

**BIOCHEMICAL ANALYSIS OF
THE mRNA SCAVENGER DECAPPING ENZYMES**

By

SHIN-WU LIU

A Dissertation submitted to the Graduate School-New Brunswick

Rutgers, The State University of New Jersey

and

The Graduate School of Biomedical Sciences

University of Medicine and Dentistry of New Jersey

in partial fulfillment of the requirements

for the degree of

Doctor of Philosophy

Graduate Program in Cell and Development Biology

written under the direction of

Dr. Megerditch Kiledjian

and approved by

New Brunswick, New Jersey

October, 2007

ABSTRACT OF THE DISSERTATION

Biochemical Analysis of the mRNA Scavenger Decapping Enzymes

by

SHIN-WU LIU

Dissertation Director

Dr. Megerditch Kiledjian

The modulation of mRNA degradation is an essential determining point for regulation of gene expression. Eukaryotic cells primarily utilize exoribonucleases and decapping enzymes to degrade their mRNAs. The scavenger mRNA decapping enzyme, DcpS, hydrolyzes the cap structure, which is the decay product in the 3'-5' mRNA degradation pathway. DcpS is a member of the histidine triad (HIT) family of hydrolases and catalyzes the cleavage of m⁷GpppN to release m⁷Gp and ppN. We have carried out a biochemical characterization of the DcpS enzyme and demonstrated that, unlike other HIT family members, DcpS requires both the core HIT fold at the C-terminus and a segment of N terminus for cap binding and hydrolysis. To further examine the cellular function of DcpS, we tested the impact of DcpS on cap-dependent translation. Interestingly, DcpS can efficiently compete for and hydrolyze the cap structure in the

presence of eIF4E, an essential cap-binding translation initiation factor. Furthermore, we demonstrated that the relative cap-dependent translation was inhibited by 40% in the DcpS knockdown cells and was partially restored by DcpS complementation. These results strongly suggest that DcpS functions to prevent the accumulation of residual cap structure that would otherwise trap eIF4E and interfere with cap-dependent translational events.

Structural analysis of DcpS revealed that it is a dimeric protein with a distinct N terminal domain and a C terminal domain, linked by a flexible hinge region, which led to a proposed dynamic decapping model, where the N terminus flips back and forth during the process of hydrolysis. To gain more insights into the decapping mechanism at the subunit level, we analyzed the kinetics of DcpS decapping and demonstrated that its decapping was negatively regulated under multiple turnover conditions, due to an allosteric conformational change caused by the excess amount of substrate. Our data have provided mechanistic details in terms of hydrolysis as well as the insights into the regulation of decapping in cells.

DEDICATION

This thesis is dedicated to my parents,

Dr. Hsiang-Chuan Liu and Fei Pan,

who have always been supportive of me and keep encouraging me from day to day;
also to my brother Tung-Sheng Liu; growing up with him has been a blessing to me.

Acknowledgement

First and foremost, I would like to thank my Lord and Savior Jesus Christ. He has brought me strength everyday and I could not gain true success in anything without Him in my life.

I would like to express my deep gratitude to my thesis advisor, Dr. Mike Kiledjian, for his guidance and support in the past five years. He has always been accessible and willing to provide his help. His knowledge, perspective, and his logical way of thinking have set up a good model which has greatly helped me to enrich my growth as student and a scientist. He has also helped me tremendously in my writing and presentation skills. The research experience I have gained through working in his lab has been one of the most exciting and rewarding experiences in my life, and I feel honored and lucky to have joined his lab.

I would like to thank my thesis committee members, Drs. Lori Covey, Samuel Gunderson, Terri Kinzy, and Smita Patel for their valuable comments and suggestions through my graduate years. In particular, I am grateful to Dr. Smita Patel, for her assistance in the kinetic analysis of DcpS decapping, which is an important part of my thesis work. Enzyme kinetics was a new field to me and Dr. Patel has taught me many important concepts during the course of this work. Her insightful opinions are also critical for the development of my thesis.

My colleagues in our lab have also contributed greatly to my research work. Everyone has helped me in some way and I am eternally grateful. I thank Hudan Liu for

spending time helping me with lab techniques when I first came to the lab. I am indebted to Xinfu Jiao, who has shared with me a lot of lab techniques which have helped me accomplish important experiments. I would like to express my thanks to Anne Carr-Schmid, for her generous contribution of time in sharing her research experiences with me in my junior years. Those conversations with Anne have greatly helped to open my eyes to science. I would like to acknowledge Sophie Bail and Vincent Shen, who have provided important support and encouragement during my thesis writing period. Also I would like to thank other lab members, You Li, Mangen Song, Yvette Wang, and Sarah Welch, as well as the former lab members Chantal Anelas, Kathy Kelly-Borja, Richie Khanna, Tao Liu and Chris Piccirillo for their support, help, and friendship.

I would like to acknowledge the members in the neighboring labs, who have provided indispensable help to my research work. First, I would like to thank the lab members in Dr. Smita Patel's lab. I would like to especially express my deep gratitude to Vaishnavi Rajagopal, who spent numerous hours assisting in data analysis, explaining concepts in enzyme kinetics to me, as well as helping me operating the quench flow machine. My thanks also go to Manjula Pandey, who has also provided important assistance with the quench flow machine; Guo-qing Tang, who helped me with the spectrophotometer; as well as other Patel lab members. I would also like to thank the wonderful people in surrounding labs in Nelson Biology for sharing their techniques, facilities and reagents. These labs include Dr. Lori Covey's lab, Dr. David Denhardt's lab, Dr. Barth Grant's lab, Dr. Sam Gunderson's lab, Dr. Alice Liu's lab, Dr. Charles Martin's lab, and Dr. Gutian Xiao's lab.

I would like to express my deep gratitude to my TA advisor, Dr. Susan Skelly. I have learned a great deal in presentation skills from working with her as a teaching assistant. I am especially grateful for her warm support and encouragement, which has been an important inspiration throughout my graduate years.

I would also like to thank my church friends Shin-Shin Chen, Jing Hao, Zhenya Jia, Linda Kuo, Ning Lee, Chanfa Lin, Shou-En Lu, Wendy Lu, Hong Li, Doreen Tang, Elizabeth Tseng, Grace Wang, Carol Yeh, Julie Zhu, as well as other members in MYPG and Saturday Choir. Without their friendships and prayers, I would not be able to have accomplished this thesis in time.

Lastly, and most importantly, I would like to express my deepest gratitude to my parents, Dr. Hsiang-Chuan Liu and Fei Pan, as well as my brother Tung-Sheng Liu, for their love and support in every aspect of my life. To them I dedicate this thesis.

TABLE OF CONTENTS

ABSTRACT OF THE DISSERTATION	ii
DEDICATION	iv
ACKNOWLEDGEMENT	v
TABLE OF CONTENTS	viii
LIST OF TABLES	x
LIST OF FIGURES	xi

INTRODUCTION

mRNA Synthesis, Maturation, and Nuclear Export	1
Nuclear mRNA turnover	7
Cytoplasmic mRNA Decay	10
Deadenylation Dependent mRNA Degradation	11
Deadenylation	11
Decapping	13
Exoribonuclease Activities	19

MATERIALS AND METHODS

Plasmid Constructs	22
Recombinant Protein Expression and Purification	25
Quantitation of the concentrations of recombinant proteins	28
Generation of Labeled RNA and Cap Structures	30
In Vitro Decapping Assay	31

Quench-Flow Decapping Assay and Data Analysis	31
Electrophoretic Mobility Shift Assay (EMSA)	33
Filter Binding Assay	34
UV-Crosslinking	34
Cell Culture and Transfections	35
Dual Luciferase Assay	35
Western Analysis	36
 CHAPTER I: Functional Analysis of mRNA Scavenger Decapping Enzymes	
Summary	37
Introduction	39
Results	41
Discussion	68
 CHAPTER II: Mechanistic and Kinetic Analysis of the DcpS Scavenger Decapping Enzyme	
Summary	74
Introduction	75
Results	77
Discussion	98
 REFERENCES	 108
CURRICULUM VITAE	126

LIST OF TABLES

Table 1.	DcpS binding.	60
Table 2.	The rate constants and maximal decapping rates under single and multiple turnover conditions	81
Table 3.	The rate constants and maximal decapping rates of DcpS ^{WT/WT} , DcpS ^{WT/Inert} , and DcpS ^{WT/HIT} under single and multiple turnover conditions	92

LIST OF FIGURES

Figure 1.	Regions outside the HIT hydrolase fold are critical for scavenger decapping activity	43
Figure 2.	The N-termini of Dcs1p and DcpS are critical for decapping	44
Figure 3.	DcpS is a modular protein	47
Figure 4.	DcpS N-terminus facilitates cap binding	49
Figure 5.	Co-crystal structure of DcpS and cap substrates revealed a dimeric structure with distinct N and C termini in an asymmetric open/closed configuration	50
Figure 6.	Mutagenesis and Biochemical analysis of DcpS decapping	52
Figure 7.	DcpS catalyzes the hydrolysis of cap structure but not capped RNA	57
Figure 8.	RNA in trans has no effect on DcpS decapping	59
Figure 9.	DcpS can displace eIF4E from the cap structure	63
Figure 10.	DcpS is involved in maintaining normal cap-dependent translation	66
Figure 11.	Increasing amount of the DcpS increases the rate constants and the decapping rates	79
Figure 12.	Excessive amount of cap substrate reduces the rate constant and the decapping rate	83

Figure 13.	Both DcpS ^{WT/WT} homodimer and DcpS ^{WT/Inert} heterodimer display decreased decapping rates under multiple turnover conditions	88
Figure 14.	Trapping of cap substrate at the HIT mutant site of DcpS ^{WT/HIT} prevents hydrolysis from the active site	96
Figure 15.	Models of decapping mechanism under single and multiple turnover conditions	102

Introduction

Control of gene expression is a fundamental characteristic of all organisms. Most eukaryotes regulate gene expression at different levels, ranging from the initiation of transcription, pre-mRNA processing, export of mature mRNA to the cytoplasm, and translation. In many cases, the abundance of mRNA directly determines the level of protein synthesis (Guhaniyogi and Brewer, 2001). The steady-state level of cytoplasmic mRNAs depends on the combined rate of their synthesis in the nucleus, their transport from the nucleus to cytoplasm, and their degradation in the cytoplasm. Thus, the mRNA decay process is an essential determining point for regulation of gene expression. In fact, expression of many genes is mainly controlled by regulating their mRNA decay rate (Wilusz and Wilusz, 2004). Over the past decade, many of the enzymes involved in mRNA decay have been identified, and the mechanism of mRNA decay regulation has begun to be elucidated. Below, we provide a brief overview of the mRNA decay.

mRNA synthesis, maturation, and nuclear export

In eukaryotic cells, genetic instructions stored in DNA are read out by transcription and translation. In transcription, nascent pre-mRNA is synthesized from the coding region in the template strand of DNA by RNA polymerase II (RNAP II), which catalyzes the polymerization of the nucleoside triphosphates in a 5'-3' direction to form a nucleic acid chain (Conaway et al., 2000). Pre-mRNAs undergo a series of co-transcriptional modification events, including 5' capping, splicing and 3' end

polyadenylation, to form mature mRNAs (Shatkin and Manley, 2000). These RNA processing steps are tightly coupled to transcription elongation through the key factor RNAP II (Bentley, 1999; Bentley, 2002; Shatkin and Manley, 2000). The largest subunit of RNAP II possesses an unstructured C terminal tail (CTD) consisting of a long tandem array of a repeated heptad YSPTSPS; the repetition is 26 times in yeast and 52 times in human (Corden, 1990; Neugebauer, 2002). CTD plays important roles in multiple steps throughout the transcription cycle, including transcription activation (Gerber et al., 1995), initiation (Meininghaus et al., 2000), elongation (Lee and Greenleaf, 1997; Morillon et al., 2003), and termination (Egyházi et al., 1996; Howe, 2002; Kim et al., 2004). During pre-mRNA processing, CTD serves as a binding platform for numerous processing factors (Bentley, 2005), the binding of which is dependent on the phosphorylation state of CTD (Phatnani and Greenleaf, 2006).

Capping is the modification a nascent pre-mRNA undergoes and is tightly coupled with transcription elongation. As soon as the RNA polymerase II has produced 20-25 nucleotides of RNA, the 5' end of the new RNA is modified by addition of a cap that consists of a modified 7-methylguanosine through a 5'-5' unusual triphosphate linkage (Neugebauer, 2002; Shatkin and Manley, 2000). The 5' cap is a signature structure exclusively belongs to Pol II transcribed mRNAs. It helps cells to distinguish mRNAs from other types of RNAs transcribed from RNA polymerase I and III, which do not contain a CTD to carry the capping enzymes. Along the life cycle of an mRNA molecule, its 5' cap structure is associated with various cap binding proteins, which regulate the activities of splicing, export, translation and degradation at later stages of the mature

mRNA (Cougot et al., 2004; Shatkin and Manley, 2000). The regulatory mechanisms of these cellular activities will be discussed in detail in subsequent sections.

The capping reaction is carried out by three enzymatic activities, which are associated with the CTD on RNAP II (Shuman, 1997; Yue et al., 1997). The 5' triphosphate end of the nascent transcript is hydrolyzed to a diphosphate end by an RNA triphosphatase; the diphosphate end is capped with GMP by an RNA guanylyltransferase; and the 5' guanine base is methylated by an RNA methyltransferase at the N7 position (Gu and Lima, 2005; Shatkin and Manley, 2000). The triphosphatase and guanylyltransferase are encoded by two different genes in yeast, and the expressed proteins form a heterodimer referred to as capping enzyme. Whereas in mammals, the capping enzyme is a single bifunctional protein that carries out both triphosphatase and guanylyltransferase activities (Howe, 2002; Shatkin and Manley, 2000). The capping enzyme is associated with the CTD on RNAP II (Shuman, 1997; Yue et al., 1997). The fact that transcripts made *in vivo* by Pol II with a truncated CTD had a lower capping efficiency (McCracken et al., 1997a) further confirmed the notion that capping is coupled to transcription by interacting with the CTD on RNAP II.

Other than the capping reaction, another important pre-mRNA processing step is splicing. The protein coding sequence in eukaryotic mRNA is typically interrupted by non-coding sequences known as introns. The pieces of discontinuous coding sequence are termed exons. Both introns and exons are transcribed into pre-mRNAs, and the introns are removed from the pre-mRNA by a dynamic macromolecular machine, spliceosome (Sanford and Caceres, 2004). The spliceosome consists of five small nuclear ribonucleoprotein particles (snRNPs) U1, U2, U4, U5 and U6, and numerous

non-snRNP factors. The pre-RNA splicing process is catalyzed by the assembly of the spliceosome on the pre-mRNA. It is initiated by the base-pairing of U1 snRNA to a consensus sequence on the 5' splice site, the recognition of 3' splice site by a U2 snRNP auxiliary factor (U2AF), followed by binding of U2 snRNP, and subsequent recruitment and rearrangement of other U snRNPs and protein factors (Sanford and Caceres, 2004). During the course of spliceosome assembly, the intron is excised and the exons are ligated. It remains unclear whether the catalysis is carried out by snRNA, proteins or both. There is growing evidence pointing to snRNA as the splicing ribozyme in spliceosome. It has been reported that the secondary structure of spliceosome is similar to the known ribozyme group II self-splicing introns (Villa et al., 2002). Moreover, both of them require metal cofactor for their catalytic activities (Gordon et al., 2000), and the metal ion is coordinated by U6 snRNA in the case of spliceosome (Yean et al., 2000). Furthermore, the protein free U2:U6 snRNAs complex was able to perform a number of catalytic reactions (Valadkhan and Manley, 2001).

Splicing can occur cotranscriptionally, immediately after the 3' splice site is transcribed (Wetterberg et al., 2001), or it can occur posttranscriptionally (Lopez and Seraphin, 2000; Wetterberg et al., 1996). Similar to capping, a number of splicing factors are physically linked to the CTD in RNAP II (Kim et al., 1997; Mortillaro et al., 1996; Vincent et al., 1996). Moreover, a truncated CTD results in inefficient splicing (McCracken et al., 1997b), indicating the coupling of transcription and co-transcriptional splicing.

Other than transcription, splicing is also linked to its downstream cellular events, such as nuclear mRNA export (Luo and Reed, 1999) and nonsense-mediated decay

(NMD) (Carter et al., 1996), an mRNA surveillance pathway to rid the mRNAs harboring a premature termination codon (PTC). During splicing, the spliceosome deposits a protein complex, termed the exon junction complex (EJC), 20-24 nucleotides upstream of the exon-exon junction (EJC)(Le Hir et al., 2000). The EJC is considered as a “mark” placed onto the splice junction of an mRNA by the spliceosome (Tange et al., 2004). It provides a binding platform for factors involved in mRNA export and NMD (Le Hir et al., 2001). For example, the mRNA export factor TAP/p15 (Le Hir et al., 2001) and the NMD factors UPF3a, Upf3b ,UPF2 and RNPS1 (Chang et al., 2007).

The last processing event is the polyadenylation of the mRNA at the 3' end. There are two major enzymatic steps in mRNA 3' end processing: the cleavage of the mRNA, followed by addition of the polyadenosine (poly(A)) tail. Prior to the first cleavage step, the polyadenylation signal, a conserved hexanucleotide AAUAAA, is recognized by the cleavage/polyadenylation specificity factor (CPSF). A downstream degenerate G/U rich sequence is recognized by the cleavage stimulation factor F (CstF) (Colgan and Manley, 1997), both of which associate with the additional cleavage factors CF1 and CF2. Once CPSF and CstF have bound to the pre-mRNA, with assistance of additional factors CF1 and CF2, the cleavage is carried out at a site between the AAUAAA and the G/U rich sequence (Colgan and Manley, 1997; Zhao et al., 1999). Recently, the 73 kD subunit of the CPSF was identified as the putative endonuclease that catalyzes the cleavage (Mandel et al., 2006). Following cleavage, an enzyme poly(A) polymerase adds adenosine nucleotides at the 3' end to form a tail with 200-250 adenosines (Wahle and Keller, 1992). In mammalian cells, poly(A)-binding protein II (PAB II) enhances the efficiency of polyadenylation and controls the length of the poly(A)

tail (Bienroth et al., 1993). As with capping and splicing processes, the CTD in RNAP II is required in polyadenylation (Fong and Bentley, 2001; McCracken et al., 1997b). There have been reports showing CTD has direct contacts on 3' processing factors, including mammalian CstF p50 and yeast Pta1, Rna14, and Pcf11 (Bentley, 2002).

As the pre-mRNA is progressing through the processing procedures, it is bound by processing factors and a variety of RNA binding proteins. Some of these proteins remain associated with the processed mRNA to form export-competent messenger ribonucleoprotein particles (mRNPs) followed by export to the cytoplasm. The aberrant mRNAs that fail to form a proper mRNP are degraded in the nucleus. mRNPs move to the cytoplasm by passing through nuclear pore complexes(NPC), a large protein complex located in the nuclear membrane and serves as the channel to connect the nucleoplasm and cytoplasm (Cole and Scarcelli, 2006b). The procedure of mRNA export involves the association of carrier to the mRNP cargo, translocation of the carrier:mRNP complex through the nuclear pore, and release of the mRNP from the carrier into the cytoplasm (Stewart, 2007). The mRNA export primarily utilizes a heterodimer Mex67:Mtr2 (TAP:p15 in higher eukaryotes) heterodimer as the mRNP carrier (Stewart, 2007). Mex67 interacts with poly(A) mRNAs and the mutation of Mex67 resulted in accumulation of the poly(A) mRNAs in the nucleus (Reed and Hurt, 2002; Segref et al., 1997). The translocation of the carrier:cargo complex through NPC initiates by the interactions between Mex67:Mtr2 and NPC components FG-nucleoporins (Braun et al., 2002; Rodriguez et al., 2004; Stewart, 2007). It has been hypothesized that the mRNPs are pulled through the NPC by the assistance of an ATPase. A supporting finding is that binding of an ATPase, Dbp5, to the cytoplasmic side of NPC, is required for mRNA

export (Cole and Scarcelli, 2006a; Schmitt et al., 1999). It has been reported the Dpb5 is also responsible for release of mRNP cargo from the Mex67:Mtr2 (Lund and Guthrie, 2005) .

Nuclear mRNA turnover

In higher eukaryotes, the introns in RNAP II produced pre-mRNAs are much longer than the exons and represent approximately 90% of nucleotides (Moore, 2002). After splicing, the majority of the removed intron RNA is degraded by exonucleases and recycled to the mRNA biogenesis machinery (Moore, 2002). However, the detailed mechanism of this exonucleolytic decay remains unclear. The remaining exon containing sequences are subjected to surveillance mechanisms to eliminate aberrant mutants or mal-processed pre-mRNAs to ensure the quality of mRNA to be exported to the cytoplasm.

The nuclear mRNA decay mechanism has been best characterized in yeast *Saccharomyces cerevisiae*. Most of the degradation activities of nuclear mRNA is carried out by the nuclear exosome, a complex of 3'-5' exonucleases and accessory factors (Mitchell and Tollervey, 2000b; van Hoof and Parker, 1999). The nuclear exosome is required *in vivo* for the degradation of normally processed mRNA (Das et al., 2003; Kuai et al., 2005), unspliced pre-mRNA (Bousquet-Antonelli et al., 2000), and incompletely processed mRNA (Burkard and Butler, 2000). Despite the abundance of the RNA substrate *in vivo*, the purified exosome displays weak activities *in vitro*. Interestingly, the individually purified exosomal component, Rrp44p, shows highly processive activities (Mitchell et al., 1997). These results suggest that the exosome in a cell is relative inactive as a default state and requires extra cofactors to reach the full

activated state. Indeed, several factors have been identified that can activate the exosome on certain types of substrates: a nuclear RNA binding protein Nrd1 was identified to recruit the exosome and facilitate degradation of target RNAs (Vasiljeva and Buratowski, 2006). In addition, a nuclear polyadenylation complex, termed TRAMP, was identified to promote nuclear exosomal activities (LaCava et al., 2005; Wyers et al., 2005).

In addition to 3'-5' exonucleolytic decay by exosome, there is also evidence for 5'-3' exonucleolytic decay in the nucleus. Rat1p is a 5'-3' exonuclease located in the nucleus (Fang et al., 2005; Johnson, 1997), which shares considerable homology with its cytoplasmic counterpart Xrn1 (Amberg et al., 1992). Rat1 is involved in the degradation of nuclear pre-mRNA (Bousquet-Antonelli et al., 2000), as well as the normal processed mRNA (Das et al., 2003). It is also involved in the processing of rRNA precursors (Geerlings et al., 2000; Henry et al., 1994), snoRNA maturation (Petfalski et al., 1998), and mRNA trafficking, as nuclear poly (A)⁺ RNA accumulates in intranuclear spots in temperature sensitive rat1-1 cells at restrictive temperature (Amberg et al., 1992).

As discussed at the beginning, the 5' end of a fully processed RNAP II transcript is modified by an m⁷GpppN cap structure, and further protected by the CBC cap binding protein. A poly(A) tail is added to the 3' end and further bound by the poly (A) binding proteins. Therefore, in order for the 3'-5' exonuclease exosome and 5'-3' rat1 to gain access to the RNA body for degradation, the 5' and 3' ends have to be deprotected. Unlike the cytoplasmic decapping events, the nuclear decapping mechanism is largely unknown. Two cytoplasmic decapping proteins, Dcp2 and DcpS are also present in the nucleus (Liu et al., 2004), suggesting they are also responsible for the nuclear cap removal. Other than Dcp2 and DcpS, a small nucleolar RNA (snoRNA)-binding protein

in *Xenopus*, X29, as well as its human homolog, have also been demonstrated to be able to hydrolyze the m⁷GpppN and m^{2,2,7}GpppN cap structure on U8 snoRNA and other mRNAs *in vitro* (Ghosh et al., 2004). The ability of X29 to remove the cap on U8 snoRNA suggests that X29 serves as a negative regulator on U8 snoRNA. U8 snoRNP has been demonstrated to be essential for processing of both 5.8S and 28S rRNA (Peculis and Steitz, 1993), thus the rate of rRNA biogenesis is indirectly regulated by the decapping of U8 snoRNA by X29. A complex of Lsm proteins, Lsm1p-7p, has been well characterized as an activator of cytoplasmic decapping in the 5' to 3' pathway (Boeck et al., 1998; Bouveret et al., 2000; Tharun et al., 2000). Similarly, nuclear decapping has been demonstrated to be stimulated by the LSM2-8p complex (Kufel et al., 2004), indicating a conserved regulating mechanism of cytoplasmic and nuclear decapping.

Prior to the degradation of the RNA body by exonucleases, the poly(A) tail of an mRNA has to be removed (deadenylation) prior to the degradation of the RNA body by the 3'-5' or 5'-3' exonucleases. Although the cytoplasmic deadenylation has been well documented (Meyer et al., 2004; Newbury, 2006), the mechanism of nuclear deadenylation remains unclear. The identified deadenylases or deadenylase complexes include Pan2:Pan3 and Ccr4:Pop2 in yeast and mammal, and PARN in mammals (Garneau et al., 2007; Meyer et al., 2004). To date, although genetic data suggest that Ccr4p and Pop2p also have nuclear roles (Collart, 2003), nuclear deadenylase activity of these factors has not yet been demonstrated. Recently, an unconventional CCR4:Caf1 complex was found to be located in the nuclear Cajal bodies in human HeLa cells, suggesting its deadenylation role in nuclear mRNA decay (Wagner et al., 2007).

Overall, the purpose of nuclear mRNA degradation is to rid the spliced intron, as well as to eliminate the aberrant mRNAs that are not properly processed. As for the degradation of normally processed mRNA in the nucleus, the exonucleases are known to play important roles and their mechanisms are extensively studied. However, the mechanistic details as to the regulation of decapping and deadenylation, and the interrelationships between these processes, still remain unclear.

Cytoplasmic mRNA decay

After a series of pre-mRNA processing events, mature mRNAs are exported to the cytoplasm and serve as substrate for the translation machinery. The abundance of the template mRNA is a critical determinant for the amount of protein produced. Since the abundance of cytoplasmic mRNAs is the net result of their transport from the nucleus to the cytoplasm and their degradation in the cytoplasm, regulation of mRNA degradation plays an important role in the gene expression process. The stability of an mRNA molecule is determined by a variety of *cis* elements on the mRNA itself, together with many *trans* factors. The *cis* elements include elements that are common to almost all mRNAs, the 5' 7-methyl guanosine cap structure and the 3' poly(A) tail which protect the RNA body against the 5' and 3' exonucleases respectively. mRNAs can also possess specific *cis* elements and one of the best characterized are the AU-rich elements (Chen and Shyu, 1995; Gingerich et al., 2004). The *trans* factors that determine the mRNA stability include RNA binding proteins that interact with the *cis* elements and enzymes that directly catalyze the degradation of the mRNA (Garneau et al., 2007; Guhaniyogi and Brewer, 2001; Newbury, 2006; Parker and Song, 2004). These *trans* factors

constitute distinct mRNA decay pathways to regulate mRNA degradation. Over the past decades, most of the enzymes and many factors have been identified, and the complex mRNA degradation mechanisms are being unraveled. Major mRNA decay pathways and the interplay between them are discussed below.

Deadenylation dependent mRNA degradation

In eukaryotes, the majority of polyadenylated mRNA undergoes degradation by the initial removal of the poly(A) tail, termed deadenylation (Decker and Parker, 1993; Muhlrad et al., 1995). Following removal of the poly (A) tail, the unadenylated mRNA is degraded by either a 5'-3' pathway or a 3'-5' pathway (Coller and Parker, 2004; Garneau et al., 2007; Liu and Kiledjian, 2006). In the 5'-3' pathway, the 5' cap is hydrolyzed by a decapping enzyme complex Dcp1/Dcp2 and the m⁷ GDP product is released (Beelman et al., 1996; Dunckley and Parker, 1999; van Dijk et al., 2002; Wang et al., 2002). The exposed mRNA 5' end is subsequently degraded in the 5'-3' direction by the XRN1 exonuclease (Decker and Parker, 1994; Johnson, 1997). In the 3'-5' pathway, following deadenylation, the unprotected 3' end is further degraded by cytoplasmic exosome in a 3'-5' manner (Wang and Kiledjian, 2001). The residual cap structure is then hydrolyzed by a scavenger decapping enzyme DcpS (Dcs1 in yeast) and the products m⁷Gp and ppN are released (Liu et al., 2002; Wang and Kiledjian, 2001). The detailed discussion regarding each step in these two major decay pathways are elaborated below.

Deadenylation

Deadenylation is the initial and generally the rate limiting step in mRNA turnover (Decker and Parker, 1993; Muhlrads et al., 1995; Parker and Song, 2004), although it remains unclear how and when the deadenylation is triggered (Garneau et al., 2007). Several deadenylases or deadenylase complexes have been characterized in yeast and mammals. In yeast *S. cerevisiae*, the first deadenylase identified was the poly(A) nuclease (PAN), which consists of the Pan2p and Pan3p subunits (Boeck et al., 1996; Brown et al., 1996). Pan2p is the catalytic subunit of the complex and its activity is Mg^{2+} dependent (Lowell et al., 1992; Uchida et al., 2004). Deletion of the PAN2 or PAN3 genes does not affect the viability of yeast, and the bulk poly(A) is approximately 20 nucleotides longer in the deficient strains. Consistent with this result, cell extract deficient for Pan2p and Pan3p polyadenylated the substrate RNA to anomalously long and heterogeneous lengths (Boeck et al., 1996; Brown and Sachs, 1998; Brown et al., 1996), suggesting an important role of PAN in the length control of the poly(A) tail. The major deadenylase of yeast is the Ccr4p:Notp complex, which contains CCR4p and Pop2p nucleases, as well as the accessory proteins Not1-Not5p, Caf4p, Caf16p, Caf40p, and Caf130p (Chen et al., 2002; Coller and Parker, 2004; Tucker M, 2002; Tucker M, 2001). PAN and Ccr4-Not deadenylases are conserved in mammals (Meyer et al., 2004). Recently, it has been shown that deadenylation in mammalian cells displays a biphasic kinetics. Using a β -globin reporter transcript, Yamashita et al. showed Pan2:Pan3 initiated deadenylation by removing about half of the A nucleotides in a relative slow and synchronous manner. Following this event, the second deadenylase complex Ccr4:Not continued the deadenylation and removed the rest of the A nucleotides in an unsynchronized processive manner (Yamashita et al., 2005).

In addition to the Ccr4-Not complex and PAN, a third deadenylase, the poly(A)-specific ribonuclease, PARN, is present in some higher eukaryotes, including mammals, some insects, plants and *Xenopus laevis* (Korner and Wahle, 1997). PARN is involved in the deadenylation of maternal mRNAs in *Xenopus laevis* oocytes during maturation (Korner et al., 1998), and it appears to be the main deadenylase in cytoplasmic extract in various cell lines (Gao et al., 2000; Milone et al., 2004).

There appears to be interplay between deadenylases and cap as well as poly(A) binding protein (PABP, Pab1 in yeast). First, the knockdown of Dcp2 resulted in accumulation of mRNA with 110nt poly(A) tail, indicating Dcp2 decapping occurs at the second phase of deadenylation by Ccr4:Not (Yamashita et al., 2005). Second, the processivity of PARN is enhanced by the presence of a 5' cap on the mRNA (Dehlin et al., 2000; Gao et al., 2000; Garneau et al., 2007; Martinez et al., 2001). Moreover, Pan2:Pan3 activity has been shown to be enhanced by PABP both in yeast and mammals (Boeck et al., 1996; Uchida et al., 2004). In contrast, the activities of both Ccr4 and Dcp2 are inhibited by PABP (Khanna and Kiledjian, 2004; Tucker M, 2002). Yamashita et al. proposed that PABP stimulates the Pan2:Pan3 activities and inhibits Ccr4 and Dcp2 activities at the initial stage of deadenylation. During this period of time PABP molecules would gradually dissociate from the poly(A) tail thus allowing Ccr4 and Dcp2 to exert mRNA degradation (Mühlemann, 2005; Yamashita et al., 2005).

Decapping

Eukaryotic mRNAs possess a 5' end 7-methylguanosine cap structure, connected to the first nucleotide of the mRNA through a non-typical 5',5' pyrophosphate linkage

(Furuichi et al., 1975). This 5'-5' linkage renders the mRNA resistant to the attack by 5' exonuclease. The cap structure plays important roles at various stages throughout the life cycle of an mRNA molecule. For example, the cap structure is required for proper pre-mRNA splicing (Edery and Sonenberg, 1985; Inoue et al., 1989; Konarska et al., 1984). It also facilitates mRNA transport from nucleus to cytoplasm (Dargemont and Kuhn, 1992; Hamm and Mattaj, 1990; Izaurralde and Mattaj, 1995; Izaurralde et al., 1992; Jarmolowski et al., 1994). After transport to the cytoplasm, the 5' cap structure is recognized and bound by the transcription initiation factor, eIF4E, which is essential for translation initiation (Muthukrishnan et al., 1975; Sonenberg, 1988). Ultimately, when a given mRNA molecule is subjected to the decay machinery, one of the critical steps is the removal of the 5' cap structure. Regulation of decapping is an important process, as hydrolysis of the cap structure is irreversible and renders the mRNA susceptible to exonucleases, leading to definitive and rapid decay of the remaining mRNA body (Coller and Parker, 2004; Cougot et al., 2004; Simon et al., 2006).

To date, two major decapping enzymes have been identified. One is Dcp1/Dcp2 decapping complex, which is responsible for the decapping in the 5'-3' decay pathway. The other one is the scavenger decapping enzyme, DcpS, which functions in the 3'-5' decay pathway. The biochemical and structural analysis of these decapping enzymes, as well as the regulation of their decapping mechanisms are discussed below.

Dcp2

In normal mRNA decay, deadenylation leads to removal of the 5' cap by a decapping enzyme Dcp2, therefore exposing the mRNA body to degradation by a 5'-3'

exonuclease (Decker and Parker, 1993; Hsu and Stevens, 1993). The substrate for Dcp2 is the capped mRNA longer than 25 nucleotides (LaGrandeur and Parker, 1998; Steiger et al., 2003). The recognition and hydrolysis of the cap structure requires an initial interaction with the RNA moiety on the substrate (Piccirillo et al., 2003). The hydrolysis of the 5' cap by Dcp2 yields the products m⁷GDP and a monophosphate terminated RNA (van Dijk et al., 2002; Wang et al., 2002).

In *S. cerevisiae*, Dcp2p and Dcp1p form a decapping complex, in which Dcp2p is the catalytic subunit and Dcp1p serves as an enhancer for Dcp2p decapping activity (Coller and Parker, 2004; She et al., 2006; Steiger et al., 2003). In higher eukaryotes, there is a third adaptor component Edc4 (Hedls or Ge-1) which stimulates decapping activity (Fenger-Gron et al., 2005; Yu et al., 2005). In addition to Dcp1 and Edc4, other Dcp2 activators have also been identified. The Lsm1-7 protein complex, as well as Pat1p, Dhh1p and the Edc1p, Edc2p, and Edc3p proteins, are also required for efficient Dcp2 decapping *in vivo* (Coller and Parker, 2004). Also, Dcp2 can be negatively impacted. PABP can inhibit Dcp2 activity *in vitro* (Khanna and Kiledjian, 2004; Wilusz et al., 2001). The cap-binding protein eIF4E inhibits Dcp2 activity both *in vitro* and *in vivo* (Caponigro and Parker, 1995; Khanna and Kiledjian, 2004; Ramirez et al., 2002; Schwartz and Parker, 1999; Schwartz and Parker, 2000). [More](#) recently, a protein VCX-A, that is implicated in x-linked nonspecific mental retardation, has also been shown to be an inhibitor of Dcp2 (Jiao et al., 2006).

The Dcp2 proteins are members of a Nudix (nucleotide diphosphate linked to an X moiety) hydrolase family. Nudix hydrolases contain a conserved Nudix motif, which is a segment of 23 amino acid sequence, GX₅EX₇REUXEEXGU, where X stands for any

residues and U denotes for hydrophobic residues (Koonin, 1993; Mejean et al., 1994) . The Nudix hydrolases are widely distributed in nature in various eukaryotes and prokaryotes, with diverse substrates including nucleoside triphosphates, nucleotide sugars, coenzymes such as NADH, FAD, or CoA, cell signaling molecules such as dinucleoside polyphosphates, and toxic metabolites such as ADP-ribose and toxic nucleotides (Bessman et al., 1996). It has been proposed that many Nudix proteins fulfill a physiological role to hydrolyze substrates that might be hazardous to cells, or to prevent the unbalanced accumulation of the substrates that are normal metabolites (Bessman et al., 1996). The structure of a Nudix protein, ADP-ribose pyrophosphatase reveals that Nudix motif is located in a larger Nudix fold, which consists of two β -sheets sandwiched between α -helices and functions as a cation-binding and catalytic site (Gabelli et al., 2001). Residues in the Dcp2 Nudix motif are required for catalysis, as mutations abolish the hydrolase activity (Dunckley and Parker, 1999; van Dijk et al., 2002; Wang et al., 2002). Similar to other Nudix proteins, Dcp2 requires cations, preferentially Mn^{2+} , as a cofactor for its decapping activity (Piccirillo et al., 2003).

In addition to the Nudix motif, there are at least two other conserved motifs in Dcp2 proteins (Wang et al., 2002). The first is Box A that precedes the Nudix fold and the second is Box B that is carboxy-terminal to the Nudix fold. Biochemical analysis revealed that the Nudix motif and the Box B were required for Dcp2 activity *in vitro*. The Box A was not absolutely required for the decapping activity *in vitro* but was a part of a N terminal region which was indispensable for the Dcp2 activity *in vivo* (Piccirillo et al., 2003; She et al., 2006). Recently, the structure of a C terminally truncated *Schizosaccharomyces pombe* Dcp2 has been resolved and it revealed a distinct N terminal

domain consisting of helices and a C-terminal domain that contained a classic Nudix fold (She et al., 2006). Consistent with the biochemical analysis results, the structural analysis revealed that B box is an essential component of the $\alpha/\beta/\alpha$ -sandwich Nudix fold (She et al., 2006). Further biochemical analysis revealed that the N terminus, which encompasses the Box A, served as the binding site for Dcp1 (She et al., 2006), consistent with the fact that the N terminus was indispensable for the decapping activity *in vivo*.

DcpS

The scavenger decapping enzyme, DcpS (Dcs1 in yeast), is the decapping enzyme responsible for the hydrolysis of the residual capped oligo nucleotide following the 3'-5' degradation by the exosome. DcpS activities were first identified from the Hela cell extracts over thirty years ago (Nuss et al., 1975), and the DcpS protein was subsequently purified (Kumagai et al., 1992; Liu et al., 2002) and cloned (Liu et al., 2002). The major difference between DcpS and Dcp2 is that, DcpS acts on a free cap dinucleotide m⁷GpppN or capped oligo nucleotides containing less than 10 nucleotides and the cleavage product is m⁷Gp. The Dcp2 substrate is capped-RNA containing at least 25 nucleotides (LaGrandeur and Parker, 1998; Steiger et al., 2003) and the cleavage product is m⁷GDP. Similar to Dcp2, DcpS has a distinct hydrolase motif, termed HIT (histidine triad) motif, and therefore is characterized as a member of the HIT protein superfamily. The members of HIT superfamily are nucleotide hydrolases and transferases, all of which possess the conserved HUHUUU HIT motif, where U denotes a hydrophobic amino acid (Brenner, 2002; Brenner et al., 1999; Guranowski, 2000; Seraphin, 1992). The

central histidine residue has been proposed to be critical for the hydrolase activity as it serves as the nucleophile attacking the α phosphate in the substrate (Lima et al., 1997).

On the basis of sequence, substrate specificity, structure, evolution and mechanism, HIT proteins are classified into the Hint (Histidine triad nucleotide-binding protein) branch, the ancestral HIT protein consisting of adenosine 5' monophosphoramidate hydrolases, the Fhit (fragile histidine triad) branch, consisting of diadenosine polyphosphate hydrolases, the GalT (Galactose-1-phosphate uridylyltransferase) branch, consisting of specific nucleoside monophosphate transferases, and Aprataxin, which is a DNA and RNA binding protein containing nucleotide hydrolase activities (Brenner, 2002; Kijas et al., 2006). DcpS is classified as a novel HIT protein branch based on a phylogenetic analysis (Kijas et al., 2006). Furthermore, structural analysis of DcpS bound to cap substrate reveals an asymmetric open/closed configuration (discussed in detail below), which is distinct from the structures of other HIT proteins (Gu et al., 2004; Gu and Lima, 2005).

The structural analysis of DcpS in complex with cap substrates has provided informative insights into its decapping mechanism. The co-crystallized DcpS enzyme and cap substrate revealed that it is a dimeric enzyme, with a distinct domain swapped N terminus and a C terminus linked by a flexible hinge (Gu et al., 2004). The DcpS dimer displayed an asymmetric architecture, with a simultaneous productive closed conformation formed at one protomer and a non-productive open conformation formed at the other protomer, with each protomer bound by a cap substrate. Based on these structural results Gu et al. proposed a dynamic decapping model where the N terminus of DcpS flips back and forth for binding and hydrolysis of the cap substrate (Gu et al., 2004).

Consistent with this model, the ligand free human and mouse DcpS exhibited a symmetric open/open configuration (Chen et al., 2005; Han et al., 2005). The structure data indicated the N-terminal domain in ligand-free DcpS was inherently flexible and in a dynamic state ready for substrate binding and product release.

In summary, Dcp2 and DcpS are the decapping enzymes responsible for the 5'-3' and 3'-5' decay pathways, respectively, with a distinct hydrolase motif in each of the decapping enzyme. Numerous Dcp2 interacting proteins have been identified and the regulatory mechanism has been well characterized. However, regulation of DcpS still remains unclear. Future focus will be to identify the regulatory network of both Dcp2 and DcpS, as well as the interplay between the two regulatory decapping mechanisms.

Exoribonuclease activities

In the 5'-3' decay pathway, following decapping the mRNA body is degraded by a 5' to 3' exonuclease, Xrn1. Mutation within the *Xrn1* gene in yeast led to the accumulation full-length mRNAs without a cap (Hsu and Stevens, 1993; Muhlrads et al., 1994). The enzyme was first characterized in yeast (Stevens, 1980), and the homolog have also been characterized in mammals (Bashkurov et al., 1997), flies (Till et al., 1998), and worms (Newbury and Woollard, 2004). The preferable substrate for Xrn1 is the RNA carrying a 5' monophosphate, and the digestion product are 5' NMPs (Stevens, 1980).

Although it has been considered to be one of the least regulated steps of mRNA decay, there are several examples showing that the 5' to 3' exoribonuclease degradation step is a regulated step. First, the mutation of eIF5A blocked the 5' exoribonucleolytic

activity following decapping (Zuk and Jacobson, 1998). Second, accumulation of pAp in cells, implicated in lithium toxicity, resulted in the inhibition of Xrn1p exoribonuclease activity (Benard, 2004; Dichtl et al., 1997). Third, the expression of Xrn1 is developmentally controlled in flies and worms (Newbury and Woollard, 2004; Till et al., 1998). Fourth, disruption of yeast DcpS homolog, Dcs1, repressed the decay rate of some mRNAs by impeding the 5' exonucleolytic decay step (Liu and Kiledjian, 2005).

The exonucleolytic decay step in the 3'-5' pathway is carried out by the RNA exosome (Jacobs et al., 1998; Mitchell et al., 1997), a 10-12 subunit complex that is present both in the nucleus and the cytoplasm. The components of exosome were first identified in yeast (Allmang et al., 1999b; Mitchell et al., 1997). The nuclear and cytoplasmic exosome share 10 common components, and they differ by the presence of Ski7 GTPase in cytoplasmic exosome, and the RNase Rrp6 as well as the putative nucleic acid binding protein Rrp47 in the nuclear exosome (Houseley et al., 2006). Other than wild type mRNAs, mRNAs with structural defects are also known as substrates of exosome. mRNAs with premature translational termination codons or mRNAs that lack the termination codon are degraded rapidly by the exosome (Frischmeyer et al., 2002; Lejeune et al., 2003; Mitchell and Tollervey, 2003; van Hoof et al., 2002). As discussed in the earlier paragraphs, exosome is relatively inactive as a default state and it requires cofactors to enhance its activities. The best characterized cytoplasmic exosome activators are the complexes formed by Ski7, Ski2, Ski3 and Ski8 proteins (Araki et al., 2001; van Hoof et al., 2000). In addition to participating in mRNA 3' to 5' decay, the Ski protein complexes are also involved in the degradation of mRNAs containing a

premature termination codon or those that lack termination codon altogether (Mitchell and Tollervey, 2003; van Hoof et al., 2002).

Materials and Methods

Plasmid constructs

Plasmids expressing amino terminal histidine-tagged recombinant proteins for DcpS (pET28-DcpS), Dcs1p (pET28-Dcs1 formerly called pET28 yDcpS), and Dcs2p (pET28-Dcs2, formerly pET28-YOR173W) have been described (Liu et al., 2002). The pET28-Dcs1/2 encodes a chimeric protein containing amino acids 1–210 of Dcs1p and 254–397 of Dcs2p. It was generated by replacing the *Bam*H I to *Pvu* I fragment of pET28-Dcs2 with the corresponding fragment of pET28-Dcs1. The pET28-Dcs2/1 plasmid encodes a chimeric protein containing amino acids 1–253 of Dcs2p and amino acids 211–350 of Dcs1p. It was generated by replacing the *Bam*H I to *Pvu* I fragment of pET28-Dcs1 with the corresponding region of pET28-Dcs2.

The plasmid pET28-Dcs1^{ΔN40} encoding Dcs1p amino acids 41–350 was generated by PCR amplification of sequences corresponding to these amino acids with a primer set introducing a *Bam*H I site on the 5' end and an *Xho* I site at the 3' end of the PCR product (5'-AGTGGATCCGCTATTATCACGGCTGAAAAG-3' and 5'-CAGCCCTCGAGTTATTTAAAACCGTTCAC-3'). The PCR product was digested with *Bam*H I and *Xho* I and inserted into the same sites of pET28a (Novagen). The plasmid pET28-Dcs1^{ΔN81}, encoding Dcs1p amino acids 82–250, was generated by digesting the pET28-Dcs1 plasmid with *Nhe* I and *Eco*R I, the ends filled in with Klenow fragment and self-ligated. The plasmid pET28-Dcs1^{ΔC285}, which encodes Dcs1p amino

acids 1–284, was generated by digesting the pET28-Dcs1 plasmid with *Sac* II and *Xho* I, the ends filled in with T4 DNA polymerase and self-ligated.

The plasmid pET28-DcpSΔN33 encoding DcpS amino acids 34–337 was generated by PCR amplification using the forward primer, 5'-ATTGGATCCAATGGTACCTGTGCTCCTGTC-3' and the reverse primer, 5'-TCTCGAGTCAGCTTTGCTGAGCCTCCTG-3' and inserted into pET28a as described for pET28-Dcs1ΔN40. The plasmid pET28-DcpSΔN71, which encodes DcpS amino acids 72–337, was generated by digesting pET28-hDcpS with *Nde* I and *Stu* I. The resulting ends were filled in with Klenow fragment and self-ligated. The pET28-DcpS1–274 plasmid encoding DcpS amino acids 1–274 was generated by PCR with the following primers, 5'-AGGATCCCGCCTCCGCGGCAGCATG-3' and 5'-TTACTC GAGGTAGTAGGAGGGCAGGTAGTG-3' that introduce a *Bam*H I and *Xho* I site, respectively. The PCR product was cloned into the same sites of pET28a. The plasmid pET-DcpSH277N expressing the HIT mutant protein DcpS^{mH} which substitutes an asparagine for the active site histidine at position 277 was described (Liu et al., 2002). All of the above pET28a-based plasmids produce a recombinant protein containing a histidine-tag at the amino terminus.

Plasmids expressing DcpS or its truncations that lack a tag were generated by PCR amplification of either full-length DcpS or DcpS sequences from amino acids 1–147 and 149–337 and inserted into to the pSMT3 TOPO directional vector (Mossessova and Lima, 2000) to generate the plasmids pSMT3-hDcpS, pSMT3-hDcpS(1–147), and pSMT3-hDcpS(149–337), respectively. The murine eIF4E protein expression plasmid pET28-eIF4E was constructed by removal of the eIF4E coding region with *Bam*H I and

Xho I from the pPROEX-melF4E plasmid (kindly provided by A.C. Gingras and N. Sonenberg, McGill Univ.) and inserted into the same sites of pET28a. The pGEX-mDAZL plasmid encoding the glutathione S-transferase (GST)-mDAZL fusion protein has been described (Jiao et al., 2002).

The pcDNA3-Flag-DcpS plasmid which expresses Flag-tagged DcpS in mammalian cells was constructed by inserting the DcpS open reading frame flanked by a *Bam*H I site at the 5' end and an *Xho* I site at the 3' end into the pcDNA3-Flag (Fenger-Gron et al., 2005) vector. pcDNA3-Flag-DcpS^{ΔKR} was derived from pcDNA3-Flag-DcpS by using site-directed mutagenesis (Stratagene) to delete amino acids 10-13 in DcpS open reading frame. The DcpS-specific shRNA expression plasmid, pSHAG1-puro-DcpS1 was generated by inserting an annealed primer set 5' GTGCTGTAGATATCATTGGAG AACTGCAGAAGCTTGTGCAGTTCTCCAATGATATCTACAGCACCTATTTTTT 3' and 5' GATCAAAAAATAGGTGCTGTAGATATCATTGGAGAACTGCACAAGCTT CTGCAGTTCTCCAATGATATCTACAGCACCG 3' into the *Bse*R I and *Bam*H I sites of the pSHAG1-puro vector (Paddison et al., 2002) modified by the addition of a puromycin selection marker to the pSHAG1 plasmid. The pSHAG1 construct was kindly provided by Dr. Gregory J. Hannon (Cold Spring Harbor Laboratory).

The Flag-tagged DcpS expression plasmid, pcDNA3-FlagDcpS-2, was constructed by inserting DcpS open reading frame (ORF) with a Flag tag fragment at the 5' end into the *Nco* I/*Xho* I sites of pcDNA3 vector (Invitrogen). Plasmids expressing a series of double-tagged homo- and heterodimer proteins were generated by inserting two tagged wild-type or mutated DcpS ORFs into the two multiple cloning regions of the commercial plasmid pETDuet-1 vector (Novagen). Plasmid pETDuet-

1HisDcpS^{WT}FlagDcpS^{WT} was constructed by inserting the *Nco* I(Klenow filled)/*Xho* I restriction fragment from pcDNA3-FlagDcpS-2, as well as the *Nco* I/*Xho* I (Klenow filled) restriction fragment from pET28-DcpS (Liu et al., 2002), into the *Eco*R V/*Xho* I sites and *Nco* I/*Eco*R I(Klenow filled) sites in pET-Duet-1, respectively. Plasmids pETDuet-1HisDcpS^{H277N}FlagDcpS^{WT} and pETDuet-1HisDcpS^{W175A}FlagDcpS^{N110A}, which express DcpS^{WT/HIT} and DcpS^{Inert/Inert} respectively, were constructed in a similar way, except with the indicated mutated sites introduced into the DcpS ORF. The mutagenesis of DcpSH277N was described in (Liu et al., 2002). The mutagenesis of N110A and W175A was carried out using the QuikChange mutagenesis system (Stratagene) with the primer sets 5'-CTC CAA TTG CAG TTC TCC GCT GAT ATA TAC AGC ACC TAT C-3', 5'-GAT AGG TGC TGT ATA TAT CAG CGG AGA ACT GCA ATT GGA G-3', and 5'-CAG AGC CTC AGC ATC CAG GCG GTG TAT AAC ATT CTC GAC-3', 5'-GTC GAG AAT GTT ATA CAC CGC CTG GAT GCT GAG GCT CTG-3', respectively.

The single tagged homodimer proteins His DcpS^{Inert/Inert} and Flag DcpS^{Inert/Inert} used in Fig 13C contain N110A and W175A double mutations. They were expressed from plasmids pET28-DcpS^{N110AW175A} and pcDNA3 Flag DcpS^{N110AW175A}, respectively. These two plasmids were generated by introducing the N110A and W175A mutations into the plasmids pET28-DcpS and pcDNA3 Flag DcpS-2 using the primer sets described above.

Recombinant protein expression and purification

Recombinant proteins expressed from the pET28 vectors were generated in *E. coli* BL21(DE3) cells. Following transformation, a single colony was grown in LB containing 50 µg/ml kanamycin to an optical density at 600 nm (OD₆₀₀) of 0.6 and induced for 3 hours with 0.4 mM isopropyl-β-D-thiogalactopyranoside (IPTG) at 30°C. The overexpressed protein was purified according to the instructions of the manufacturer (Novagen), except that 300 mM urea was included in the binding buffer. Protein eluted from the nickel column was dialyzed against PBS (0.14 M NaCl, 2.7 mM KCl, 1.5 mM KH₂PO₄, 8.1 mM Na₂HPO₄, pH 7.4) and concentrated by Centricon centrifugal filter columns (Amicon). The Dcs1^{ΔC285} and DcpS¹⁻²⁷⁴ proteins were purified under denaturing conditions with 4M urea according to the manufacturer's instructions (Novagen) and dialyzed against renaturing buffer (50 mM Tris-HCl, 500 mM L-arginine, 5 mM EDTA, 0.4% PEG 4000, 5 mM reduced Glutathione, 1 mM oxidized glutathione) overnight to remove the urea. The renaturing buffer was subsequently replaced by PBS in a stepwise manner by concentration using Centricon centrifugal filtration. The GST-mDAZL protein was purified by glutathione beads as described (Jiao et al., 2002) except that 300 mM urea was included in the binding and wash buffer.

Recombinant proteins used in Fig 3, 4, 6, 7, 9C, 14C are kind gifts from Dr. Chris Lima (Sloan-Kettering Institute). They were expressed from the pSMT3 vector in *E. coli* BL21 (DE3) CodonPlus RIL cells (Novagen). Proteins were initially purified by metal-affinity chromatography under native conditions and subsequently subjected to proteolysis by Ulp1 to remove the His₆-Smt3 tag (Mossessova and Lima, 2000). The resulting proteins were further purified by gel filtration (Superdex 75, Pharmacia).

Recombinant Flag DcpS is expressed from pcDNA3-flag DcpS in 293T cells and purified using Anti-Flag M2 agarose beads (Sigma). 1×10^8 293T cells were transfected with 120 μ g pcDNA3-flag DcpS and incubated at 37°C, 5% CO₂ to allow transient protein overexpression. Forty-eight hours posttransfection, cells were harvested and washed with PBS and resuspended in sonication buffer (150 mM KCl, 20 mM Tris HCl pH 7.9, 0.2 mM EDTA, 10% glycerol, 0.01% NP40) followed by sonication for 30 seconds. The cell debris were then spun down, and the supernatant was incubated with 300 μ L pre-washed Anti-Flag M2 agarose beads at 4°C for 3 hours with mild shaking to allow the Flag DcpS bind to the beads. The beads were then washed twice with 10 ml wash buffer (300 mM KCl, 20 mM Tris HCl pH 7.9, 0.2 mM EDTA, 10% glycerol, 0.025% NP40). The bound Flag DcpS proteins were then eluted by 1 ml elution buffer (wash buffer with 100 μ g/ml Flag peptide, Sigma). The eluted proteins were subsequently concentrated by Centricon centrifugal filter columns (Amicon).

The expression of double tagged recombinant homodimer and heterodimer proteins was performed using the pETDuet-1 expression system. Plasmids pETDuet-1-His-DcpS/Flag-DcpS, pETDuet-1-His-DcpS^{N277A}/Flag-DcpS, and pETDuet-1-His-DcpS^{W175A}/Flag-DcpS^{N110A} were used to transform BL21-CodonPlus(DE3)-RIPL competent cells (Stratagene) according the the manufacturer's instructions. A single colony was picked and grown in two liters LB medium containing 100 μ g/ml ampicillin and 20 μ g/ml chloramphenicol to 0.6 OD₆₀₀ and induced with 0.2 mM IPTG at 30°C for 2-3 hours. The bacterial cells were then washed and resuspended in binding buffer (300 mM urea, 5mM imidazole, 500 mM NaCl, 20 mM Tris-HCl pH 7.9) and sonicated for three times for 30 sec at 1 min intervals in ice. The cell debris was then spun down and the cell

lysate containing the recombinant homo- or heterodimer proteins was subjected to a two-column affinity purification procedure. The dimer protein was initially purified on a nickel charged column for His tagged protein binding, according to the manufacturer except 300 mM urea and 0.5% Triton X-100 was included in the binding buffer. The bound His-tagged proteins were eluted in 1.5 ml elution buffer (500 mM imidazole, 500mM NaCl, 20 mM Tris-HCl pH 7.9) from the nickel column. The eluted proteins were then slowly added into 15 ml Flag IP binding buffer (150 mM KCl, 20 mM Tris HCl pH 7.9, 0.2 mM EDTA, 10% glycerol, 0.01% NP40) and incubated with 200 μ l prewashed Anti-Flag M2 agarose beads at 4°C for 3 hours with mild shaking to allow the Flag tagged protein to bind to the beads. The bound proteins were then washed with wash buffer and eluted as described for Flag DcpS proteins above. The eluted proteins are His and Flag dual tagged homo- or heterodimers since they underwent both His and Flag column procedures. They were subsequently concentrated by Centricon centrifugal filter columns (Amicon).

The purified recombinant proteins used in Chapter I resolved in SDS-PAGE were stained with Coomassie Blue. The proteins used in Chapter II resolved in SDS-PAGE were stained with Sypro Ruby (Invitrogen).

Quantitation of the concentrations of recombinant proteins

The concentrations of recombinant proteins used in Chapter I were determined by comparing the intensity of recombinant protein bands with the BSA protein bands with known concentrations (New England Biolab) on a SDS-PAGE gel. The concentrations of homo- and heterodimer DcpS proteins used in Chapter II were determined based on

the measurement of their absorbance using spectrophotometry (Gill and von Hippel, 1989). The concentration of Flag-DcpS shown in Fig 11A was calculated based on the equation below:

$$A_{280} = \epsilon C \quad (\text{Eq 1})$$

A₂₈₀ is the absorbance of protein solution under UV light with wavelength 280 nm, ϵ is the extinction coefficient of the protein under A₂₈₀, and C represents the concentration of protein solution. 10 μ l protein solution was added into 990 μ l 6M Guanidine HCl solution and left at room temperature for 20 minutes for complete denaturation of protein. Denatured protein was subsequently transferred to a quartz cuvette with a standard pathlength 10 mm, followed by A₂₈₀ measurement by using a spectrophotometer (Bechman DU 640 spectrophotometer). The extinction coefficient ϵ was computed from the amino acid sequence of protein by using a ExPASy ProtParam webtool (Gasteiger et al., 2005) provided on the website <http://ca.expasy.org/tools/protparam.html>. The protein concentration was calculated from Equation 1.

The homo- and heterodimer DcpS protein solutions shown in Fig 13B and Fig 14A contain a co-purified protein with an approximate size 50 kD. This co-purified protein was analyzed by mass spectrometry and its identity was confirmed as GroEL, a bacterial chaperonin that functions in assisting folding of nascent polypeptide (Sigler et al., 1998).

The measured A280 represents a combined absorbance from both the DcpS protein and the co-purified GroEL. Therefore, both DcpS and GroEL were taken into account in the calculation of DcpS concentrations using the equation below:

$$A280_{\text{total}} = \epsilon_S C_S + \epsilon_G C_G \quad (\text{Eq 2})$$

$A280_{\text{total}}$ is the absorbance of the protein solution containing both the DcpS dimer and GroEL. ϵ_S and C_S represent the extinction coefficient and concentration of DcpS, while ϵ_G and C_G represent the extinction coefficient and concentration of GroEL. The concentration ratio of DcpS dimer and GroEL, C_S/C_G , was then obtained by comparing the intensity of bands using the software ImageQuant 5. The obtained ratio was integrated into Equation 2 and the concentration of the DcpS dimer, C_S , was calculated.

Generation of labeled RNA and cap structures

Unlabeled, uncapped RNA corresponding to the pcDNA3 polylinker spanning from the SP6 promoter to the T7 promoter (pcP) with 16 guanines at the 3' end was transcribed by SP6 RNA polymerase from a PCR-generated template using the primers 5'-CGATTAGGTGACACTATAG-3' and 5'-CCCCCCCCC CCCCCCGTAATACGACTCACTATAGGG-3'. Cap labeled RNA was generated with the vaccinia virus capping enzyme utilizing α -³²P GTP and S-adenosyl-methionine (SAM) to label the first phosphate within the cap relative to the methylated guanine (m⁷G*pppG-) and the RNA gel-purified as described (Wang et al., 1999). Labeled cap structure without the RNA body was generated by treating the cap-labeled RNA with 1

unit Nuclease P1 (Roche) for 1.5 h at 37°C to hydrolyze the RNA body leaving the intact cap structure as described (Wang and Kiledjian, 2001). Uniformly labeled uncapped RNA was generated with SP6 RNA polymerase using α -³²P UTP according to the manufacturer (Promega).

***In vitro* decapping assays**

Decapping assays shown in Fig 1B, Fig 2B and 2D, Fig 3, Fig 6, Fig 7A, Fig 8, and Fig 9B were carried out with the indicated substrate and recombinant proteins in IVDA buffer (10 mM Tris pH 7.5, 100 mM KOAc, 2 mM MgOAc, 2 mM DTT, 10 mM creatine phosphate, 0.1 mM spermine) for 15 min at 37°C. For the decapping assays shown in Figure 9B, the labeled cap structure was pre-incubated with the His-eIF4E protein for 10 min, followed by the addition of DcpS and an additional 10-min incubation at 37°C. Decapping reactions were terminated by extracting once with phenol:chloroform (1:1). An aliquot of each reaction was spotted onto PEI-cellulose TLC plates (Sigma) that were prerun in H₂O and air dried, and the products were developed with 0.45 M (NH₄)₂SO₄ at room temperature. The TLC plates were air dried and exposed to Kodak BioMax film or Phosphoroimager for quantitation. All quantitations were conducted with a Molecular Dynamics Phosphoroimager (Storm860) using ImageQuant 5 software.

Quench-flow decapping assay and data analysis

Decapping assay in Fig 13C was carried out with the indicated monomer concentrations of proteins and 200 nM unlabeled cap structure (New England Biolab)

spiked with hot cap structure in decapping buffer (10 mM Tris pH 7.5, 100 mM KOAc, 2 mM MgOAc, 2 mM DTT) for 30 sec at room temperature. Decapping reactions were terminated by 1.7N formic acid. An aliquot of each reaction was spotted onto PEI-cellulose TLC plates (Sigma) that were prerun in H₂O and air dried, and the products were developed with 0.45 M (NH₄)₂SO₄ at room temperature. The TLC plates were air dried and exposed to PhosphorImager for quantitation. All quantitations were conducted with a Molecular Dynamics Phosphorimager (Storm860) using ImageQuant 5 software.

The decapping assays in the rest of the Figures in Chapter II were carried out on a rapid quench-flow instrument (KinTek Corp., Austin, TX) at 25°C. DcpS protein in decapping buffer was loaded into one syringe of the quench-flow apparatus. The cold cap substrate spiked with ³²P-labeled cap substrate was loaded in a second syringe. The reactions were initiated by rapidly mixing equal volumes of solutions from both syringes. After the mixtures of enzyme and substrate were incubated for indicated amounts of time, the reactions were quenched by 2.3N formic acid added from a third syringe. An aliquot of each reaction was spotted onto TLC plates, developed, dried and exposed to PhosphorImager and quantitated as stated in previous paragraph. The kinetics in Fig 11C, Fig12B, Fig 13F were fit to Equation 3 using SigmaPlot 10.0 software (Systat Software, Inc.)

$$Y=Y_0+A(1-\exp(-KT)) \quad (\text{Eq 3})$$

Y is the fraction of generated product m⁷Gp over total substrate; Y₀ is the interception representing the fraction of background m⁷Gp hydrolyzed from the input

substrate in the absence of enzyme; A is the maximal decapping rate. Decapping rate is defined as the fraction of substrate converted to products by the enzyme. K is the rate constant, and T represents the reaction time.

The concentrations of product generated by enzymatic hydrolysis were plotted against enzyme concentrations in Fig 11E. The data were fit to a hyperbola with Equation 4.

$$A = Y_0 + A_0[E]/(K_d + [E]) \quad (\text{Eq 4})$$

A is the concentration of product generated by enzymatic hydrolysis. Y_0 is the interception, and A_0 is the highest amount of substrate converted to product. E represents the enzyme concentration, and K_d is the dissociation constant.

The kinetics of DcpS^{WT/HIT} under single turnover conditions in Fig 14E was fit to Equation 5.

$$Y = Y_0 + A(1 - \exp(-KT)) + B(1 - \exp(-CT)) \quad (\text{Eq 5})$$

Y , Y_0 , A , and K represent the same parameters as that of Equation 3.

Electrophoretic mobility shift assay (EMSA)

EMSAs were carried out by incubating proteins with labeled cap structure or capped RNA in RNA binding buffer (RBB; 75 mM KCl, 10 mM Tris HCl, pH7.5, 1.5 mM MgCl₂, and 0.5 mM DTT) containing 4μg heparin and 40 units RNase inhibitor

(Promega) per reaction on ice for 15 min. The resulting protein–cap or protein–RNA complexes were resolved on a 5.6% native polyacrylamide gel. The gel was dried and exposed to Kodak BioMax film.

Filter binding assays

Filter binding assays were carried out with an increasing concentration of DcpS^{mH} incubated with ³²P-labeled cap structure or ³²P cap labeled RNA similar to that described for the EMSAs above. Following the binding reaction, the samples were filtered through 0.2 μM nitrocellulose filters (Millipore) prewashed with RBB to retain the protein–cap or protein–RNA complexes. The filters were subsequently washed twice with 2 mL ice-cold RBB to remove the nonspecifically bound labeled cap or capped RNA. The filters were air dried, and the amount of bound complex was determined by a liquid scintillation counter. The values were corrected by subtracting the background counts obtained from negative control reactions containing only the ³²P-labeled substrate. The values for the bound cap-DcpS^{mH} complex were plotted relative to DcpS^{mH} concentration, and apparent dissociation constants were determined as the concentration of protein at which 50% of cap was bound (Wilson and Brewer, 1999). The average of three independent experiments is reported.

UV-crosslinking

His-eIF4E was pre-incubated with ³²P-labeled cap structure in IVDA buffer on ice for 10 min, followed by addition of His-DcpS^{mH} for an additional 10-min incubation on ice. The samples were then covalently crosslinked by exposure to a 15 W germicidal UV

lamp for 10 min. Following crosslinking the samples were resolved by 12.5% SDS-PAGE and visualized by autoradiography.

Cell culture and transfections

Human HEK293T cell lines were grown in DMEM (Invitrogen) supplemented with 10% fetal bovine serum, penicillin-streptomycin, and fungizone under 5% CO₂ at 37°C. Cells were grown in the growth media containing 100 µg/ml G418. All transfections were carried out using Lipofectamine 2000 (Invitrogen) according to the manufacturer instruction, except the transfection mixtures were added to the cells prewashed with PBS and incubated at room temperature for 15 minutes, followed by addition of the normal growth media. The HEK293T cell line stable transfectants expressing a shRNA targeting DcpS or expressing empty pSHAG1-puro vector were generated by transfecting pSHAG1-puro-DcpS1 or pSHAG1-puro empty vector, respectively. After 48 hours of transfection, 500µg/ml G418 and 3µg/ml puromycin were included in the cell culture for selection. Clonal cell lines were isolated by plating the population into a 96 well plate such that only one colony grows in a single well under puromycin selection. The colony with the most efficient DcpS protein level knockdown was expanded and used.

Dual Luciferase Assay

293T DcpS knockdown cell line expressing the shRNA against DcpS, or 293T control cell line expressing the shRNA vector construct were transfected with the pcDNA3.1-IRES-RF renilla and luciferase dicistronic reporter plasmid with either

pcDNA3-Flag-DcpS or pcDNA3-Flag vector co-transfected. Cells were harvested 36 hours posttransfection and washed with PBS and the cells were lysed in the lysis buffer provided by the Dual Luciferase Kit (Promega). Cells were then frozen at -80°C for 10 minutes followed by thawing at 37°C. The cell debris was then spun down and the cleared cell lysate was subsequently used in a dual luciferase assay according to the instruction provided by the manufacturer (Promega). Luciferase activities were measured using the GLOMAX 20/20 (Promega, Madison) luminometer.

Western analysis

Protein samples were resolved on 12.5% sodium dodecyl sulfate (SDS) gels and transferred to nitrocellulose membrane (Bio-Rad) using a semi-dry transfer apparatus. The endogenous DcpS and exogenous Flag DcpS were probed by a rabbit polyclonal DcpS antiserum, and the endogenous Dcp2 was probed by an affinity purified rabbit polyclonal anti-Dcp2 antibody. The affinity purification of the Dcp2 polyclonal antibody was carried out by using a Hitrap column (Pharmacia) conjugated with His-Dcp2 recombinant protein. The blots were then probed with goat anti-rabbit secondary antibodies conjugated with peroxidase (Jackwon Immuno Research), and visualized by Amersham ECL Western blotting Detection Reagents (GE Healthcare).

Chapter I: Functional Analysis of mRNA Scavenger Decapping Enzymes

Summary

Eukaryotic cells primarily utilize exoribonucleases and decapping enzymes to degrade their mRNAs. Two major decapping enzymes have been identified. The hDcp2 protein catalyzes hydrolysis of the 5' cap linked to the RNA polynucleotide, whereas the scavenger decapping enzyme, DcpS, functions on a cap structure lacking the RNA body. DcpS is a member of the histidine triad (HIT) family of hydrolases and catalyzes the hydrolysis of m⁷GpppN. HIT proteins are homodimeric and contain a conserved 100-amino-acid HIT fold domain in each protomer, with an independent active site that is sufficient to bind and hydrolyze the substrate. We carried out a biochemical characterization of the DcpS enzyme and demonstrate that unlike other HIT proteins, DcpS requires both the core HIT fold at the carboxyl-terminus and sequences at its amino-terminus for cap binding and hydrolysis. Interestingly, DcpS can efficiently compete for and hydrolyze the cap structure *in vitro* in the presence of excess eIF4E, a cytoplasmic cap binding protein and also an essential translation initiation factor. This *in vitro* finding implies that DcpS could function to scavenge the accumulated 3' to 5' decay product, the cap structure, which would otherwise sequester eIF4E and in turn interfere with the eIF4E mediated translational events. Consistent with this *in vitro* finding, the knockdown of DcpS in cells reduced the relative cap-dependent translation of a reporter

transcript by 40%, supporting the hypothesis that DcpS functions to control the global concentration of accumulated 3'-5' decay product, the cap structure.

Introduction

Turnover of mRNA is a regulated process that influences gene expression. The major mRNA degradation pathways in eukaryotes involve exonucleolytic decay initiated by deadenylation that is followed by either a continuation of 3' to 5' decay and decapping, or decapping and subsequent 5' to 3' decay (Parker and Song, 2004). The scavenger decapping enzyme, DcpS in human and Dcs1p in *Saccharomyces cerevisiae*, hydrolyzes the resulting cap structure following decay by the 3' to 5' decay pathway (Liu et al., 2002). Hydrolysis of capped mRNA primarily involves the Dcp2 protein in mammalian cells (Lykke-Andersen, 2002; van Dijk et al., 2002; Wang et al., 2002) and the Dcp1p/Dcp2p enzyme complex in yeast cells (Steiger et al., 2003).

Each decapping enzyme possesses a distinct hydrolase motif that is essential for decapping. The Dcp2 protein contains a **Nucleotide Diphosphate** linked to an **X** moiety (Nudix) hydrolase motif (Dunckley and Parker, 1999; van Dijk et al., 2002; Wang et al., 2002), whereas DcpS contains a histidine triad (HIT) hydrolase motif required for its decapping activity (Liu et al., 2002). The Nudix motif was originally identified in a class of hydrolase proteins and shown to be critical for pyrophosphatase activity (Koonin, 1993; Mejean et al., 1994). A Nudix motif consisting of a 23-amino-acid consensus sequence within a larger Nudix fold (Bessman et al., 1996) was shown to be critical for Dcp2 decapping activity (Dunckley and Parker, 1999; van Dijk et al., 2002; Wang et al., 2002). Interestingly, the human Dcp2 (hDcp2) protein is an RNA-binding protein that only hydrolyzes the cap structure that is linked to the RNA polynucleotide, requiring both the

RNA-binding property and the Nudix motif to recognize and hydrolyze the capped RNA substrate (Piccirillo et al., 2003). The prerequisite for RNA binding precludes hDcp2 from functioning on cap structure and restricts its activity to capped RNA.

The HIT motif present in the DcpS decapping enzyme is characterized by three histidine residues separated by hydrophobic amino acids (Seraphin, 1992). This motif is located within a larger 100-amino-acid HIT fold (Brenner, 2002). Structural analysis of several HIT proteins revealed that these proteins exist as homodimers through formation of a 10-stranded antiparallel β -sheet. Each protomer possesses an active site and nucleotide binding pocket containing the catalytic HIT motif, in which the three histidine residues coordinate the pyrophosphate bond of the substrate (Brenner et al., 1997; Lima et al., 1997; Pace et al., 1998). Unlike hDcp2, DcpS does not function on long capped RNA, instead it functions on capped oligonucleotides shorter than 10 nucleotides (Liu et al., 2002). This property led to the initial hypothesis that DcpS is a scavenger decapping enzyme that hydrolyzes resulting cap dinucleotide following mRNA decay (Nuss and Furuichi, 1977; Nuss et al., 1975; Wang and Kiledjian, 2001). This hypothesis was subsequently confirmed with a mammalian *in vitro* RNA decay system where decapping products were detected following prior deadenylation and exosome-mediated decay of the reporter RNA (Rodgers et al., 2002). Furthermore, cap structure was shown to accumulate in the *dcs1 Δ* *S. cerevisiae* strain (Liu et al., 2002). DcpS activity can be copurified with the exosome 3' to 5' exoribonuclease complex, implying a link between decay of the mRNA body and the final decapping step (Wang and Kiledjian, 2001). Interestingly, in *S. cerevisiae* there are two DcpS homologs, Dcs1p and Dcs2p. Although they are highly conserved with each other and both of them share an equal level of

identity with DcpS, only Dcs1p is capable of hydrolyzing the cap structure, whereas Dcs2p does not have a detectable decapping activity.

In this chapter we demonstrate that the sequences in the N terminus, which are outside of the HIT fold in the C terminus, are also critical for the decapping activity of DcpS. We also demonstrate that DcpS specifically act on cap structure, not capped RNA, and this specificity is due the higher affinity between DcpS and the cap structure. Furthermore, we show that DcpS can efficiently replace eIF4E for access to the cap structure *in vitro*. Lastly, we demonstrate that DcpS is involved in maintaining the cap-dependent translation, consistent with the hypothesis that the high affinity between DcpS and cap structure prevents the sequestration of eIF4E by the cap structure.

Results

Regions outside the HIT hydrolase fold are critical for decapping

The *S. cerevisiae* Dcs1p and Dcs2p proteins share 65% identity and 90% similarity, with the highest degree of identity observed within the C-terminal HIT hydrolase domain of the two proteins. Despite this high degree of identity and the fact that the HIT fold was shown in previously characterized HIT proteins to contain both nucleotide-binding and hydrolase activities (Brenner, 2002; Brenner et al., 1999), only Dcs1p has detectable cap hydrolysis activity (Liu et al., 2002). To determine whether the Dcs2p HIT motif is competent to hydrolyze a methylated cap structure and whether regions of the protein outside the HIT motif are required for cap hydrolysis, the N-

terminal and C-terminal segments of the two proteins were swapped. A schematic of the two proteins is shown in Figure 1A, along with the domain-swapped proteins. One fusion protein consisted of the N-terminal half of Dcs1p linked to the C-terminal half of Dcs2p (Dcs1/2p); the second consisted of the N-terminal half of Dcs2p fused to the C-terminal half of Dcs1p (Dcs2/1p). The capacity of each recombinant histidine-tagged protein to hydrolyze cap structure labeled with ^{32}P at the first phosphate relative to the methylated guanosine (m7G*pppG) was tested, and the products were resolved by polyethylenimine (PEI) cellulose thin-layer chromatography (TLC). Consistent with our previous findings (Liu et al., 2002), Dcs1p was capable of hydrolyzing the cap structure whereas Dcs2p was not (Fig 1B, lanes 2,3). However, a chimeric protein containing the N-terminus of Dcs1p and the HIT motif containing C-terminal segment of Dcs2p was capable of catalyzing cap hydrolysis, whereas the converse protein containing the N-terminus of Dcs2p linked to the C-terminus of Dcs1p was not functional (Fig 1B, cf. lanes 4 and 5). These data demonstrate that N-terminal domains of Dcs1 proteins mediate the potential of their decapping.

The amino terminus of Dcs1p and DcpS is critical for decapping

To further refine the region within the N-terminus of Dcs1p that was essential for decapping, a series of N-terminal truncation proteins were generated (Fig 2A). Removal of the N-terminal 40 amino acids of Dcs1p (Dcs1p Δ^{N40}) had a deleterious consequence on decapping where no decapping was detected (Fig 2B, lane 3). Conversely, removal of 65 residues at the C-terminus of the protein that still retained the HIT hydrolase fold was still capable of decapping, albeit with lower efficiency (Fig 2B, lane 5). These data further demonstrate a requirement for the N-terminus of Dcs1p in decapping and implicate the

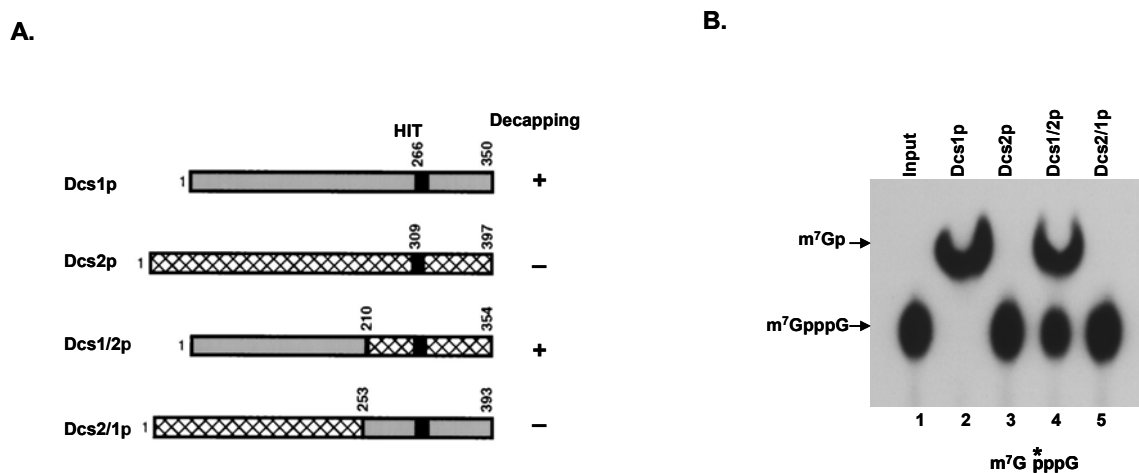


Figure 1. Regions outside the HIT hydrolase fold are critical for scavenger decapping activity.

(A) Dcs1p and Dcs2p are represented schematically in gray and hatch bars, respectively. The chimeric Dcs1/2p and Dcs2/1p proteins containing the swapping portions are indicated. The black box denotes the 6-amino-acid HIT motif. A summary of decapping activity for each protein is shown on the right, where "+" and "-" represent the ability or inability to catalyze cap structure hydrolysis, respectively.

(B) The presence of Dcs1p N-terminus corresponds to decapping. A decapping assay using 0.5 pmoles of each histidine-tagged recombinant protein was carried out at 37°C for 15 min using ^{32}P -labeled cap analog where the first phosphate relative to the methylated guanosine is labeled ($\text{m}^7\text{G}^*\text{pppG}$) as substrate. Reaction products were resolved on PEI TLC plates. Migration of the unhydrolyzed cap substrate and m^7Gp product were shown at the left. A schematic of the ^{32}P -labeled cap analog substrate is shown at the *bottom*, with the labeled phosphate denoted by *.

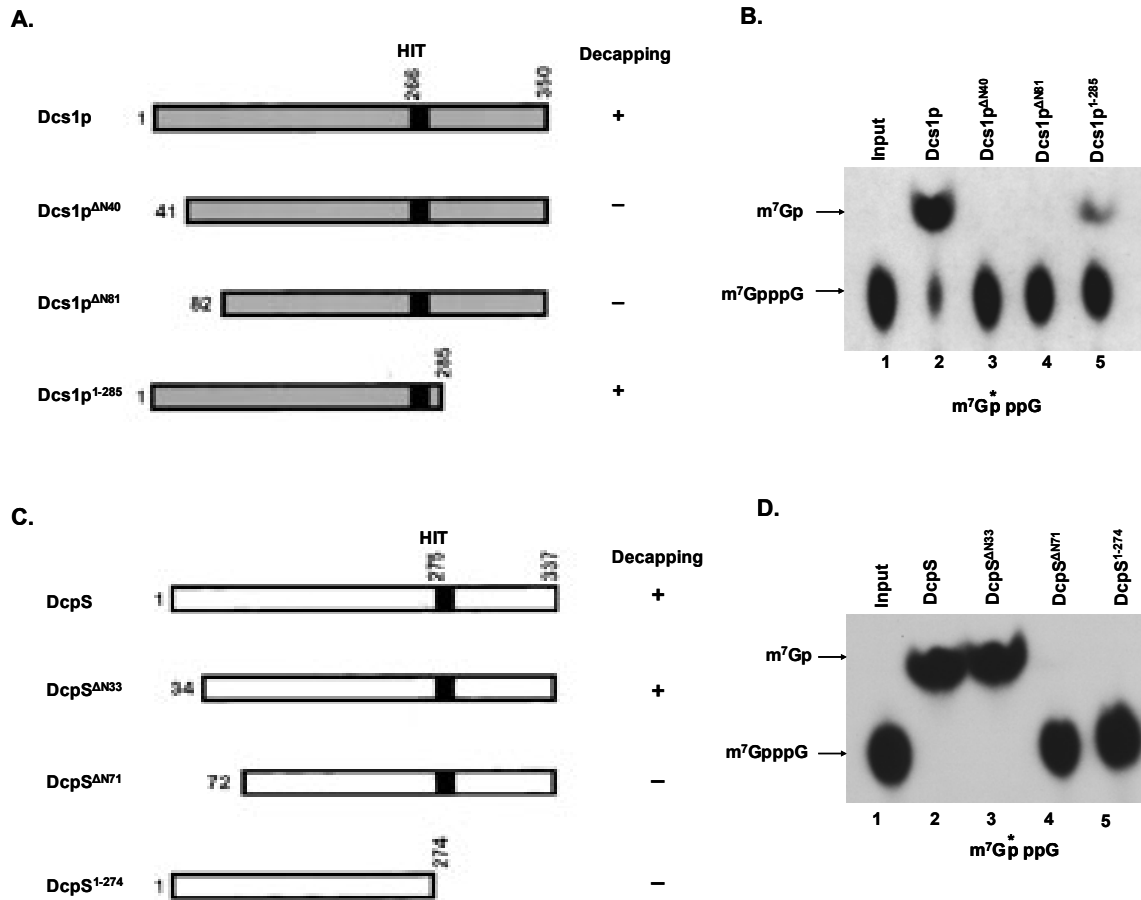


Figure 2. The N-termini of Dcs1p and DcpS are critical for decapping.

(A) A schematic of Dcs1p and its truncated derivatives is shown.

(B) Decapping activity obtained from each protein represented in panel A.

(C) A schematic of the human DcpS protein and its truncated derivatives is shown.

(D) The corresponding decapping activity for each protein is shown. Labeling and assay conditions are as described in the Figure 1 legend.

first 40 amino acids as an essential component of the Dcs1p decapping activity. The requirement of the N-terminus in decapping was also tested for the human DcpS protein. Amino acid sequence alignment of DcpS with Dcs1p indicates that DcpS contains a 33-amino-acid extension at the N-terminus (data not shown). We first determined whether this extended region is required for DcpS function. A schematic of the recombinant proteins used for this set of experiments is shown in Figure 2C. Removal of the N-terminal 33 amino acids of DcpS (DcpS^{ΔN33}) did not have an adverse affect on decapping (Fig 2D, lane 3). However removal of sequences up to amino acid 72 (DcpS^{ΔN71} which is analogous to the Dcs1p^{ΔN40}) completely abrogated decapping activity of the truncated protein (Fig 2D, lane 4), demonstrating the significance of the N-terminal domain for the human DcpS decapping protein as well. As expected, a C-terminal truncation removing the HIT motif also resulted in an enzymatically inactive protein (Fig 2D, lane 5). Together, these data demonstrate that both the HIT motif and sequences at the N-terminus of DcpS and Dcs1p are required for the decapping activity of these proteins.

DcpS is a modular protein whose activity can be reconstituted in *trans*

The above data suggest that both the N-terminus and the C-terminus of DcpS are essential for decapping. In a related study, we obtained the crystal structure of DcpS, which revealed that the protein consisted of an N-terminal domain and a C-terminal domain separated by a hinge region (Gu et al., 2004)(also see Discussion). To test whether DcpS can consist of two modular domains that can form a decapping enzyme,

two halves of the human DcpS protein separated at the hinge region were generated and tested for decapping. Consistent with the above data, a protein containing the first 147 amino acids of DcpS, corresponding to the N-terminal domain lacking the HIT motif, was unable to hydrolyze the ^{32}P -labeled cap structure substrate (Fig 3, lane 3). Similarly, the C-terminal 189 amino acids of the protein containing the complete HIT hydrolase fold were also incompetent to hydrolyze the labeled cap structure (Fig 3, lane 4). Interestingly, reconstitution of the two halves of the protein in *trans* generated a functional decapping activity (Fig 3, lane 5). We conclude that DcpS contains at least two distinct modular domains that together generate a functional decapping enzyme.

The DcpS N-terminal domain facilitates cap binding

The inability of N-terminal truncated DcpS protein to hydrolyze the cap could be due to either the inability to bind the cap substrate, or the inability to hydrolyze the cap once it binds the substrate. To distinguish between these two possibilities, we used an electrophoretic mobility shift assay (EMSA) with DcpS and ^{32}P -labeled cap structure. The DcpS N-terminal truncation proteins, DcpS $^{\Delta\text{N}33}$, which was competent to hydrolyze the cap structure, and DcpS $^{\Delta\text{N}71}$, which was unable to hydrolyze the cap structure, were tested for their ability to bind the cap. A mutation substituting an asparagine for the active site histidine (DcpS $^{\text{mH}}$) at amino acid 277 within the HIT motif was introduced into these constructs to render the resulting proteins inactive for hydrolysis activity (Liu et al., 2002) and enable detection of cap binding. Full-length DcpS $^{\text{mH}}$ and DcpS $^{\text{mH}\Delta\text{N}33}$, both of which would be expected to contain decapping activity without the histidine 277

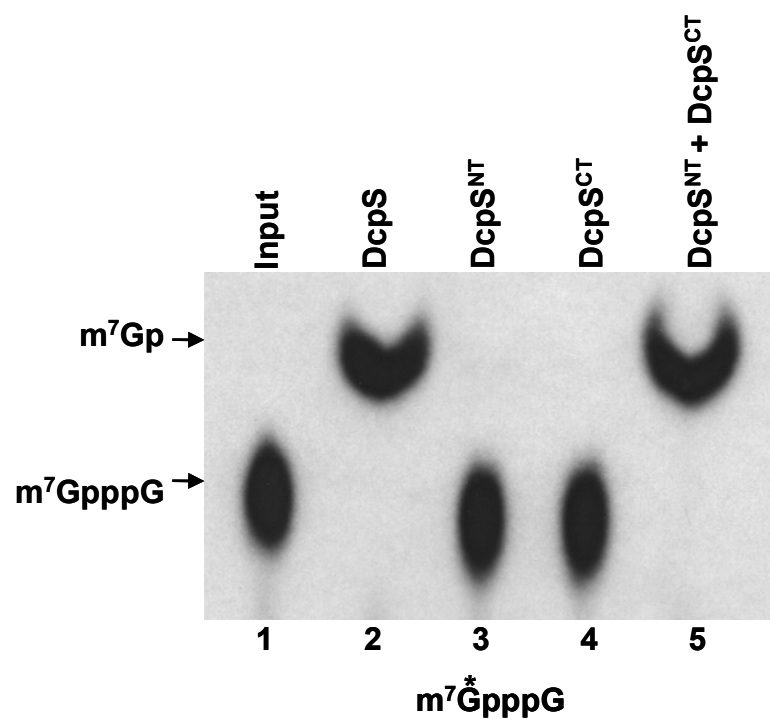


Figure 3. DcpS is a modular protein.

Decapping assay using the N-terminal 147 amino acids of DcpS (DcpS^{NT}) or the C-terminal 189 amino acids spanning residues 149–337 (DcpS^{CT}) individually or both simultaneously in *trans* (lane 5) is shown. Five pmoles of DcpS was used in lane 2; 1 μg of each truncated protein was used in lanes 3–5. Labeling and assay conditions are as described in the Figure 1 legend.

substitution (Fig 2), were capable of binding the cap structure as demonstrated by the slower migration on the ^{32}P -labeled cap structure substrate (Fig 4, lanes 2,3). Binding to cap structure was not detected with the DcpS^{mH Δ N71} protein (Fig 4, lane 4) nor with the individual N-terminal (Fig 4, lane 5) and C-terminal (Fig 4, lane 6) domains under these assay conditions. These results demonstrate that an intact N-terminal domain is necessary but not sufficient for binding of DcpS to the cap structure.

Overview of DcpS structure

The co-crystallized structure of DcpS HIT mutant and cap substrates were resolved by Gu et al and the amino acids 38-337 for protomer A and 40-337 for protomer B were modeled. The DcpS is a dimeric protein which possesses two distinct domains, an N terminal domain consisting of amino acids 38-145 or 40-145, and a C terminal domain consisting of amino acids 146-337, linked by a hinge region centered near Arg 145 (Fig 5A), with each protomer bound to a distinct cap substrate. The N-terminal domain is made up of a region containing three non-swapped anti-parallel β -strands (β 1-3) contributed by each protomer, followed by a region containing swapped α -helix (α A) and two anti-parallel β -strands (β 4-5) by the other protomer, and a subsequent region of another non-swapped β -strand (β 6) and α -helix (α B) contributed by each protomer (Fig 5B). Each C-terminal DcpS protomer is formed by five α -helices and eight β -strands, six of which form a continuous anti-parallel β -sheet (Fig 5C). The catalytic HIT motif is located on β 12.

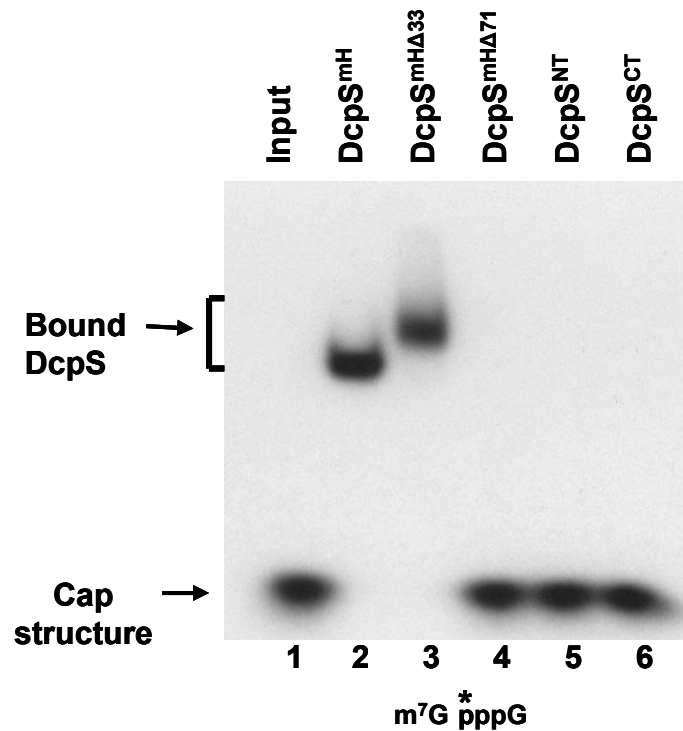


Figure 4. DcpS N-terminus facilitates cap binding.

An EMSA was used to test the ability of DcpS and its truncated derivatives to bind ^{32}P -labeled cap analog. Recombinant DcpS or the truncated derivatives removing N-terminal residues of 33 and 71 amino acids and containing the HIT motif mutant H277N (DcpS^{mH}, DcpS^{mH Δ 33}, and DcpS^{mH Δ 71} respectively) were used. Proteins with a mutant HIT motif were used to uncouple cap binding and hydrolysis to enable detection of binding. DcpS^{NT} represents the DcpS protein from amino acids 1–147, and DcpS^{CT} contains amino acids 149–337. The cap structure substrate and bound DcpS-cap structure complex are indicated by the arrows on the left, and a schematic of the substrate is shown at the bottom, where * denotes the ^{32}P .

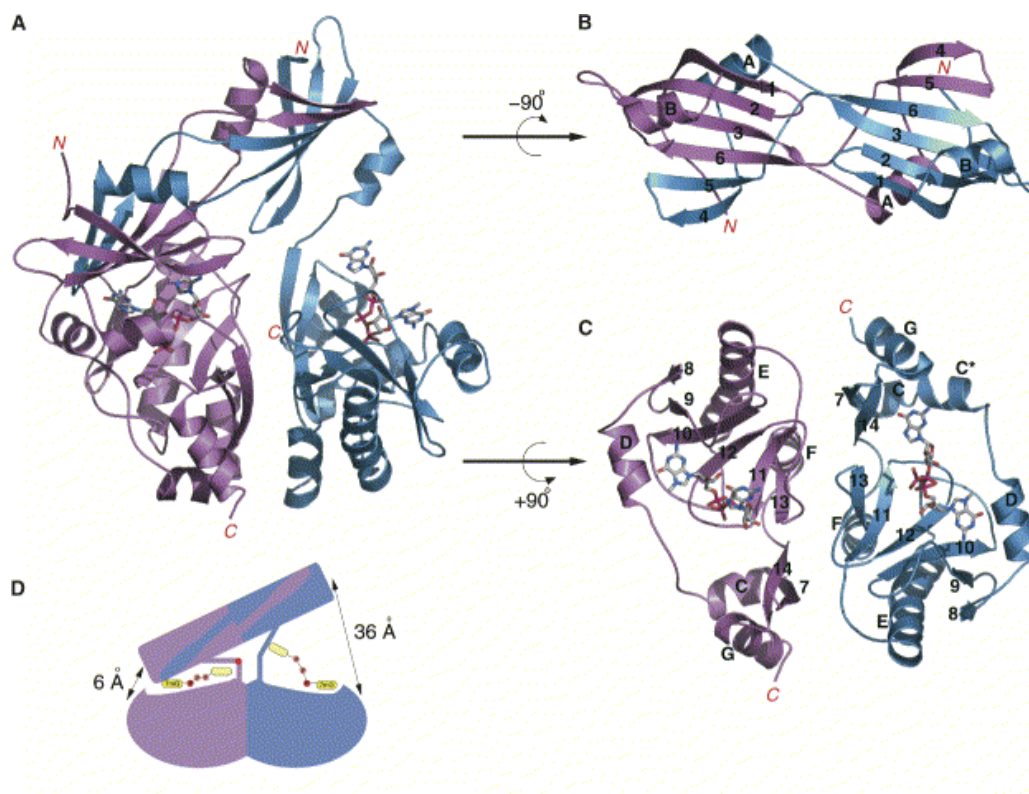


Figure 5. Co-crystal structure of DcpS and cap substrates revealed a dimeric structure with distinct N and C termini in an asymmetric open/closed configuration.

(A) Ribbon diagram of the DcpS co-crystal structure with m^7GpppG with two protomers colored pink and blue, respectively. N and C denote the termini of both protomers.

(B) Orthogonal view of the N-terminal domain-swapped dimer (residues 38(40)-145).

(C) Orthogonal view of the C-terminal domain dimer (residues 146-336(337)), with helices denoted by letters and strands denoted by numbers.

(D) Cartoon of the DcpS dimer in a simultaneous open/closed configuration.

The co-crystal structure of DcpS dimer and the substrates revealed an asymmetric, simultaneous open (blue) and closed (pink) conformations on opposite sides of the dimer (Fig 5A, 5D). The rigidity of the dimeric N- and C-terminal domains led to the proposal that the N terminal domain flips back and forth to generate a simultaneous open/closed configuration of the dimer (Fig 5D). In an open conformation, there are few contacts between the N and C termini, with the cap substrate bound to the C terminal domain, close to the HIT catalytic center (Fig 5A, 5D). In a closed conformation, a conformational change brings the N terminus to the C terminus, creating a substrate binding pocket, with the cap substrate directly interacting with numerous amino acid residues on both N and C terminal domains (Fig 5A, 5D). Consistent with these findings, another group recently resolved the co-crystal structure of wild-type DcpS and m⁷GDP, which yields a similar asymmetric configuration (Chen et al., 2005).

Important residues for DcpS binding and hydrolysis

By inspection on the resolved DcpS-cap substrate co-crystal structure, numerous amino acid residues were observed to interact with the cap substrate. These amino acid residues were classified into four groups. They are the amino acids that interact with (1) the cap phosphates, (2) the methyl guanosine base (3) the second cap base. Other than the above residues that contact the cap substrate, the fourth group of amino acids which are involved in conformational switch were also classified (Fig 6). To determine the relative importance of these residues regarding cap binding and hydrolysis, they were

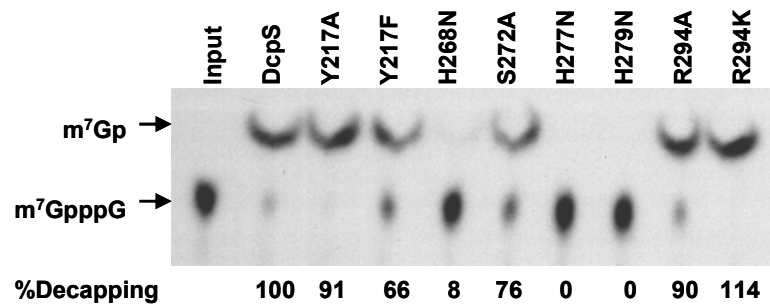
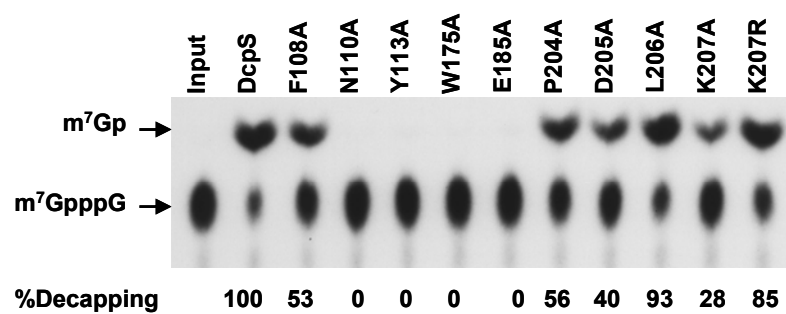
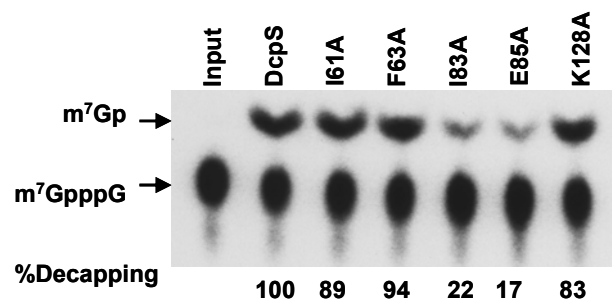
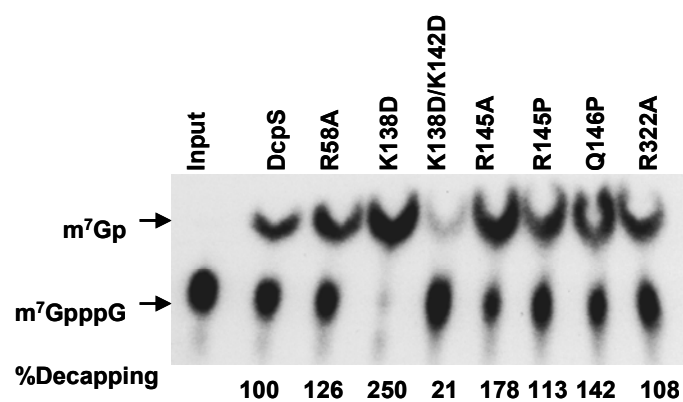
A.**B.****C.****D.****Fig 6**

Figure 6. Important residues for DcpS decapping.

The important amino acids that contact the substrate or involved in conformational switch were classified into four groups and each individual mutant was tested for decapping activities.

(A) Amino acids that interact with cap phosphates.

(B) Amino acids that interact the methyl guanosine base.

(C) Amino acids that interact with the second cap base.

(D) Amino acids that are associated with the conformational switch between the open and closed conformation.

substituted by mutagenesis and individual mutant proteins were tested for decapping activity (Fig 6). In residues classified into group 1, His277 and His279 located in the HIT motif and are conserved among DcpS family members. H277N and H279N mutants were both inactive in decapping assays (Fig 6A). His279 makes direct contacts to the cap α and β phosphate. In the cases of other HIT protein family members, the central His277 is the nucleophile that attacks the α phosphate (Lima et al., 1997). The α phosphate in a cap structure is defined as the phosphate that is most proximal to the methylated guanosine. His268 is proximal to the α phosphate and H268N inactivated the decapping activity (Fig 6A). His268 is not a conserved histidine in other HIT proteins, therefore the decapping inactivation in H268N indicates a unique role for His268 in DcpS activity.

The C-terminal domain makes similar contacts to the m^7G base, ribose, and α - phosphate in m^7GpppG structure in either open or closed states (Gu et al., 2004). Mutation of Trp175 or Glu185 abolished decapping activities. Mutations of Pro204 (contacts m^7G base) or Asp205 (contacts m^7G ribose) also caused the reduction of decapping activity by 50% compared to that of wild-type (Fig6B). Also K207R resulted in a protein with 85% activity, and K207A resulted in protein with less than 30% activity.

Several additional contacts between DcpS and the m^7G base in the closed configuration are contributed from the N-terminal domain-swapped dimer (Gu et al., 2004). These interactions include Van der Waals (VDW) interactions between m^7G and residues Phe108 as well as Tyr 113, and hydrogen bond interactions between Asn110 and Glu185 (Gu et al., 2004). N110A or Y113A completely abolished decapping activity (Fig 6B). In addition, residues from the N-terminal domain make VDW contacts to the

second cap base. I61A, F63A, and K128A caused mild reduction of decapping activity, while I83A and E85A caused more significant reduction of decapping activity (Fig 6C).

The residues between Tyr143 and Arg149 form a hinge that links the N and C termini (Gu et al., 2004). This hinge region is extended in an open state which enables interactions of several residues to the second cap base, and even to the N-terminal domain (Gu et al., 2004)(Fig 5A). In the closed state, the hinge bends and brings Arg149 into contact to Asp147, and Leu144, Arg145 into contact with Leu53 and Val52, respectively, as well as Tyr143 close of the second cap base (Gu et al., 2004). Other than these residues involved in the hinge, there are additional residues that are proposed to stabilize the open or closed conformations. To determine their relative importance on activity, several residues involved in hinge movement and stabilization of the open or closed configurations were mutated and tested for activities. Many mutants displayed activities higher than the wild type enzyme: R58A, K138D, R145A, R145P, and Q146P exhibited 125%, 250%, 178%, 113%, and 142% activity compared to the wild type (Fig 6D). These results suggest that the destabilization of the closed confirmation does not prevent closure of the N terminus, but rather facilitate the product release thus to enhance the decapping activities (Gu et al., 2004).

DcpS specifically hydrolyzes cap structure relative to capped RNA

We previously reported that DcpS functioned on capped RNAs 10 nt or smaller (Liu et al., 2002). However, Nhm1p, the *Schizosaccharomyces pombe* homolog of DcpS,

was recently reported as a decapping enzyme capable of catalyzing hydrolysis of capped RNA (Salehi et al., 2002). To more precisely address the specificity of DcpS for cap structure versus capped RNA, a titration of DcpS was carried out with the two different substrates. As shown in Figure 7A, DcpS efficiently hydrolyzed the ^{32}P -labeled cap structure, where almost 100% of the substrate was decapped with 24 fmoles of DcpS (Fig. 7A, lane 5). Conversely, at the highest concentration of DcpS used in this assay (1200 fmoles), the capped RNA was hydrolyzed <2% (Fig 7A, lane 12). Therefore DcpS has at least a 2500-fold higher capacity to hydrolyze the cap structure substrate relative to capped RNA substrate.

We next determined whether a correlation existed between the inability of DcpS to hydrolyze capped RNA and its capacity to bind capped RNA, using an EMSA. As expected, binding of the catalytically inactive DcpS^{mH} to the ^{32}P -labeled cap structure was detected (Fig. 7B, lanes 3–5). Surprisingly, binding to cap-labeled RNA was also detected, although higher amounts of protein were required to detect binding (Fig. 7B, lanes 8, 9). The binding was dependent on the cap, because DcpS did not bind uncapped RNA with the same concentrations of protein (data not shown), and the presence of the uncapped RNA has no effect on DcpS decapping (Fig 8). A filter binding assay with limiting ^{32}P -labeled substrate was used in the presence of increasing concentrations of DcpS to assess binding affinities. The dissociation constants were determined as the concentration of protein at which 50% of the substrate was bound. DcpS bound to cap structure with an apparent dissociation constant (K_d) of 7.5×10^{-8} M, whereas the apparent K_d for capped RNA was 1.25×10^{-6} M (Table 1). No significant binding was detected to uncapped RNA with a $K_d \gg 10^{-6}$ M. These data indicate that DcpS is a cap binding

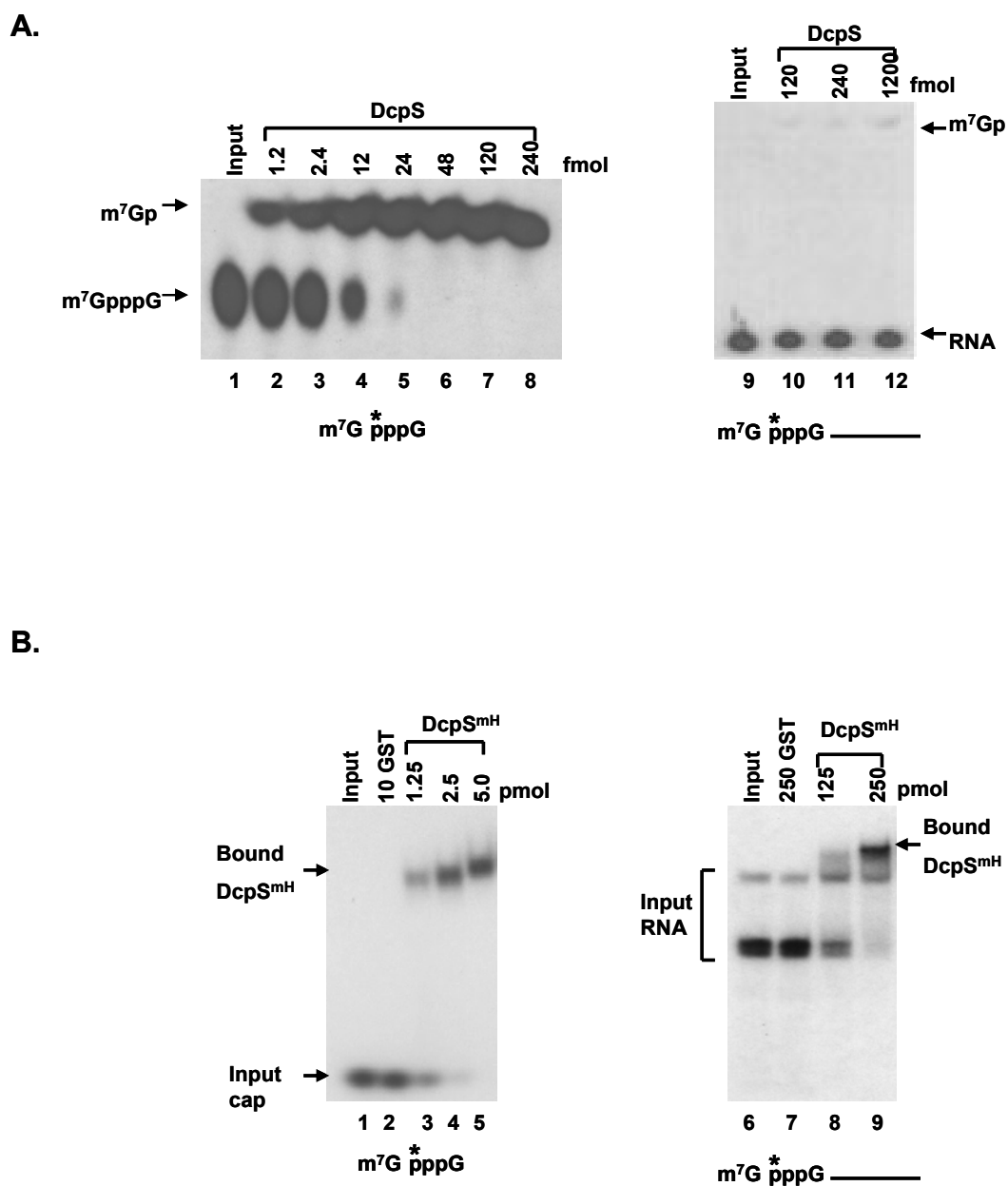


Figure 7. DcpS catalyzes the hydrolysis of cap structure but not capped RNA.

(A) Decapping assays were carried out with the indicated amounts of His-DcpS. Left panel: ^{32}P -labeled cap structure was used as substrate. Right panel: ^{32}P -labeled cap

containing a track of 16 guanosines at the 3' end to minimize nonspecific 3' end degradation (Wang and Kiledjian 2001) was used. The substrates are schematically represented at the bottom; the line denoting the RNA body.

(B) EMSA of DcpS HIT mutant DcpS^{mH} binding to ³²P-labeled cap structure (left panel) or ³²P cap-labeled RNA substrates (right panel) using the indicated amount of protein. The glutathione S-transferase domain was used as a negative control (GST; lanes 2,7). The input cap structure, capped RNA, and the corresponding bound complex are indicated.

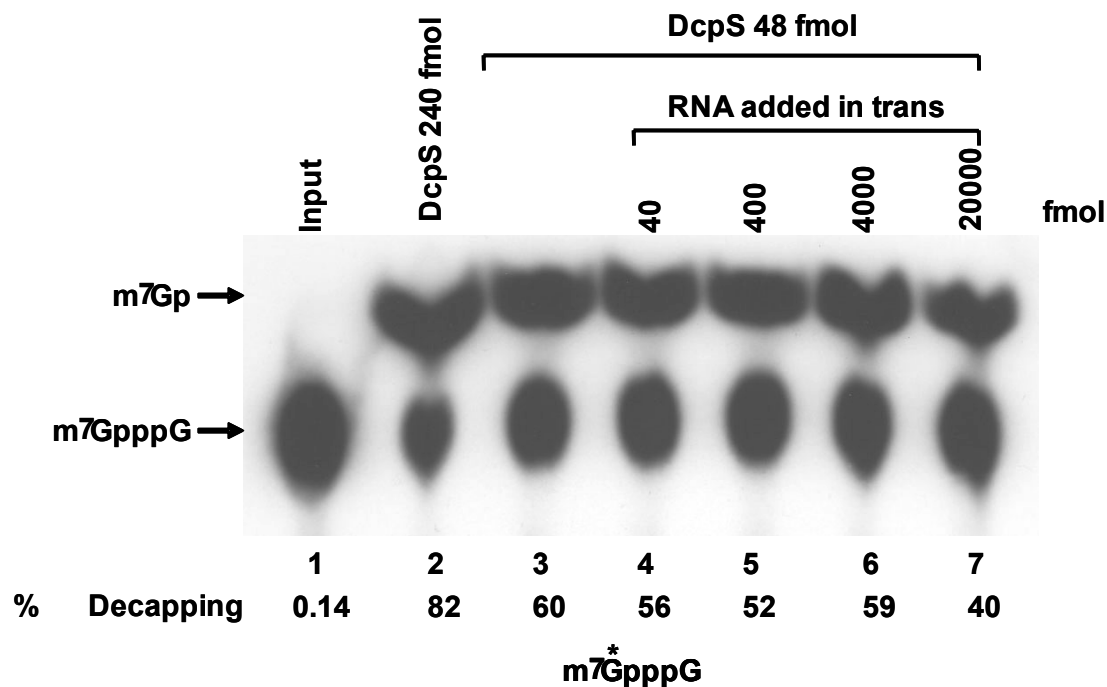


Figure 8. RNA in *trans* has no effect on DcpS decapping.

Decapping assay was carried out using 240 and 48 fmol recombinant DcpS and substrate ^{32}P -labeled cap analog, with addition of indicated amount of RNA into the reactions containing 48 fmol DcpS. Migration of the unhydrolyzed cap substrate and m^7Gp product were shown at the left. The percentage of decapping was indicated at the bottom.

Table 1. DcpS binding

Binding of DcpS^{mH} to:	K_d (μM)^a
Cap structure (m⁷G*pppG)	0.075
Capped RNA (m⁷G*ppp-RNA)	1.2
Uncapped RNA (*ppp-RNA)	>>1

^a

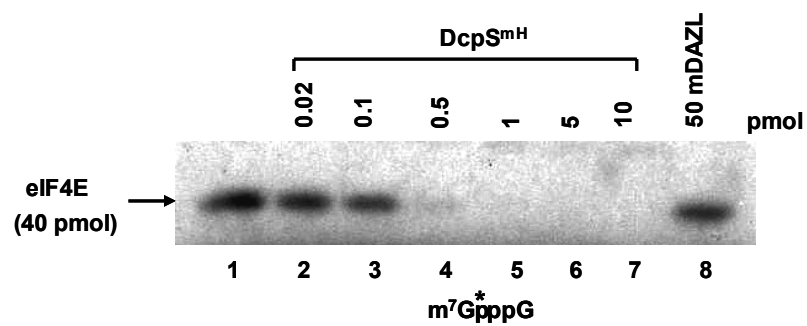
Dissociation constant determined as the concentration of His-DcpS^{mH} protein at which 50% of the labeled cap analog substrate was bound. Average of three independent experiments is indicated.

protein that is capable of binding both cap structure and capped RNA, but is only capable of efficiently hydrolyzing cap structure.

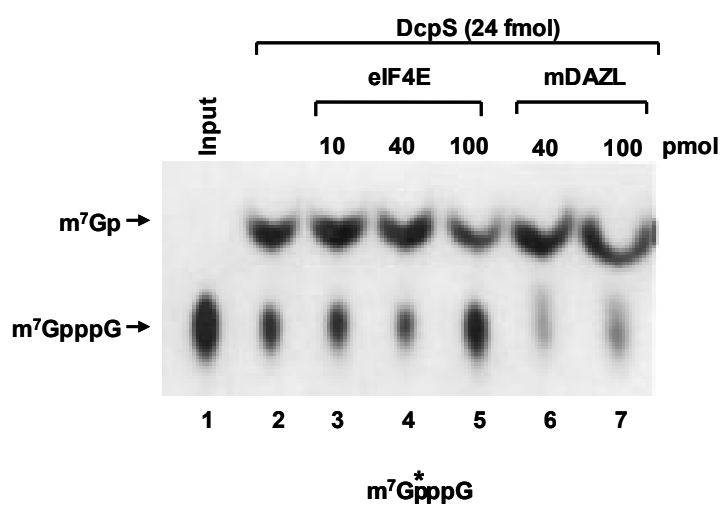
DcpS can efficiently compete with eIF4E for access to the cap structure

Because DcpS is a cap binding protein, UV crosslinking analysis was used to determine the capacity of DcpS to compete for cap binding with the major cytoplasmic cap binding protein, eIF4E. A constant concentration of histidine-tagged eIF4E was preincubated with ^{32}P -labeled cap structure followed by addition of an increasing titration of catalytically inactive DcpS^{mh} mutant protein. Crosslinking of eIF4E under these assay conditions (Fig. 9A, lane 1) was efficiently competed by the addition of DcpS where 50% of eIF4E was displaced from the cap structure with a 400-fold lower molar ratio of the DcpS^{mh} protein (Fig. 9A, lane 3). Complete displacement of eIF4E was detected with an 80-fold lower molar concentration of DcpS^{mh} (Fig. 9A, lane 4). Addition of an unrelated RNA-binding protein had no affect (Fig. 9A, lane 8). eIF4E was equally ineffective at preventing hydrolysis of the cap structure by DcpS (Fig. 9B), where partial inhibition of decapping was only detected when a 4000-fold molar excess of eIF4E was preincubated with the cap structure (Fig. 9B, lane 5). However, consistent with the lower affinity of DcpS for capped RNA, DcpS was less efficient at competing eIF4E binding to capped RNA (Fig. 9C). Collectively, these data demonstrate that DcpS is able to compete effectively with eIF4E for cap structure, but not capped RNA.

A.



B.



C.

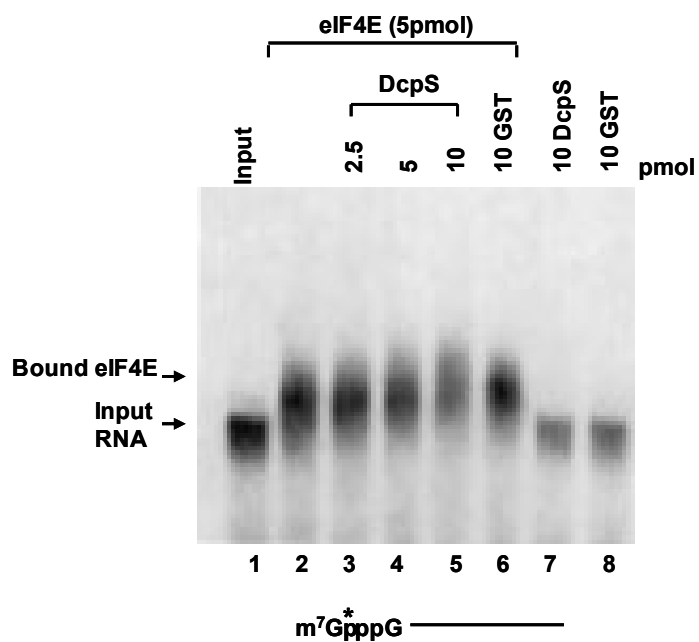


Fig 9

Figure 9. DcpS can displace eIF4E from the cap structure.

(A) The ability of DcpS to displace eIF4E from the cap structure was tested. Forty pmoles of histidine-tagged eIF4E was preincubated with ^{32}P -labeled cap structure on ice for 10 min, followed by addition of the indicated amounts of histidine-tagged DcpS^{mh} for an additional 10 min (lanes 1–7). The reactions were subsequently UV-crosslinked and resolved by SDS-polyacrylamide gel. The mDAZL RNA binding protein was used as a control (lane 8). DcpS can efficiently displace eIF4E from the cap structure.

(B) eIF4E is ineffective at inhibiting DcpS-mediated decapping. Indicated amounts of His-eIF4E (lanes 3–5) or control His-mDAZL (lanes 6,7) protein were preincubated with cap structure, followed by the addition of 24 fmoles of DcpS in a decapping assay.

(C) DcpS is inefficient at removing eIF4E from capped RNA relative to cap structure. ^{32}P cap-labeled RNA was preincubated with 5 pmoles of His-eIF4E for 10 min on ice, and competed with the indicated amounts of competitor proteins. Migration of the input RNA and bound eIF4E–RNA complex are indicated on the left, and the RNA is denoted schematically at the bottom.

DcpS plays a role in maintaining cap-dependent translation

Considering DcpS is able to displace excess molar amounts of eIF4E from cap structure *in vitro*, we had initially hypothesized that one potential cytoplasmic function of DcpS was to control the global accumulation of cap structure as the 3'-5' mRNA decay product. Otherwise, eIF4E would be sequestered by the aberrantly high level of cap structure thus the eIF4E mediated translation would be impeded. To test this hypothesis, we established a 293T stable cell line expressing an shRNA against DcpS transcripts. As shown in Figure 10D, lanes 1-3, the endogenous DcpS expression was reduced by more than 95%, relative to a control stable cell line transfected with an shRNA empty vector(lanes 4-7). Consistent to this result, the DcpS activity was reduced by 80% (data not shown). Moreover, the DcpS knockdown cells exhibited an accumulation of the cap structure as the 3'-5' decay product (data not shown), consistent with the reduced DcpS activities and validate the hypothesis that cap structure accumulates in the absence of DcpS which could in turn sequester eIF4E.

To determine whether a reduction of endogenous DcpS levels would impact eIF4E-mediated cap-dependent translation, a dual luciferase assay was used to monitor translation efficiency. A dicistronic reporter transcript that translates renilla luciferase in a cap-dependent manner and firefly luciferase in a cap-independent manner was used to assess the impact on the ratio of cap-dependent translation by reduced DcpS activity (Fig 10A). The dicistronic reporter construct was expressed in DcpS

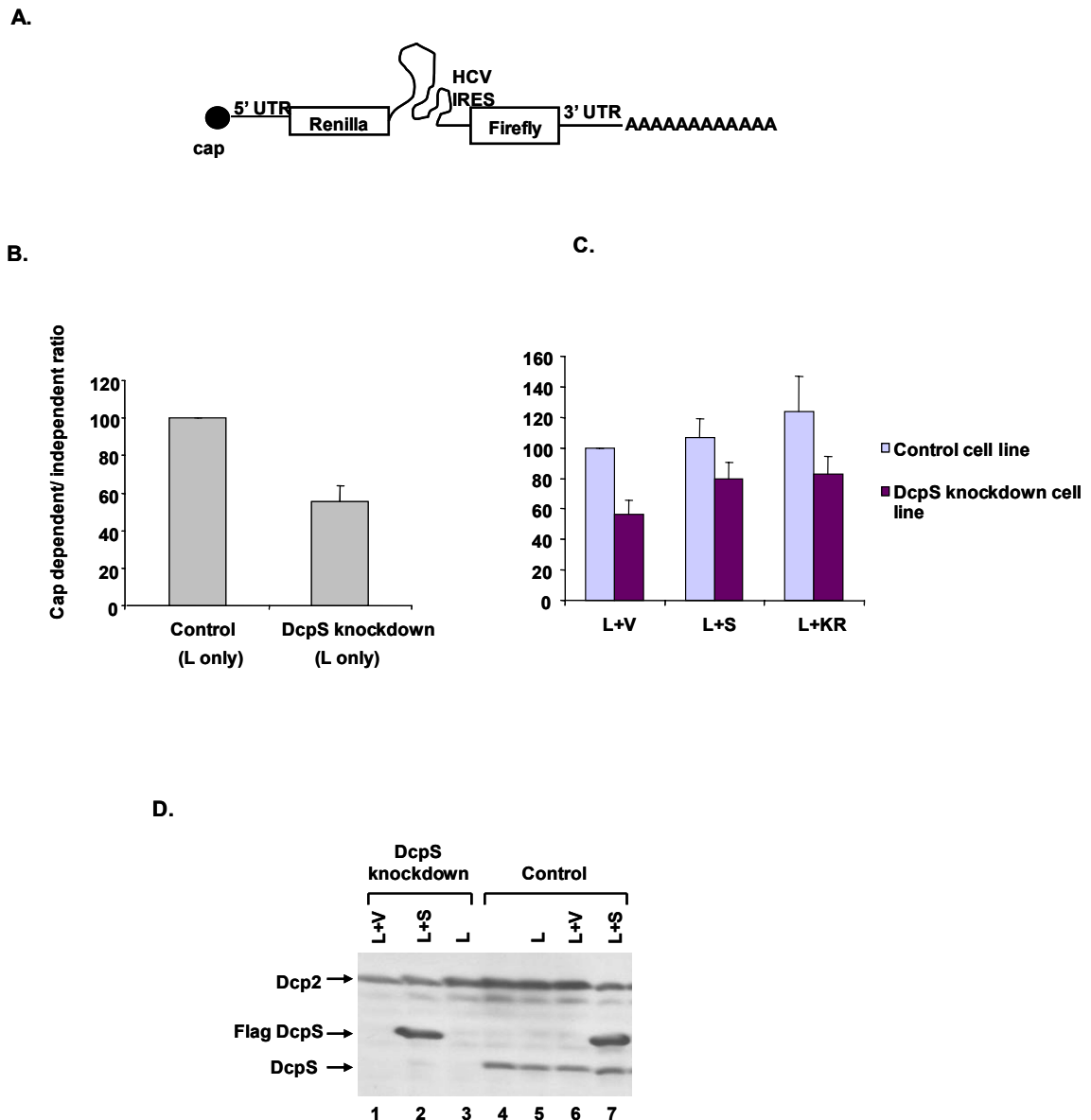


Figure 10. DcpS is involved in maintaining normal cap-dependent translation.

The ability of DcpS to affect protein translation was tested by *in vivo* dual luciferase assays.

(A) A schematic showing a dicistronic luciferase plasmid encoding cap dependent renilla and cap-independent firefly luciferase with a 5' HCV IRES.

(B) 2 μ g of the plasmid described in (A) was transfected into either shRNA vector expressing or DcpS shRNA expressing cell lines. The cap dependent renilla luciferase activity was normalized to that of the HCV IRES driven firefly luciferase activity to obtain the fold change of cap-dependent translation. Relative to control cells (the first bar), DcpS knockdown cells (the second bar) exhibited a 40% fold reduction in cap dependent translation. L, dicistronic luciferase plasmid described in (A).

(C) The decreased translation could be restored over 50% by complementation with exogenous wild type DcpS, or a DcpS truncation mutant that only localizes in the cytoplasm, whereas the vector alone failed to complement. L, Cells transfected with 2 μ g dicistronic luciferase plasmid described in (A); V, Cells transfected with 4 μ g empty vector; S, Cells transfected with 4 μ g wild-type DcpS; KR, Cells transfected with 4 μ g DcpS truncation mutant that only localizes in the cytoplasm.

(B) and (C) represent the average of four independent experiments. The corresponding standard deviations are denoted by the error bars.

(D) Western blotting analysis was carried out to confirm the knockdown of endogenous DcpS and over-expression of exogenously expressed Flag DcpS. Endogenous Dcp2, DcpS and exogenously expressed Flag DcpS are indicated by arrows. Note the endogenous DcpS was knockdown by over 95% in the cells expressing DcpS shRNA(compare lanes1-3 and lanes 4-7), whereas the Flag DcpS was over-expressed in the cells transiently co-transfected with pcDNA3-Flag DcpS(lanes 2 and 7).

knockdown cells and control cells and cap-dependent protein translation activity of renilla luciferase normalized to cap-independent translation activity of firefly are presented in Figure 10B. A 40% reduction of cap-dependent translation is detected in the DcpS knockdown cells compared to the control cells expressing the shRNA vector. This result is consistent with cap structure accumulation precluding eIF4E access to capped RNA for productive protein translation. To validate the specificity of the effect of DcpS on translation, the DcpS knockdown cell line and the control cell line were cotransfected with a plasmid expressing Flag-tagged DcpS, and a partial restoration was observed in the DcpS knockdown cell line, while no difference was detected when the cells were cotransfected with an empty vector (Fig10C). Interestingly, a 10-20% enhancement of cap dependent translation was also observed in the control cell line co-transfected with Flag-tagged DcpS plasmid, consistently suggesting a positive effect DcpS has on cap-dependent translation. The expression of the cotransfected Flag-tagged DcpS is verified by western analysis. As shown in Fig 10D, the cell lines transfected with the Flag DcpS plasmids had significant expression level of Flag tagged DcpS (Fig 10D, lanes 2, 7). Collectively, these *in vivo* data showed that a reduction of DcpS levels leads to reduction of cap-dependent translation, which in turn support our initial hypothesis that DcpS acts to scavenge the accumulated of cap structure that would otherwise trap eIF4E and interfere with the eIF4E-mediated translation.

Discussion

We present evidence that DcpS is a unique member of the HIT hydrolase protein family. It is a modular protein comprised of at least two distinct domains that are inactive

individually but together reconstitute decapping activity in *trans*. One of these domains contains the 100-amino-acid HIT domain, demonstrating that this element is not sufficient for efficient substrate binding and hydrolysis activity as observed for other HIT motif proteins. Furthermore, with the DcpS structure being resolved, we tested the decapping activities of various mutants, whose mutated residues were predicted to be important for substrate binding and hydrolysis based on the structure, and determined the requirement of these residues for hydrolysis. We further demonstrate that DcpS can efficiently compete with eIF4E for binding cap structure, consistent with a role for DcpS in ensuring that eIF4E is not sequestered by byproducts of mRNA decay.

Our analysis of Dcs1p and DcpS revealed that regions outside the HIT fold, namely the N-terminal domains, are essential for decapping activity. This point is underscored by the following observations. First, mutational analysis removing either the N-terminal 40 amino acids of Dcs1p or sequences C-terminal to amino acid 33 in DcpS results in an inactive protein (Fig 2). Second, dissection of DcpS into an N-terminal domain and a C-terminal domain maintaining an intact HIT fold region abrogated the ability of the HIT fold to hydrolyze the cap, but interestingly, a mixture of the two domains in *trans* reconstituted decapping activity (Fig 3). These data demonstrate that the N-terminal domain coordinates the activity of these proteins. This is further underscored by a functional decapping enzyme generated by the fusion of the N-terminal domain of the catalytically active Dcs1p to the C-terminal domain of the catalytically inactive Dcs2p containing the HIT motif (Dcs1/2p). A Dcs2/1p fusion protein containing the Dcs2p N-terminal domain and the Dcs1p C-terminal domain was unable to catalyze cap hydrolysis (Fig 1), demonstrating that the active state of the protein can be dictated

by the composition of the N-terminal domain. In conjunction with biochemical studies we were able to obtain the cocrystal structure of DcpS bound to monomethylated cap analog in collaboration with Meigang Gu and Christopher Lima (Sloan-Kettering Institute) (Gu et al., 2004). Consistent with the data presented herein indicating that cap binding and hydrolysis of DcpS require the HIT fold as well as the N-terminal domain, the structure revealed DcpS to be an asymmetric dimer containing distinct N-terminal and C-terminal domains that are separated by a hinge region (Fig5) (Gu et al., 2004). The structure illustrated that a productive active site is composed of amino acid residues emanating from both the N-and C-terminal domains, several of which were critical for cap binding and hydrolysis (Gu et al., 2004). The substitution of N terminal amino acids that interact with the cap substrate disrupted protein activities (Fig 6), confirming that generation of a closed decapping competent confirmation requires interactions of the N terminus with the cap substrate.

Analyses of the N-terminal truncation of DcpS indicate that this domain primarily functions to facilitate cap binding. A direct correlation was detected between N-terminal truncations that were able to hydrolyze the cap structure and those that can bind the cap. The DcpS^{ΔN33} mutant, which retained decapping activity, was competent to bind the cap structure, whereas the DcpS^{ΔN71} mutant, which was unable to hydrolyze the cap, was also unable to bind the cap (Fig 4). Similarly, N-terminal truncations of Dcs1p that were inactive for decapping were also unable to bind cap structure (data not shown). These data are in agreement with the observed structure of DcpS where removal of the terminal 33 amino acids would not disrupt the N-terminal domain, whereas a larger truncation

removing the first 71 amino acids would be expected to disrupt the overall structure of the N-terminal domain.

The generation of a functional decapping enzyme by substitution of the Dcs2p N-terminus with that of the Dcs1p N-terminus demonstrates that Dcs2p contains a productive HIT motif capable of hydrolyzing a pyrophosphate linkage within a cap. The lack of cap analog hydrolysis activity with recombinant Dcs2p and endogenous Dcs2p in yeast cells devoid of Dcs1p (Liu et al., 2002) indicates that Dcs2p is not involved in decapping the m⁷GpppG cap structure. Furthermore, Dcs2p also lacks the ability to catalyze the hydrolysis of capped RNA, indicating that it does not have a Dcp2-like decapping activity (data not shown). Interestingly, Dcs2 seems to be a modulator of Dcs1 activity. Under conditions of stress, Dcs2 can heterodimerize with Dcs1, thus suppressing the substrate specificity and k_{cat} of Dcs1 decapping (Malys and McCarthy, 2006). Surprisingly, a Dcs2 homolog is not present in mammalian cells and this regulation appears to be restricted to yeast cells.

An interesting property of DcpS is its specificity to hydrolyze cap structure relative to capped RNA (Liu et al., 2002; Wang and Kiledjian, 2001). DcpS preferentially hydrolyzes cap structure at least 2500-fold more efficiently than capped RNA (Fig 7A). Interestingly, DcpS was able to bind the cap structure of capped RNA, although at a 17-fold lower affinity than that of cap structure (Table 1). As the addition of uncapped RNA competitor did not interfere with DcpS-mediated hydrolysis of cap analog (Fig 8), it is unlikely that the RNA moiety competitively inhibits DcpS activity. Structural analysis of DcpS suggests that in addition to the lower binding affinity, the

increased size and entropy of a longer RNA molecule might hinder closure of the enzyme and formation of a productive decapping complex (Gu et al., 2004).

The *S. pombe* homolog of DcpS, Nhm1p, was recently identified as an enzyme capable of catalyzing the decapping of intact capped RNA (Salehi et al., 2002). The reason for the different decapping properties of Nhm1p compared to DcpS or Dcs1p is not obvious, considering the conservation of critical residues among these proteins as determined by the structure of DcpS. On the basis of the conservation, we would predict that Nhm1p also contains scavenger-decapping activity that will efficiently function on cap structure. Further analyses are necessary to determine the relative decapping efficiency of Nhm1p for cap structure versus capped RNA.

At least one function of DcpS is to hydrolyze the cap structure remaining after 3' - 5' exoribonucleolytic decay of the mRNA in both yeast cells and mammalian extract (Liu et al., 2002; Rodgers et al., 2002; Wang and Kiledjian, 2001). A functional consequence of this hydrolysis activity could be to eliminate the removal of a potential substrate that can sequester the cytoplasmic eIF4E cap binding protein. The ability of DcpS to efficiently hydrolyze the cap structure in the presence of excess eIF4E is consistent with this hypothesis. Furthermore, the lower affinity of eIF4E to m⁷GMP relative to cap structure (Niedzwiecka et al., 2002; Zuberek et al., 2003) also supports such a function. Moreover, the relative reduction of cap-dependent translation in a DcpS knockdown cell line (Fig 10) further supports the hypothesis. Under physiological conditions, eIF4E is a component of translation initial complex eIF4F, which also contains eIF4A and eIF4G and functions to recruit ribosomes to mRNA (Gingras et al., 1999). Furthermore, our in

vivo results indicate that, despite the fact that eIF4E is associated with other protein partners, it is still capable of binding to the cap structure therefore sequestered by the accumulated cap structure when DcpS level is reduced. The relatively lower capacity of DcpS to compete with eIF4E for capped RNA and its inability to hydrolyze capped RNA appears to provide a multilevel regulatory mechanism to ensure that capped RNAs are not prematurely hydrolyzed prior to degradation of the mRNA body. The relative lower efficiency of DcpS to displace eIF4E from capped RNA could also serve to minimize potential competition with eIF4E for capped mRNA, thus preventing potential interference with mRNA translation. Interesting questions remain: when during the demise of an mRNA does eIF4E dissociate from the cap and when does DcpS gain access to the cap? Curiously, Nhm1p was initially isolated as a protein associated with the *S. pombe* eIF4F cap binding complex (Salehi et al., 2002). A more detailed analysis of the affinities of eIF4E and DcpS to capped RNAs of varying lengths as well as additional proteins that can associate with the cap including PARN (Dehlin et al., 2000; Gao et al., 2000; Martinez et al., 2000) and the poly(A) binding protein PABP (Khanna and Kiledjian, 2004) will begin to address the interplay between the cap and cap binding proteins during degradation.

Chapter II: Mechanistic and Kinetic analysis of the DcpS Scavenger Decapping Enzyme

Summary

In eukaryotic cells, decapping is an important process in the control of mRNA degradation. The scavenger decapping enzyme DcpS, is a major decapping enzyme that functions to hydrolyze a cap structure lacking the RNA body. It is a member of the histidine triad (HIT) family of hydrolases and catalyzes the cleavage of m⁷GpppN into m⁷Gp and ppN. Previous structural analysis has revealed that DcpS is a dimeric protein with an amino-terminus swapped domain. The protein dimer contains two cap binding/hydrolysis sites and displays a symmetric structure with both binding sites in the open conformation in the ligand-free state and an asymmetric conformation with one site open and one site closed when ligand-bound. The structural data are suggestive of a dynamic decapping mechanism where each protomer alternates between an open and closed state. However, the detailed kinetics in terms of binding and hydrolysis remains unclear. In this chapter, we analyzed the kinetic properties of DcpS enzymatic activity to address the decapping mechanism at the subunit level. We demonstrate that the binding step is the rate limiting step under single turnover conditions, whereas the hydrolysis step is rate limiting under multiple turnover conditions. This alteration of the kinetics appears to be due to an allosteric conformation change in the presence of excess substrate. The dynamic and mutually exclusive cap hydrolysis activity of the two cap binding sites was further confirmed with the use of mixed active and inactive heterodimers. Our data have

provided mechanistic details in terms of hydrolysis as well as insights into the regulation process of decapping in cells.

Introduction

The control of mRNA degradation is a critical step in the posttranscriptional regulation of gene expression, since the steady state level of any mRNA species depends on both the rate of mRNA synthesis and its breakdown. In eukaryotic cells, cytoplasmic mRNA degradation predominantly proceeds through an initial deadenylation step (Decker and Parker, 1993; Muhlrud et al., 1995) followed by 5' to 3' or 3' to 5' decay (Coller and Parker, 2004; Liu and Kiledjian, 2006). In the 5'-3' decay pathway, the 5' cap structure is cleaved by the catalytic activity of the Dcp2 decapping enzyme to release the m⁷GDP and monophosphorylated RNA (Beelman et al., 1996; Dunkley and Parker, 1999; LaGrandeur and Parker, 1998; Piccirillo et al., 2003; Steiger et al., 2003; van Dijk et al., 2002). The resulting uncapped monophosphorylated RNA is digested by a 5'-3' exonuclease, Xrn I (Decker and Parker, 1993; Hsu and Stevens, 1993). In the 3'-5' pathway, subsequent to deadenylation the capped-RNA body is continuously degraded by an exosome complex (Anderson and Parker, 1998; Wang and Kiledjian, 2001). The resulting capped oligonucleotide m⁷GpppN(pN)_n (n<9) is hydrolyzed by a second type of decapping enzyme, DcpS, to release the m⁷Gp and ppN(pN)_n products (Liu et al., 2002; Wang and Kiledjian, 2001). These pathways need not be mutually exclusive and could occur simultaneously (Murray and Schoenberg, 2007) and an interplay between the two pathways could also exist. DcpS, which was originally characterized as the decapping enzyme in the 3'-5' pathway, is able to hydrolyze the 5'-3' decapping product m⁷GDP to

release m^7Gp (Chen et al., 2005; van Dijk et al., 2003). Furthermore, disruption of yeast DcpS homolog, Dcs1p, impeded the 5' exonuclease activity (Liu and Kiledjian, 2005), indicating the Dcs1p decapping products might serve as signaling molecules for the 5' decay pathway. DcpS is a member of the Histidine triad (HIT) hydrolase family of proteins that contain a stretch of His-X-His-X-His-X residues, where X denotes hydrophobic amino acid residues. HIT proteins are dimeric nucleotide binding proteins that have hydrolase activities (Brenner, 2002; Brenner et al., 1999; Guranowski, 2000). The central histidine residue has been proposed to be critical for the hydrolase activity as it serves as the nucleophile attacking the cap α -phosphate in m^7GpppG (Lima et al., 1997) and is also critical for DcpS hydrolysis (Liu et al., 2002).

Structural analysis of DcpS has revealed that it is a homodimer with a symmetric structure when in the ligand-free form (Chen et al., 2005; Han et al., 2005), or asymmetric homodimer in the ligand-bound form (Chen et al., 2005; Gu et al., 2004). Each DcpS protomer possesses a distinct N terminal domain and a C terminal domain containing the HIT motif linked by a hinge region. The N-terminal domain displays a domain swapped form by exchanging an identical α -helix and two anti-parallel β -strands with the second protomer. The DcpS homodimer contains two cap binding pockets which serve as the active sites for cap hydrolysis. In the ligand bound form, DcpS forms a simultaneous closed conformation on one side and an open conformation on the other, with a substrate bound at the C-terminal domain of each side (Figure 5) (Gu et al., 2004). The structure suggests that the closed conformation constitutes the cap hydrolysis productive site while the open site would be nonproductive. The N terminal domains can either both be in the open state or one side in an open state with the second in a

productive closed state with the hinge enabling the N-terminus to flip back and forth, alternating on each side (Chen et al., 2005; Gu et al., 2004). The catalytic cycle was proposed as follows: upon interacting of a cap substrate at one protomer, DcpS dimer undergoes a conformational change from the symmetric open/open configuration to an asymmetric open/close one, as the cap interacting protomer adopts a close form. The subsequent hydrolysis of the cap structure leads to a second conformational change, which weakens the binding affinity of the product m^7Gp and enhances release of the product (Chen et al., 2005).

Here, we examined the enzymatic kinetics of recombinant DcpS and demonstrate that negative cooperativity is present during the binding and hydrolysis processes. Furthermore, by comparing the enzymatic behaviors of wild type DcpS homodimer and HIT mutant heterodimer, we have further confirmed the previously proposed dynamic decapping model in which the N terminus pivots back and forth for binding and hydrolysis (Chen et al., 2005; Gu et al., 2004).

Results

Hydrolysis of cap structure by DcpS is rate limiting at the binding step under single turnover conditions

To gain a better understanding of the mechanism by which the DcpS scavenger decapping enzyme functions to hydrolyze cap structure, we undertook an enzymatic kinetic analysis of DcpS decapping. Recombinant Flag-tagged DcpS was purified and its concentration quantitated as described in Materials and Methods. The purified protein was resolved in SDS-PAGE and stained with Sypro-Ruby as shown in Fig 11A. *In vitro*

decapping assays were performed under single turnover conditions by a rapid chemical quench-flow apparatus to determine the rate limiting step in its kinetic pathway. An enzyme titration of 20nM, 50nM, 100nM, and 200nM of DcpS monomer concentrations, were used with 10nM cap structure substrate spiked with α - 32 P labeled cap. The label is exclusively at the first phosphate following the methylated guanosine to enable detection of both the cap structure substrate (m^7Gp^*ppG) and the decapping product (m^7Gp^*). Reactions were carried out with increasing time intervals ranging from 0.1 second to two minutes at 25°C, followed by the addition of 2.3N formic acid to quench the reaction. The decapping rate was determined by separation of the decapping products and substrate by polyethylenimine (PEI) cellulose thin-layer chromatography (TLC) (Fig 11B). The decapping rate is defined as the hydrolyzed cap substrate (or the product m^7Gp generated) over the total substrate input. The decapping rate was plotted against the logarithmic value of the reaction time (Fig11C). The curves in Fig 11C were fit to a single exponential equation (Equation 3 in Materials and Methods). The rate constants and maximal decapping rates (20nM-200nM) were determined from the equation and listed in Table 2.

Examination of the different DcpS concentrations reveal interesting insights into the rate limiting step under single turnover conditions. As shown in Fig11D and Table 2, the rate constants increase with increasing amounts of DcpS, indicating that the initial enzyme-substrate binding step is rate limiting. As the enzyme concentration increases, the probability of molecular collisions between the enzyme and substrate increases to overcome the time-consuming slow binding step under limiting substrate conditions.

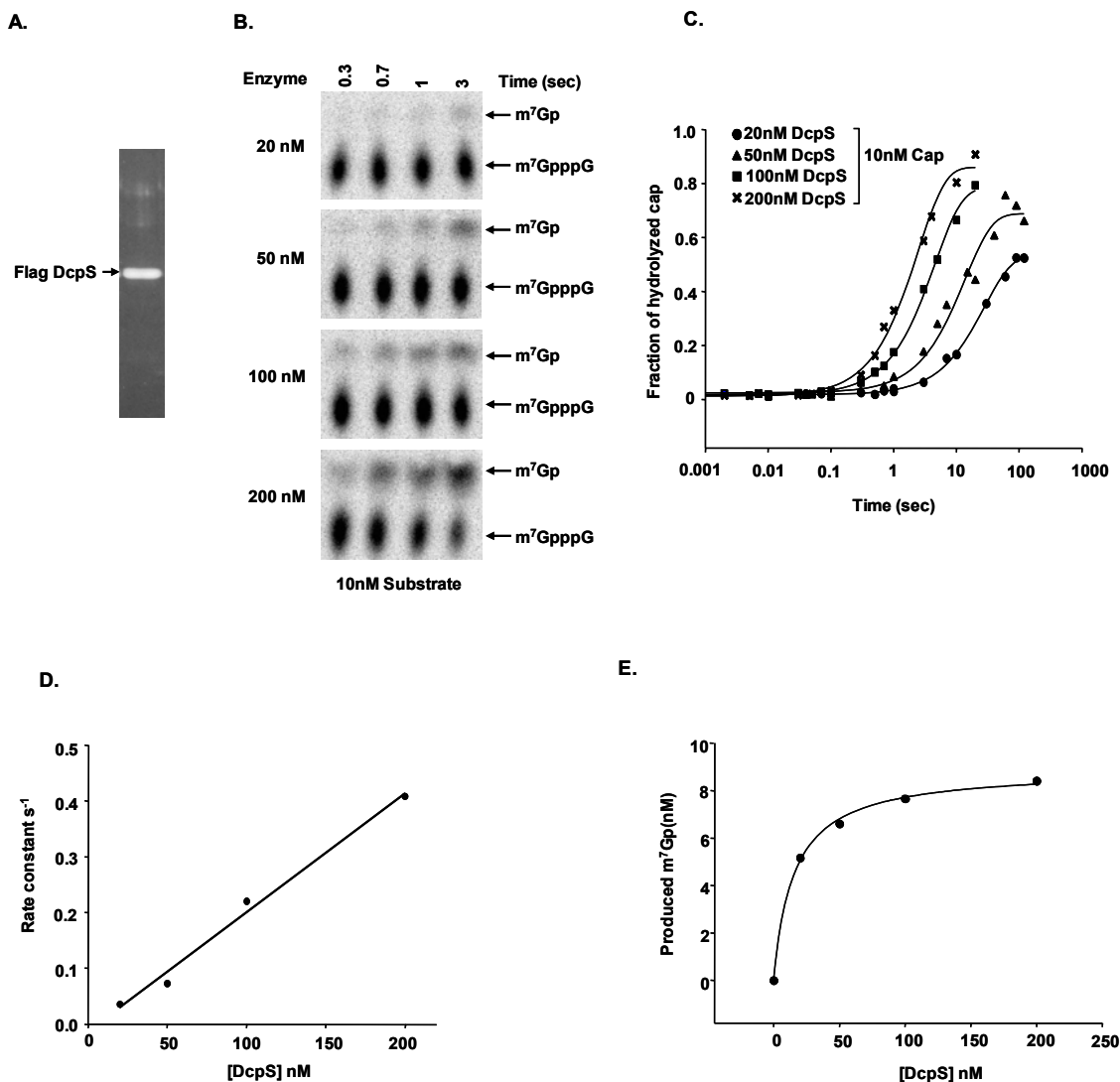


Figure 11. Increasing amount of the DcpS increases the rate constants and the decapping rates.

Decapping rate is defined as the fraction of generated decapping product m^7Gp over total substrate input.

(A) Purified Flag-tagged DcpS was resolved by SDS-PAGE and stained with Sypro Ruby.

The quantitation of purified Flag DcpS is stated in Materials and Methods.

(B) A titration of monomer concentrations, 20nM, 50nM, 100nM, and 200nM DcpS were used with 10nM cold cap structure substrate spiked with α -³²p labeled cap to perform rapid quench-flow *in vitro* decapping assays at 25°C and the kinetics analyzed. The hydrolyzing products and unhydrolyzed substrates were resolved by thin-layer chromatography (TLC) developed in 0.45 M (NH₄)₂SO₄ and exposed to PhosphorImager (see Materials and Methods).

(C) The decapping rate was quantitated and plotted against the logarithmic value of the reaction time. The decapping rate is defined as the fraction of generated decapping product m⁷Gp over total substrate input. The data points of each experiment were fit to a single exponential equation (Equation 3) to obtain the rate constants.

(D) The rate constants derived from (C) were plotted against the DcpS concentrations.

(E) The product m⁷Gp concentrations were calculated from (C) and plotted against DcpS concentrations. The data points were fit to a hyperbola (Equation 4) to obtain a K_d 15.5 nM.

Table 2. The rate constants and maximal decapping rates under single and multiple turnover conditions

Low substrate		E20	E50	E100	E200
	S10	C=0.036s ⁻¹ R=0.516	C=0.073s ⁻¹ R=0.663	C=0.22s ⁻¹ R=0.765	C=0.41s ⁻¹ R=0.847
High substrate		S200	S400	S800	S1600
	E100	C=0.045s ⁻¹ R=0.59	C=0.055s ⁻¹ R=0.5084	C=0.054s ⁻¹ R=0.4810	C=0.059s ⁻¹ R=0.4411

C=rate constant, R=maximal decapping rate, E=Enzyme, S=substrate

Conversely, if the rate limiting step is after the enzyme-substrate binding, increasing the amount of enzyme would have no effect on the reaction rate provided the substrate is limiting. Our data is consistent with the rate limiting step being the initial binding step.

To obtain the dissociation constant (K_d) for DcpS with the cap structure substrate, the amount of m^7Gp product produced was plotted against the respective DcpS concentrations (20-200nM). The generated curve was fit to a hyperbolic equation (Equation 4) and a K_d of 15.5 nM was obtained (Fig 11E). The nanomolar range of the derived K_d value is consistent with the K_d of 75nM we previously reported (Liu et al., 2004).

The chemistry step is the rate limiting step under high substrate conditions

The above analysis demonstrates that the binding between DcpS and cap substrate is the rate limiting step under conditions where the enzyme is in excess over the substrate. We next tested parameters with excess substrate and limiting enzyme concentrations. *In vitro* decapping assays were performed by the rapid chemical quench-flow approach as above except a DcpS monomer concentration of 100nM and excessive cap substrate concentrations of 200nM, 400nM, 800nM and 1600nM were used. The reaction products were resolved by thin-layer chromatography (Fig 12A). The decapping rate was plotted against the logarithmic value of reaction time (Fig 12B). The curves in Fig 12B were fit to a single exponential equation (Equation 3 in Materials and Methods) with various coefficients for each curve. The rate constants and the maximal decapping rates were determined from the equation coefficients and listed in Table 2. The rate constants

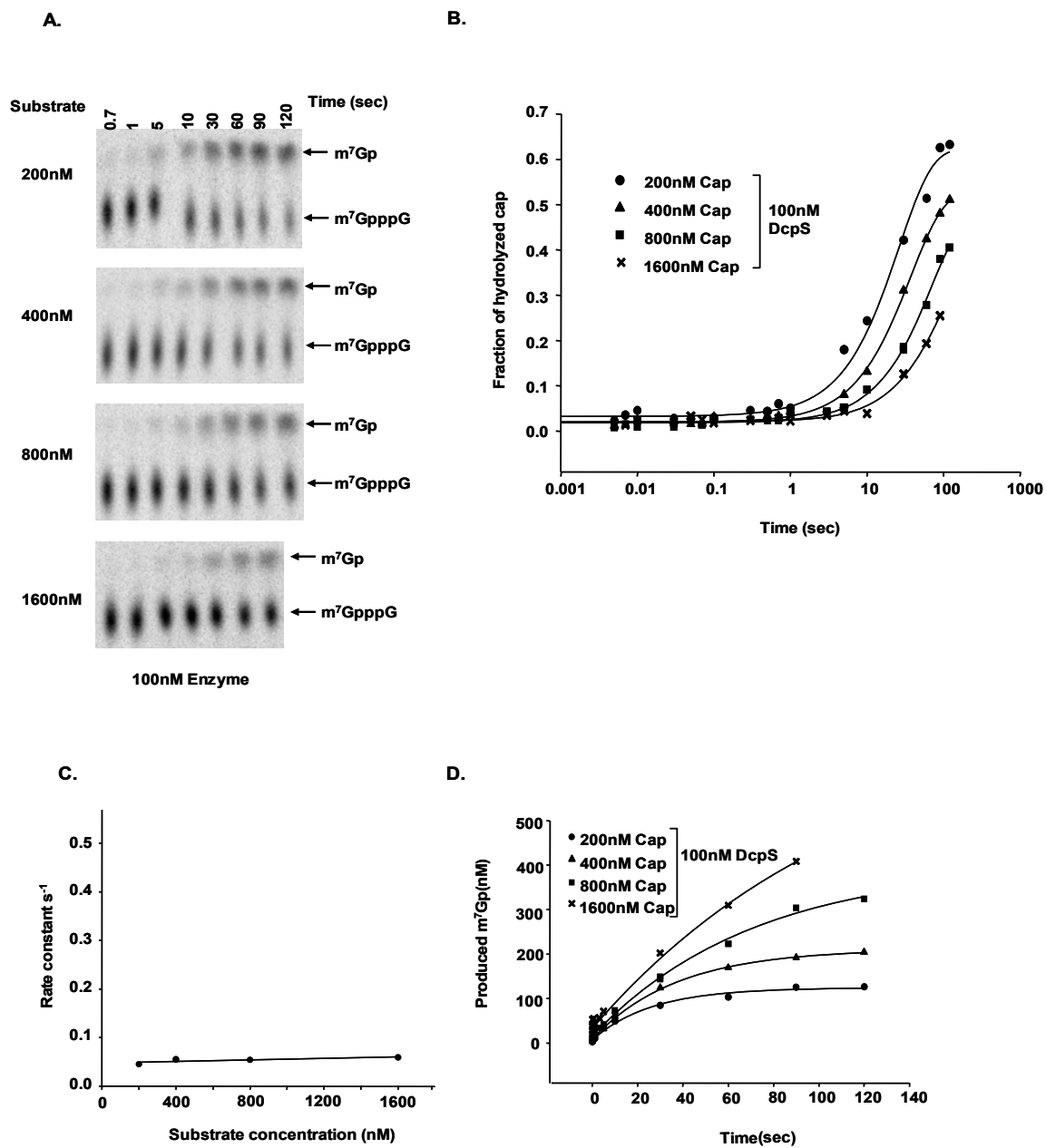


Figure 12. Excessive amount of cap substrate reduces the rate constants and the decapping rates.

(A) 100 nM monomer concentration of DcpS were used with a titration of excessive amount of substrate 200, 400, 800, 1600 nM to perform rapid quench-flow decapping assays as in Fig11B.

(B) The decapping rate was plotted against the logarithmic value of the reaction time. The data points of each experiment were fit to a single exponential equation (Equation 3) to obtain the rate constants.

(C) The rate constants derived from (B) were plotted against the DcpS concentrations.

(D) The concentrations of the decapping product m^7Gp were calculated and plotted against the reaction time. No initial bursts of first round turnover were observed from these curves. All four curves exhibit a single prolonged exponential phase.

derived from Equation 3 were further plotted against the substrate concentrations (200-1600 nM) (Fig 12C). As shown in Fig 12C and Table 2, the increasing amount of cap substrate had no effect on rate constants, indicating that the substrate binding is not rate limiting under excess substrate conditions.

Having ruled out the substrate binding as the rate limiting step, we next determined whether one of the steps subsequent to binding, the hydrolysis or product release step, is rate limiting. The data was represented as the concentration of m⁷Gp produced over the reaction time (Fig 12D). Representation of the data under these parameters enables the distinction of whether the reaction proceeds through an initial burst for the first round of substrate turnover. An initial steep slope with a subsequent shallow slope would indicate the reaction proceeds through an initial rapid burst but the subsequent rounds of hydrolysis are slower due to a slow release of the product. The observed data points fit to a single exponential curve and are plotted in Figure 12D. Examination of the data demonstrates the reaction does not proceed through an obvious burst of product formation, indicating the product release is not a rate limiting slow step. The above data is consistent with the chemical step of cap hydrolysis constituting the rate limiting step under excess substrate conditions.

The accumulation of products is inhibitory to cap hydrolysis by DcpS

An interesting observation from Figure 12B is the decapping rate varies with the concentration of substrate being used despite the fact that all reactions are under excess substrate concentrations. A decrease of decapping rate is observed with increasing

substrate concentration. Therefore, an increase in substrate resulted in an inhibition of the hydrolysis, indicating the accumulation of increasing product was inhibitory. Furthermore, the fact that the data points fit to a single exponential curve that has a relatively prolonged exponential phase also suggests product inhibition where the accumulation of the product was inhibitory to the hydrolysis step (Fig12D). The above observations suggest that the accumulation of the m^7Gp generated throughout multiple turnover rounds competes for substrate binding and leads to inhibition of hydrolysis.

The lowering of the rate constants is indicative of negative cooperativity

DcpS functions as a dimer with the domain swapped N-terminal domains separated from the C-termini by a hinge (Gu et al., 2004). Each N-terminus can pivot between a closed or open conformation to hydrolyze the cap structure and release the m^7Gp product (Gu et al., 2004) (Chen et al., 2005). Examination of the rate constants for 100nM DcpS decapping under single turnover conditions ($0.22s^{-1}$) revealed it to be 4 times higher than the rate observed at multiple turnover conditions with excess substrate ($0.045s^{-1}$ to $0.059s^{-1}$) (Table 2). This is indicative of negative cooperativity under excessive substrate conditions and suggests a possible negative feedback mechanism to regulate DcpS mediated decapping under high substrate conditions (see Discussion).

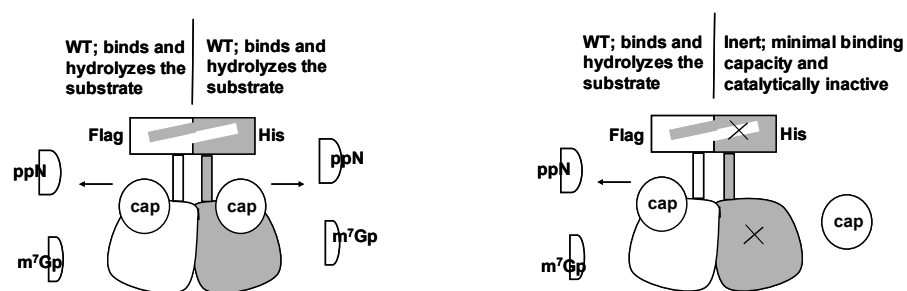
Decapping by a DcpS heterodimer containing one inert subunit displayed decreased negative cooperativity

To further confirm the negative cooperativity between the two active sites within the DcpS dimer, a DcpS heterodimer containing one wild-type active site and a mutated

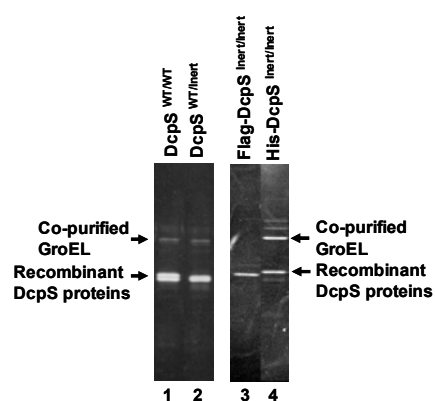
second site with reduced binding ability to cap substrate was generated. With a heterodimer containing only one active site and a second that was rendered relatively inert, we would expect there to be minimal if any cooperativity with this heterodimer since only one side of the protein can effectively interact with the cap substrate. To generate the heterodimer with one inert site, mutants were constructed such that two residues within one active site of the dimer critical for cap structure binding were substituted with alanine to abolish the cap binding function. Two mutations that each individually are essential for cap hydrolysis, asparagines 110 and tryptophan 175 (Gu et al., 2004), were used. The rationale was to maximize the disruption of cap binding by using a double mutation. Asparagines 110 and tryptophan 175 were each substituted with alanine (N110A and W175A respectively) at only one of the cap binding and hydrolysis sides to minimize the cap binding at one site of the DcpS dimer. A schematic of this heterodimer is shown in Figure 13A, and purified proteins are shown in Fig 13B. As the N-terminus is constituted by a domain swapped dimer with contributions of cap binding from both protomers at each active site, each mutant was made in distinct monomers. Upon formation of a heterodimer, the N110A from the first monomer and W175A from the second monomer assemble on the same side of the protein within the same catalytic site. Each monomer of this heterodimer contained a distinct tag (Flag tag and His tag) for the purpose of protein purification (see Materials and Methods).

We previously showed that a homodimer containing the N110A or W175A mutation at each cap binding site contained less than 5% activity of the wild type DcpS, thus we initially set out to ascertain whether the N110A and W175A double mutant retained any catalytic activity. To test this, a homodimer of N110A and W175A

A.



B.



C.

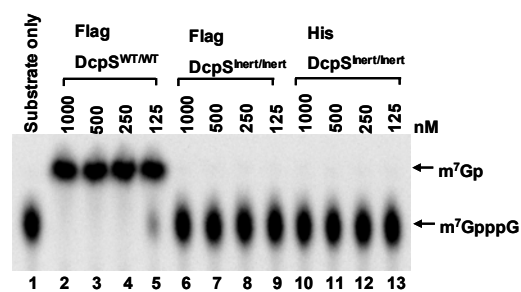


Fig 13

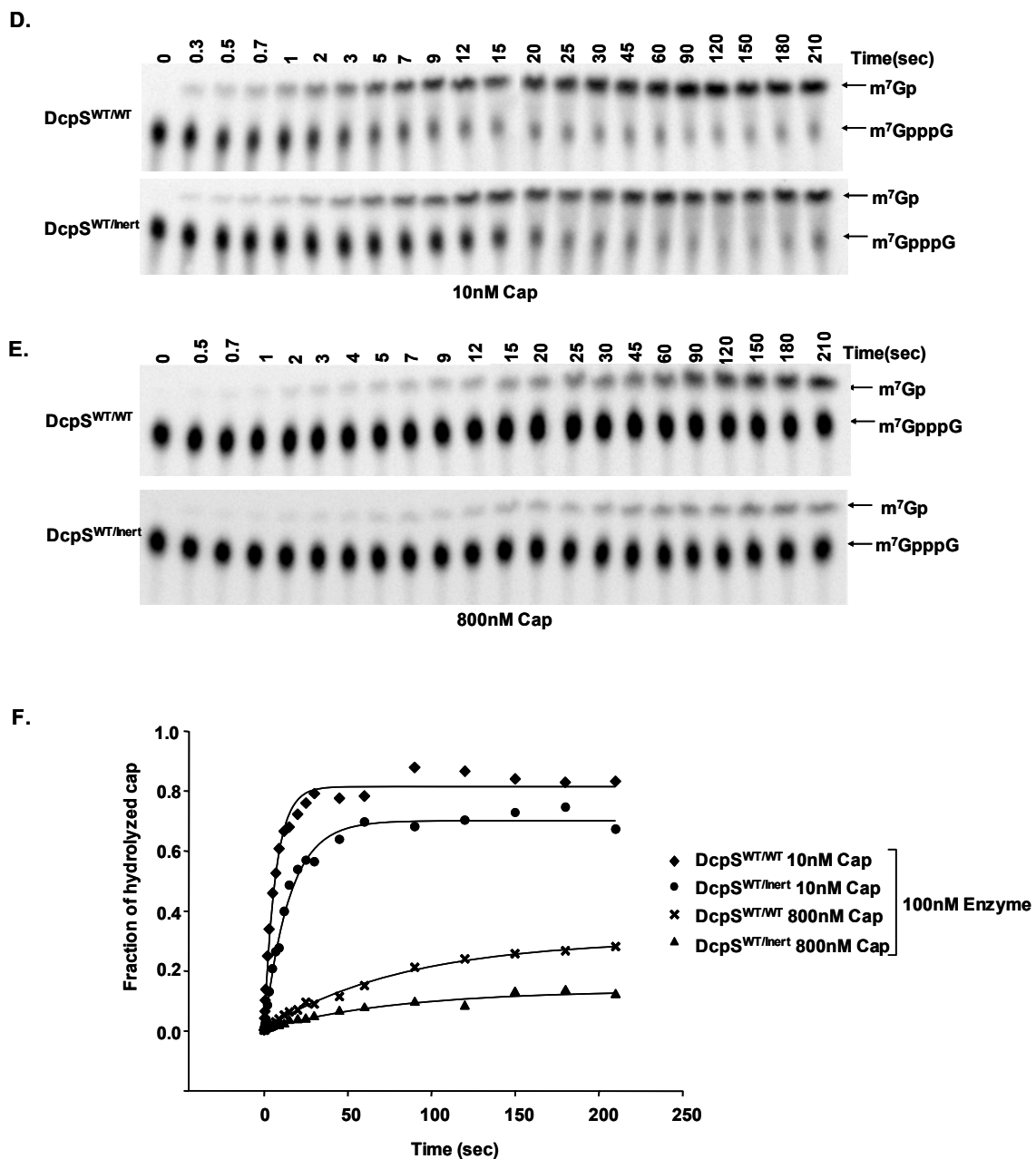


Fig 13. Both DcpS^{WT/WT} homodimer and DcpS^{WT/Inert} heterodimer display decreased decapping rates under multiple turnover conditions.

(A) Cartoon representations of DcpS^{WT/WT} homodimer and DcpS^{WT/Inert} heterodimer with double tags. Note that part of the N terminus is exchanged in the DcpS dimer. With this domain swapping nature, DcpS^{WT/Inert} was constructed in a way that two mutated residues

from distinct protomers actually assemble on the same binding site rendering this site catalytically inactive (see Results). The cartoon format of the DcpS dimer was adopted and modified from (Gu et al., 2004).

(B) Purified DcpS^{WT/WT} and DcpS^{WT/Inert} were resolved by SDS-PAGE and stained with Sypro Ruby. A co-purified protein GroEL was also shown. The quantitation of the concentrations of DcpS proteins is stated in Materials and Methods.

(C) The DcpS^{Inert/Inert} homodimer has no detectable decapping activity. An *in vitro* decapping assay was carried out with the indicated amount of DcpS^{Inert/Inert} homodimer (monomer concentration, nM) and 200 nM cold cap structure spiked with hot cap structure. The reactions were incubated for 30 sec at room temperature and terminated by 1.6N formic acid. The hydrolyzed product m⁷Gp and unhydrolyzed cap structure substrate were resolved by thin-layer chromatography (TLC) and exposed to PhosphorImager.

(D) The rapid quench-flow decapping assays of DcpS^{WT/WT} and DcpS^{WT/Inert} carried out under single turnover conditions. 100 nM monomer concentration of DcpS^{WT/WT} and DcpS^{WT/Inert} were used with 10 nM of cold cap substrate spiked with hot cap substrate.

(E) The rapid quench-flow decapping assays of DcpS^{WT/WT} and DcpS^{WT/Inert} carried out under multiple turnover conditions. 100 nM monomer concentration of DcpS^{WT/WT} and DcpS^{WT/Inert} were used with 800 nM of cold cap substrate spiked with hot cap substrate.

(F) The decapping rates in (D) and (E) were quantitated and plotted against the reaction times. The data points for each set of experiment were fit to a single exponential equation (Equation 3) to obtain the rate constants. As shown in the curves, the decapping rates for both DcpS^{WT/WT} and DcpS^{WT/Inert} decreased over increasing amount of substrate.

Table 3. The rate constants and maximal decapping rates of DcpS^{WT/WT}, DcpS^{WT/Inert}, and DcpS^{WT/HIT} under single and multiple turnover conditions

	DcpS ^{WT/WT}	DcpS ^{WT/Inert}	DcpS ^{WT/HIT}
E100S10	C=0.14 s⁻¹ R= 0.79	C=0.067 s⁻¹ R=0.70	C=0.52 s⁻¹ R=0.18
E100S800	C=0.028 s⁻¹ R= 0.30	C= 0.026 s⁻¹ R= 0.13	
Rate constant change, Low substrate /High substrate	5 fold	2.5 fold	

Table 3. The rate constants and decapping rates from experiments in Fig 13 and Fig 14 were listed in Table 3. Under multiple turnover conditions, the rate constants and decapping rates of both DcpS^{WT/WT} and DcpS^{WT/Inert} decreased. The fold change of rate constants were calculated as listed. The rate constant was reduced by 5 fold for DcpS^{WT/WT}, but only 2.5 fold for DcpS^{WT/Inert}. The reduced fold change for DcpS^{WT/Inert} indicates a decreased negative cooperativity under multiple turnover conditions.

double mutant within each monomer was constructed and the expressed protein with a dual mutation within each of the two cap binding sites ($\text{DcpS}^{\text{Inert/Inert}}$) was generated and tested for decapping activity. As shown in Fig 13C, the $\text{DcpS}^{\text{Inert/Inert}}$ homodimer did not contain detectable decapping activity (lanes 6-13) as opposed to 100% decapping activity from the same concentration of wild type protein ($\text{DcpS}^{\text{WT/WT}}$, lanes 2-5). The decapping results demonstrate that the presence of both the N110A and W175A substitutions within the same active site has the capacity to disrupt decapping to undetectable levels within our assay system. Furthermore, these data suggest that a heterodimer that generates one wild type active site and the other site with the N110A and W175A mutations should contain only one active site capable of binding and decapping cap structure while the site with the double mutation would be inactive and contains only minimal, if any, binding ability to the cap structure.

Decapping of the double tagged $\text{DcpS}^{\text{WT/WT}}$ compared to the heterodimer with one wild type site and one inert site ($\text{DcpS}^{\text{WT/Inert}}$) was next tested. Decapping assays were carried out with $\text{DcpS}^{\text{WT/WT}}$ or $\text{DcpS}^{\text{WT/Inert}}$ under single turnover conditions (50nM dimer concentration of DcpS enzyme, 10nM cap substrate) and multiple turnover conditions (50nM dimer concentration enzyme, 800nM cap substrate). The decapping products were resolved by TLC (Fig 13D, E) and the decapping rate was plotted against the reaction time (Fig 13F). The curves in Fig 13F were fit to a single exponential equation (Equation 3). The rate constants and maximal decapping rates were determined from the equation coefficients and listed in Table 3. The rate constant for $\text{DcpS}^{\text{WT/WT}}$, under multiple turnover conditions was reduced by 5 fold compared to the single turnover conditions (0.028 s^{-1} vs. 0.14 s^{-1}), consistent with the data shown in Fig11, Fig12, and

Table 2, suggesting the existence of negative cooperativity. Interestingly, under steady state condition, the $\text{DcpS}^{\text{WT/Inert}}$ rate constant was reduced by only 2.5 fold compared to the single turnover conditions (0.026s^{-1} vs. 0.067s^{-1}), indicating similar to the $\text{DcpS}^{\text{WT/WT}}$ wild type homodimer, higher substrate negatively impacts hydrolysis of the active site but the impact is half as great. These data demonstrate negative cooperativity between the two active sites of the DcpS enzyme. The failure of the $\text{DcpS}^{\text{WT/Inert}}$ heterodimer to be completely resistant to negative cooperativity rather than partially resistant could be due to the ability of the double mutant inert site to still have partial binding capacity (see Discussion).

A requirement for pivoting of the N-terminus for efficient cap binding and hydrolysis

Structural analysis of DcpS has revealed that it is a dimeric protein, with two active sites that are created with contributions from both the N-terminal and C-terminal domains (Gu et al., 2004). By virtue of the hinge that separates the two domains, the N-terminus has the capacity to flip from one side to the other creating a closed complex bound to a cap substrate on one side to initiate hydrolysis which in turn would force an open conformation on the other side, and vice versa (Gu et al., 2004). Therefore, the structural data does not support a simultaneous and independent activity of both active sites but rather is consistent with a mutually exclusive activity of both sites. If this proposed mechanism is true, both sides of the DcpS protein are not able to close at the same time. A prediction would be that when one side is locked into the closed confirmation, the other side would remain open and would not be able to close freely to

cleave its bound cap. To test this hypothesis biochemically, a heterodimer with one wild type active site and the other containing an asparagine substitution at His 277 in the HIT motif which renders the protein inactive (Liu et al., 2002) yet still competent to bind cap, was generated and tested in decapping assays (Fig 14B).

The DcpS H277N (DcpS^{HIT/HIT}) homodimer was first characterized for its binding property to cap ligand. Interestingly, it was able to bind the cap structure as assessed by the detection of a bound complex by an electrophoretic mobility shift assay (Figure 14C). Neither the wild type nor any of the other mutant proteins containing mutations in amino acids that contact the cap, were able to stably bind the cap structure (Fig 14C). Therefore, the HIT mutant cap binding site within the DcpS^{WT/HIT} is expected to function similarly and trap the cap substrate without hydrolyzing it while the second site should remain analogous to a wild type active site capable of binding and hydrolyzing the cap substrate.

Rapid quench-flow decapping assays were carried out with the DcpS^{WT/HIT} heterodimer under single turnover (50nM protein dimer, 10nM substrate) and multiple turnover (50nM protein dimer, 800 nM substrate) conditions and the decapping products were resolved by TLC (Fig 14D). The data points for single turnover experiment were fit to a biphasic, double exponential curve (Fig 14E and Equation 3), and the kinetic values were calculated from the equation and listed in Table 2. As shown in Fig 14D, under single turnover conditions the DcpS^{WT/HIT} protein was catalytically active, however, the decapping amplitude only reached 20% at the first exponential phase, compared to 76% for DcpS^{WT/WT} (compare Fig14E and Fig 11C). These data suggest that 80% of the cap

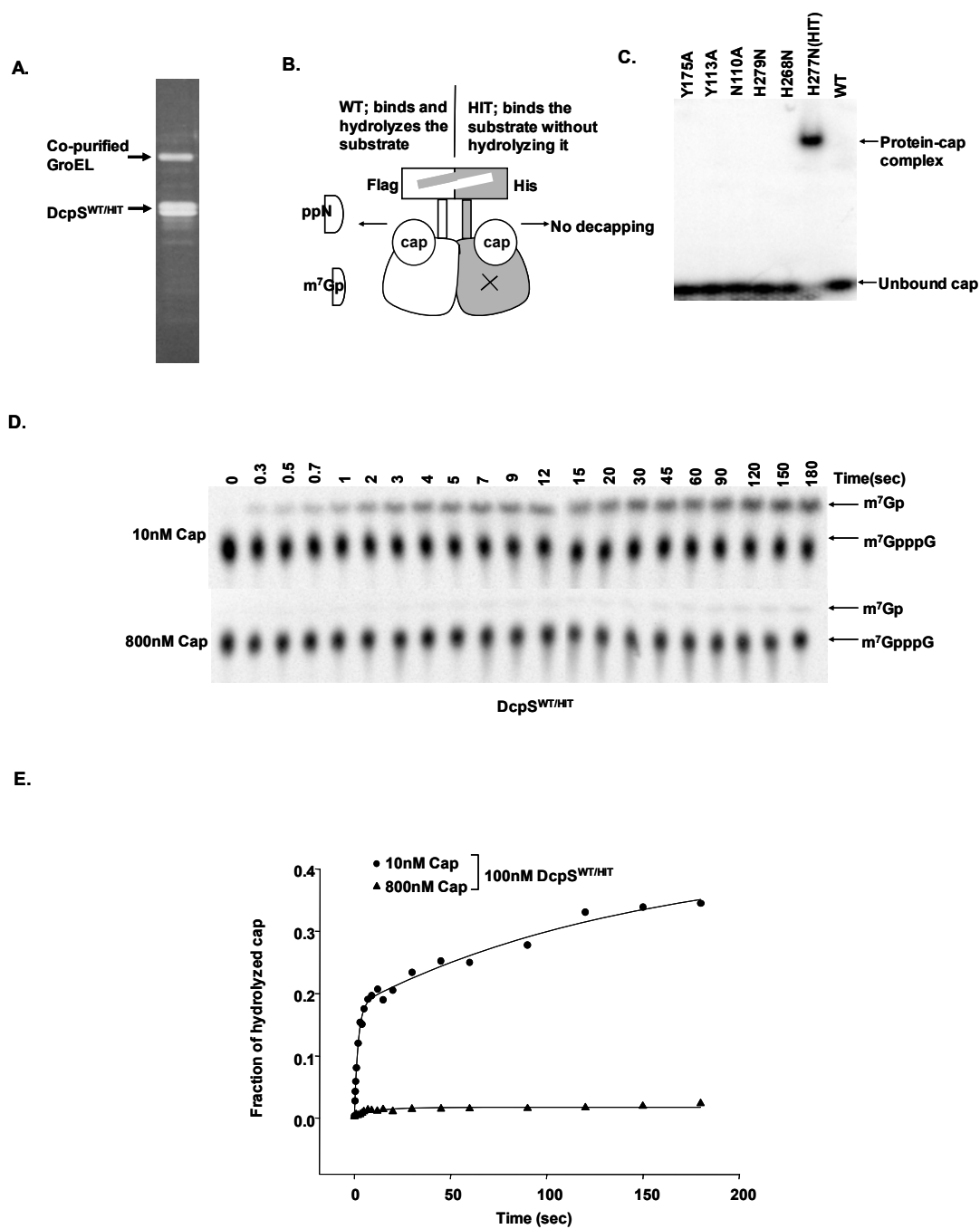


Figure 14. Trapping of cap substrate at the HIT mutant site of DcpS^{WT/HIT} prevents hydrolysis from the active site.

- (A) Purified DcpS^{WT/HIT} was resolved on SDS-PAGE and stained by Sypro Ruby. A co-purified protein GroEL was also shown.
- (B) Cartoon representations of DcpS^{WT/HIT} heterodimer with double tags. The HIT site binds cap structure but is unable to hydrolyze it.
- (C) An EMSA was used to test the ability of WT DcpS and the other mutant proteins to bind the ³²P-labeled cap analog. The DcpS H277N (DcpS^{HIT/HIT}) is the only protein that bound to the labeled cap analog under the given EMSA conditions.
- (D) The rapid quench-flow decapping assays of DcpS^{WT/HIT} carried out under single and multiple turnover conditions. Single turnover: 100 nM monomer concentration of enzyme and 10 nM substrate. Multiple turnover: 100 nM monomer concentration of enzyme and 800 nM of substrate.
- (E) The decapping rates in each set of experiments were quantitated and plotted against the reaction times. The data points of the single turnover condition were fit to a biphasic, double exponential curve (Equation 5). The maximal decapping rate of the multiple turnover experiment is lower than 2%.

substrate was captured at the inactive HIT side, while only 20% was bound by the WT side and was hydrolyzed. They further suggest that the HIT mutant-containing cap binding site had a stronger affinity for the cap substrate and was able to bind and trap a majority of the cap substrate. The second exponential phase might represent the fact that substrates bound at the HIT side were slowly released and eventually hydrolyzed by the wild type side. As expected, under multiple turnover conditions, there was a precipitous decrease in decapping with less than 2% of decapping observed. This latter data suggests that the HIT mutant side of all the DcpS dimers were bound and locked by the cap substrates, therefore the WT side was forced to remain in the open confirmation and unable to hydrolyze other cap substrates. These data confirm the proposed mechanism that the N-termini of DcpS dimer cannot simultaneously function to hydrolyze a cap at both binding sites with both sites in the closed confirmation. They demonstrate that only one site can be closed while the second site is obligatorily forced into an open confirmation.

Discussion

In this report, we present kinetic analysis of DcpS and elucidate several novel insights into its decapping mechanism at the subunit level. Interestingly, the rate limiting step of the decapping reaction varied depending on the substrate concentration. The reaction was limited at the initial binding step under single turnover conditions but shifted to the hydrolysis step under high substrate conditions (Table 2 and Table 3). Furthermore, the DcpS decapping reaction was susceptible to product inhibition (Figures

12B and 12D) as well as negative cooperativity (Table 2 and Table 3). Lastly, we demonstrate that a dynamic conformational change of the N-terminal domain relative to the C-terminal domain which closes and opens on a cap substrate is necessary for productive decapping, as mutant heterodimers that remained locked on one side in the closed conformation failed to function in cap hydrolysis on the second site confirming a mutually exclusive hydrolysis function for both sites.

The first interesting finding in this report is that the rate-limiting step changed from the initial binding step to the subsequent hydrolysis step when higher amounts of substrate were used (Figures 11 and 12). One possible reason is that higher substrate concentrations induce allosteric conformational changes between the two protomers, resulting in a slower hydrolysis step. Negative allosteric regulation of DcpS is supported by several observations. First, the rate constant was reduced by 5 fold with wild type DcpS homodimer under high substrate conditions, while the DcpS^{WT/Inert} heterodimer with one wild type active site and an inert active site, only displayed a 2.5 fold reduction of the rate constant (Table 3). Although we expected the DcpS^{WT/Inert} to be highly resistant to negative cooperativity rather than only partially resistant, since two residues essential for cap binding were mutated, it appears that the mutant protomer we predicted would be inert, still retains some level of cap binding. This is not surprising considering the extensive network of contacts from numerous amino acid residues between DcpS and the cap structure (Gu et al., 2004).

Our data are consistent with an inherent negative cooperativity of the two active sites within DcpS as indicated by the cap bound co-crystal structure (Chen et al., 2005; Gu et al., 2004). A model was proposed whereby the N termini of both protomers within

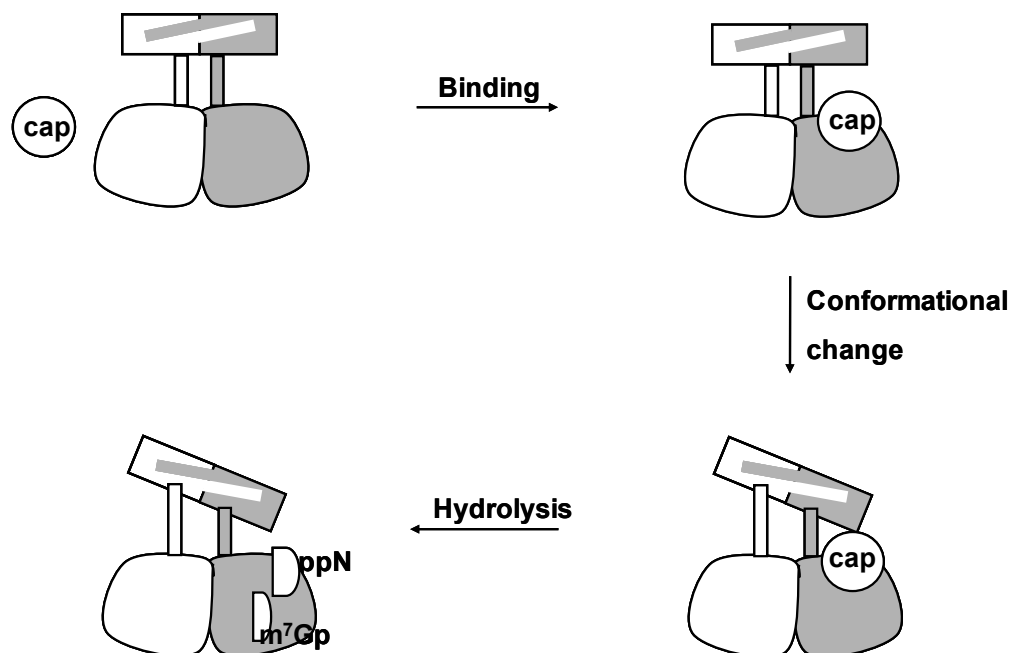
the DcpS dimer acts as a single inflexible domain that can alternate back and forth to form a hydrolysis competent closed and open conformations, or an intermediate state of both sites in the open confirmation (Chen et al., 2005; Gu et al., 2004). The high rigidity of the two intertwined N terminal domains prevents them from closing at the same time. Therefore, when an N terminus on a protomer closes for hydrolysis, the one on the other is forced into an open position. Although the site in the open conformation is capable of cap substrate binding (Gu et al., 2004), the affinity would be lower than that of the closed site, since the open protomer lacks the interacting forces contributed by the N terminus to stabilize the association of the cap substrate (Fig 15B). Therefore, the DcpS dimer displays inherent negative cooperativity between the first and second binding of its substrate. The fact that the hydrolysis on the second site has to wait until the one on the first site has completed hydrolysis and converts to the open confirmation contributes to the reduced overall chemical hydrolysis step. Our results with the DcpS^{WT/HIT} heterodimer provide experimental confirmation for the negative allosteric model where less than 2% decapping activity was detected with high substrate (Fig 14C). Therefore, the biochemical analysis indicates that the WT site was not able to conform to a closed productive confirmation for hydrolysis when the HIT mutant site was bound and “locked” by the substrate.

Taken together, our analysis of the heterodimer combined with the decapping observed with the wild type DcpS homodimer under both low and high substrates and the known structural properties of DcpS collectively suggests the following model of hydrolysis: Under single turnover conditions, upon binding to the cap substrate at one binding site, the N terminus at this site closes for substrate cleavage, followed by release

of the m^7Gp and ppN decapping product to complete a catalytic cycle (Fig 15A). Since the amount of substrate is lower than the enzyme, only one protomer is used per cycle. Therefore, there is no allosteric communication between the first and second protomer. Under multiple turnover conditions, upon binding of a cap substrate at the first binding site, the N terminus closes for substrate cleavage. The rigidity of the domain swapped region forces the N terminus of the second protomer to stay in an open position. Subsequently, a second cap substrate can associate with the C terminus of the second site with weaker affinity, waiting for its turn for cleavage. After the substrate bound at the first site is hydrolyzed, the hydrolyzed products are released and the N terminus of the second site closes for hydrolysis. Following the cleavage at the second site, the hydrolyzed products are released, and the ligand free DcpS returns to its symmetric open/open form to complete a catalytic cycle (Fig 15B).

DcpS is also negatively regulated by product inhibition. A reduction of DcpS decapping rate was observed with increasing cap substrate concentrations. Since m^7Gp is as effective a competitor of DcpS decapping as is cap structure (Liu et al., 2002), this rate reduction can be attributed to an accumulation of the m^7Gp decapping product. As the decapping product accumulates, it can serve as a negative competitor and inhibit DcpS decapping and provide a means to regulate its activity.

Negative allosteric regulation has also been reported in another domain swapped protein, bovine seminal ribonuclease (BS-RNase). Similar to DcpS, BS-RNase is a dimeric domain swapped protein with the two protomers exchanging N terminal segments (Capasso et al., 1983; Piccoli et al., 1992). Interestingly, the negative cooperativity modulates its enzymatic reaction at the rate-limiting hydrolytic step under

A.**Fig 15**

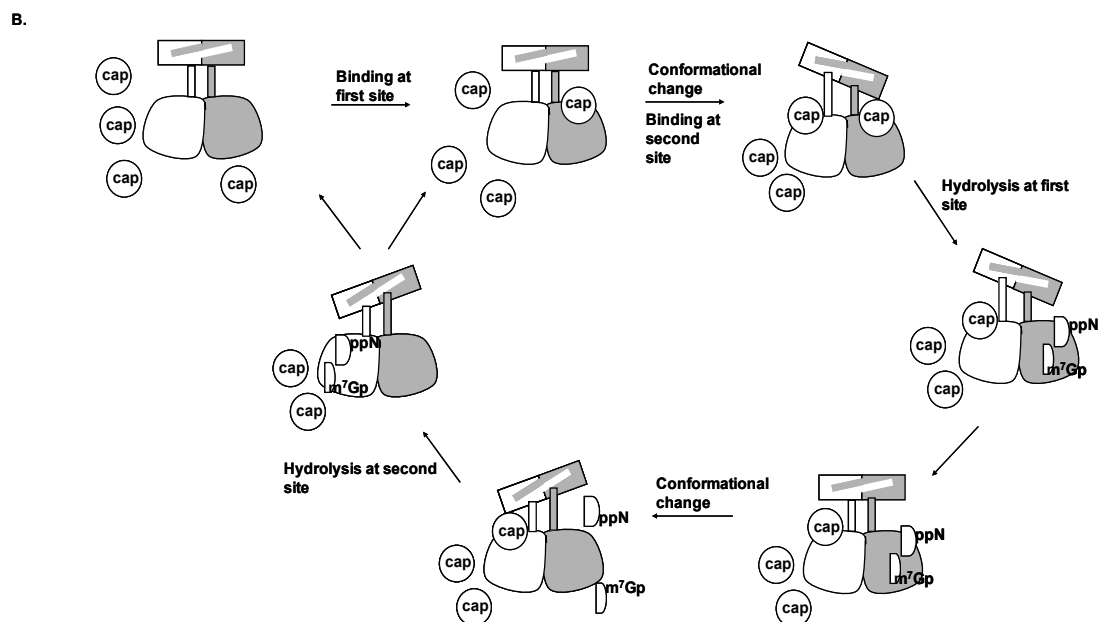


Figure 15. Models of decapping mechanism under single (low substrate) and multiple turnover (high substrate) conditions.

(A) Decapping model with low substrate displays no cooperativity between two protomers. The ligand-free DcpS dimer exhibits a symmetric conformation. Upon binding to the cap substrate at one binding site, the N terminus at this site closes for substrate cleavage, followed by releasing of the decapping product m⁷Gp and ppN to complete a catalytic cycle. Only one protomer is used per cycle, therefore there is no allosteric communication between the first and second protomer.

(B) DcpS hydrolysis of cap substrate displays negative cooperativity under multiple turnover conditions. Upon binding of a cap substrate at the first binding site, the N terminus closes for substrate cleavage. The rigidity of the domain swapped region

forcing the N terminus of the second protomer to stay in an open position. Subsequently, a second cap substrate is associated to the C terminus of the second site. The binding affinity of the cap to the second site is weaker as it lacks the stabilizing contacts from the N terminus which is in the open position. After the substrate bound at the first site is hydrolyzed, the decapping products are released, and the N terminus of the second site closes for hydrolysis followed by product release to complete the catalytic cycle. The ligand free DcpS then returns to the symmetric open/open configuration.

high substrate concentrations (Piccoli et al., 1988; Piccoli et al., 1982), analogous to what we observed for DcpS (Figure 12). The negative cooperativity was ascribed to the domain swapped nature of BS-RNase, as no cooperativity was observed for its non-swapped dimeric form or monomeric form (Piccoli et al., 1988; Piccoli et al., 1992),.

Allosteric regulation of the rate-limiting enzyme is an important mechanism to tightly control the flux through a metabolic pathway. This type of regulation is widespread in oligomeric proteins and is an important mechanism to regulate enzyme activity and receptor-ligand binding, particularly in enzymes at key branch points in metabolic pathways and in receptors that are sensitive to small signals (Koshland, 1996; Koshland and Hamadani, 2002). A classic example is phosphofructokinase (PFK), a key regulatory enzyme in glycolysis pathway. PFK is a tetrameric enzyme composed of four identical subunits. It catalyzes the phosphorylation of fructose-1,6-bisphosphate (F6P) to fructose-1,6-bisphosphate, the rate-limiting step in glycolytic pathway. Binding of the substrate F6P to PFK is highly positively cooperative, whereas binding of a later step product in the glycolytic pathway, phosphoenolpyruvate (PEP) is negatively cooperative (Blangy et al., 1968; Schirmer and Evans, 1990). Since PFK is the rate limiting enzyme of the glycolytic pathway, the feedback inhibition reduces the rate of glycolysis when the cell does not require energy and is important to finely tune the flux of glycolysis in cells.

An interesting mechanism that regulates DcpS protein activity has been revealed in *Saccharomyces cerevisiae*. This organism contains two DcpS homologs, Dcs1p and Dcs2p with only Dcs1p containing decapping activity (Liu et al 2002). Dcs1p and

Dcs2p, are involved in a stress response mechanism to survive glucose deficiency (Malys et al., 2004). Under glucose-deprived conditions, the catalytically inactive paralog, Dcs2p, was shown to heterodimerize with catalytically active Dcs1p and compromise its substrate specificity and K_{cat} (Malys et al., 2004; Malys and McCarthy, 2006). The DcpS^{WT/HIT} human protein heterodimer is analogous to this situation with one active and one inactive protomers and similarly led to a dramatic decrease in decapping (Figure 14). However, there does not appear to be a Dcs1p-like protein in human cells suggesting that a heterodimer mediated inhibition is unlikely, however our data indicates that nonhydrolyzable substrates or compounds could bind in one active site and inhibit decapping by trapping the protein in an inactive state.

DcpS has been characterized as an mRNA decapping enzyme that is involved in mRNA decay. Whether DcpS is involved in other cellular processes is still an open question. An obvious metabolic pathway DcpS may impact includes nucleotide biogenesis and catabolic pathways due to its ability to hydrolyze cap dinucleotides. Although DcpS acts as the last step of an mRNA decay pathway to “scavenge” the 3'-5' decay leftover cap oligonucleotide and release the decapping product m⁷G, previous studies showed that the end product m⁷G was further hydrolyzed by an unknown enzyme activity to release m⁷Guanine (Gang and Lavers, 1980). Moreover, a more recent report showed that m⁷Gp is dephosphorylated by an unknown phosphatase (Wang and Kiledjian, 2001). The results from both reports indicate that m⁷Gp is not the actual end product of the decay pathway. After cleaved from m⁷Gp, m⁷Guanine might be further processed, possibly by demethylation. Although the cellular activity representing the removal of the methyl group is unclear, it would not be surprising if a demethylase activity exists in cells.

It is well known that the modifications of macromolecules are reversible, such as phosphorylation, glycosylation, and acetylation, indicating the enzymatic activities that remove these modifications coexist in cells. Furthermore, a recent finding of demethylase AlkB, which removes the methyl group of 1-methyladenine and 3-methylcytosine lesions in mRNAs and tRNAs (Aas et al., 2003; Ougland et al., 2004; Yu et al., 2006), is supportive of the possible existence of the m^7 Guanine demethylase. The demethylated guanine base can be either reutilized for nucleotide biosynthesis by a salvage reaction, or catabolized into the end product uric acid (Watts, 1983; Wyngaarden, 1976). The negative modulation of DcpS decapping under high substrate conditions may possibly provide a regulating point to control the amount of uric acid generated, whose rapid accumulation is harmful to human body. Thus, when there is high amount of cap structure accumulated in cells, DcpS adopts the negative allosteric regulation strategy in cap hydrolysis to prevent a sudden burst of downstream uric acid formation. When the cellular cap structure drops to the low level, DcpS switches to the single turnover kinetics without the allosteric regulation.

In addition, regulation of DcpS activity impacts earlier steps of mRNA decay, as the disruption of yeast Dcs1p (DcpS homolog) decapping activity results in inhibition of 5' to 3' exonuclease activity (Liu and Kiledjian, 2005). As shown in this report, local increase of the substrate, as well as the decapping product would inhibit DcpS decapping, which is analogous to the disruption of Dcs1. Thus, substrate and product inhibition of DcpS, which is part of the last step in mRNA decay, could be a means to feedback and regulate earlier steps in mRNA decay. Therefore, the negative cooperative nature of DcpS activity may provide a regulatory point for crosstalk between both pathways.

In conclusion, our data provide evidence that DcpS exhibits different enzymatic kinetics under low and high substrate conditions. The presence of negative cooperativity between two wild type subunits, as well as the dramatically reduced decapping activity displayed by the DcpS^{WT/HIT} heterodimer under high substrate conditions validate our previous dynamic decapping model (Gu et al., 2004). Future studies to determine the local concentrations of DcpS protein and cap dinucleotide will begin to test the negative allosteric regulatory model proposed.

References

- Aas, P.A., Otterlei, M., Falnes, P.O., Vågbo, C.B., Skorpen, F., Akbari, M., Sundheim, O., Bjørås, M., Slupphaug, G., Seeberg, E. and Krokan, H.E. (2003) Human and bacterial oxidative demethylases repair alkylation damage in both RNA and DNA. *Nature*, **421** 859-863.
- Allmang, C., Petfalski, E., Podtelejnikov, A., Mann, M., Tollervey, D. and Mitchell, P. (1999b) The yeast exosome and human PM-Scl are related complexes of 3' → 5' exonucleases. *Genes Dev*, **13**, 2148-2158.
- Amberg, D.C., Goldstein, A.L. and Cole, C.N. (1992) Isolation and characterization of RAT1: an essential gene of *Saccharomyces cerevisiae* required for the efficient nucleocytoplasmic trafficking of mRNA. *Genes Dev*, **6**, 1173-1189.
- Anderson, J.S.J. and Parker, R.P. (1998) The 3' to 5' degradation of yeast mRNAs is a general mechanism for mRNA turnover that requires the SKI2 DEVH box protein and 3' to 5' exonucleases of the exosome complex. *Embo J*, **17**, 1497-1506.
- Araki, Y., Takahashi, S., Kobayashi, T., Kajiho, H., Hoshino, S. and Katada, T. (2001) Ski7p G protein interacts with the exosome and the Ski complex for 3'-to-5' mRNA decay in yeast. *EMBO J*, **20**, 4684-4693.
- Bashkirov, V.I., Scherthan, H., Solinger, J.A., Buerstedde, J.M. and Heyer, W.D. (1997) A mouse cytoplasmic exoribonuclease (mXRN1p) with preference for G4 tetraplex substrates. *J Cell Biol*, **136**, 761-773.
- Beelman, C.A., Stevens, A., Caponigro, G., LaGrandeur, T.E., Hatfield, L., Fortner, D.M. and Parker, R. (1996) An essential component of the decapping enzyme required for normal rates of mRNA turnover. *Nature*, **382**, 642-646.

- Benard, L. (2004) Inhibition of 5' to 3' mRNA degradation under stress conditions in *Saccharomyces cerevisiae*: from GCN4 to MET16. *Rna*, **10**, 458-468.
- Bentley, D. (1999) Coupling RNA polymerase II transcription with pre-mRNA processing. *Curr Opin Cell Biol*, **11** 347-351.
- Bentley, D. (2002) The mRNA assembly line: transcription and processing machines in the same factory. *Curr Opin Cell Biol*, **14**, 336-342.
- Bentley, D.L. (2005) Rules of engagement: co-transcriptional recruitment of pre-mRNA processing factors. *Curr Opin Cell Biol*, **17**, 251-256.
- Bessman, M.J., Frick, D.N. and O'Handley, S.F. (1996) The MutT proteins or "Nudix" hydrolases, a family of versatile, widely distributed, "housecleaning" enzymes. *J Biol Chem*, **271**, 25059-25062.
- Bienroth, S., Keller, W. and Wahle, E. (1993) Assembly of a processive messenger RNA polyadenylation complex. *EMBO J.*, **12**, 585-594
- Blangy, D., Buc, H. and Monod, J. (1968) Kinetics of the allosteric interactions of phosphofructokinase from *Escherichia coli*. *J Mol Biol* **31**, 13-35.
- Boeck, R., Lapeyre, B., Brown, C.E. and Sachs, A.B. (1998) Capped mRNA degradation intermediates accumulate in the yeast *spb8-2* mutant. *Mol Cell Biol*, **18**, 5062-5072.
- Boeck, R., Tarun, S., Jr., Rieger, M., Deardorff, J.A., Muller-Auer, S. and Sachs, A.B. (1996) The yeast Pan2 protein is required for poly(A)-binding protein-stimulated poly(A)-nuclease activity. *J Biol Chem*, **271**, 432-438.
- Bousquet-Antonelli, C., Presutti, C. and Tollervy, D. (2000) Identification of a regulated pathway for nuclear pre-mRNA turnover. *Cell*, **102**, 765-775.
- Bouveret, E., Rigaut, G., Shevchenko, A., Wilm, M. and Seraphin, B. (2000) A Sm-like protein complex that participates in mRNA degradation. *Embo J*, **19**, 1661-1671.
- Braun, I.C., Herold, A., Rode, M. and Izaurralde, E. (2002) Nuclear export of mRNA by TAP/NXF1 requires two nucleoporin-binding sites but not p15. *Mol Cell Biol*, **22**, 5405-5418.
- Brenner, C. (2002) Hint, Fhit, and GalT: function, structure, evolution, and mechanism of three branches of the histidine triad superfamily of nucleotide hydrolases and transferases. *Biochemistry*, **41**, 9003-9014.
- Brenner, C., Bieganowski, P., Pace, H.C. and Huebner, K. (1999) The histidine triad superfamily of nucleotide-binding proteins. *J Cell Physiol*, **181**, 179-187.

- Brenner, C., Garrison, P., Gilmour, J., Peisach, D., Ringe, D., Petsko, G.A. and Lowenstein, J.M. (1997) Crystal structures of HINT demonstrate that histidine triad proteins are GalT-related nucleotide-binding proteins. *Nat Struct Biol*, **4**, 231-238.
- Brown, C.E. and Sachs, A.B. (1998) Poly(A) tail length control in *Saccharomyces cerevisiae* occurs by message-specific deadenylation. *Mol Cell Biol*, **18**, 6548-6559.
- Brown, C.E., Tarun, S.Z., Jr., Boeck, R. and Sachs, A.B. (1996) PAN3 encodes a subunit of the Pab1p-dependent poly(A) nuclease in *Saccharomyces cerevisiae*. *Mol Cell Biol*, **16**, 5744-5753.
- Burkard, K.T. and Butler, J.S. (2000) A nuclear 3'-5' exonuclease involved in mRNA degradation interacts with Poly(A) polymerase and the hnRNA protein Npl3p. *Mol Cell Biol*, **20**, 604-616.
- Capasso, S., Giordano, F., Mattia, C.A., Mazzarella, L. and Zagari, A. (1983) Refinement of the structure of bovine seminal ribonuclease. *Biopolymers*, **22**, 327-332.
- Caponigro, G. and Parker, R. (1995) Multiple functions for the poly(A)-binding protein in mRNA decapping and deadenylation in yeast. *Genes Dev*, **9**, 2421-2432.
- Carter, M.S., Li, S. and Wilkinson, M.F. (1996) A splicing-dependent regulatory mechanism that detects translation signals. *EMBO J* **15**, 5965-5975.
- Chang, Y.F., Imam, J.S. and Wilkinson, M.F. (2007) The nonsense-mediated decay RNA surveillance pathway. *Annu Rev Biochem*, **76**, 51-74.
- Chen, C.Y. and Shyu, A.B. (1995) AU-rich elements: characterization and importance in mRNA degradation. *Trends Biochem Sci*, **20**, 465-470.
- Chen, J., Chiang, Y.C. and Denis, C.L. (2002) CCR4, a 3'-5' poly(A) RNA and ssDNA exonuclease, is the catalytic component of the cytoplasmic deadenylase. *Embo J*, **21**, 1414-1426.
- Chen, N., Walsh, M.A., Liu, Y., Parker, R. and Song, H. (2005) Crystal structures of human DcpS in ligand-free and m7GDP-bound forms suggest a dynamic mechanism for scavenger mRNA decapping. *J Mol Biol*, **347**, 707-718.
- Cole, C.N. and Scarcelli, J.J. (2006a) Transport of messenger RNA from the nucleus to the cytoplasm. *Curr Opin Cell Biol*, **18**, 299-306.
- Cole, C.N. and Scarcelli, J.J. (2006b) Unravelling mRNA export. *Nat Cell Biol*, **8**, 645-647.

- Colgan, D.F. and Manley, J.L. (1997) Mechanism and regulation of mRNA polyadenylation. *Genes Dev*, **11**, 2755-2766.
- Collart, M.A. (2003) Global control of gene expression in yeast by the Ccr4-Not complex. *Gene*, **313**, 1-16.
- Coller, J. and Parker, R. (2004) Eukaryotic mRNA Decapping. *Annu Rev Biochem*, **73**, 861-890.
- Conaway, J.W., Shilatifard, A., Dvir, A. and Conaway, R.C. (2000) Control of elongation by RNA polymerase II. *Trends Biochem Sci* **25**, 375-380.
- Corden, J.L. (1990) Tails of RNA polymerase II. *Trends Biochem Sci*, **15**, 383-387.
- Cougot, N., van Dijk, E., Babajko, S. and Séraphin, B. (2004) 'Cap-tabolism'. *Trends Biochem Sci* **29**, 436-444.
- Dargemont, C. and Kuhn, L.C. (1992) Export of mRNA from microinjected nuclei of *Xenopus laevis* oocytes. *J. Cell Biol.*, **118**, 1-9.
- Das, B., Butler, J.S. and Sherman, F. (2003) Degradation of normal mRNA in the nucleus of *Saccharomyces cerevisiae*. *Mol Cell Biol*, **23**, 5502-5515.
- Decker, C.J. and Parker, R. (1993) A turnover pathway for both stable and unstable mRNAs in yeast: evidence for a requirement for deadenylation. *Genes Dev*, **7**, 1632-1643.
- Decker, C.J. and Parker, R. (1994) Mechanisms of mRNA degradation in eukaryotes. *Trends Biochem Sci*, **19**, 336-340.
- Dehlin, E., Wormington, M., Korner, C.G. and Wahle, E. (2000) Cap-dependent deadenylation of mRNA. *Embo J*, **19**, 1079-1086.
- Dichtl, B., Stevens, A. and Tollervy, D. (1997) Lithium toxicity in yeast is due to the inhibition of RNA processing enzymes. *Embo J*, **16**, 7184-7195.
- Dunckley, T. and Parker, R. (1999) The DCP2 protein is required for mRNA decapping in *Saccharomyces cerevisiae* and contains a functional MutT motif. *Embo J*, **18**, 5411-5422.
- Edery, I. and Sonenberg, N. (1985) Cap-dependent RNA splicing in a HeLa nuclear extract. *Proc Natl Acad Sci U S A*, **82**, 7590-7594.

- Egyházi, E., Ossoinak, A., Pigon, A., Holmgren, C., Lee, J.M. and Greenleaf, A.L. (1996) Phosphorylation dependence of the initiation of productive transcription of Balbiani ring 2 genes in living cells. *Chromosoma*, **104**, 422-433.
- Fang, F., Phillips, S. and Butler, J.S. (2005) Rat1p and Rai1p function with the nuclear exosome in the processing and degradation of rRNA precursors. *RNA*, **11**, 1571-1578.
- Fenger-Gron, M., Fillman, C., Norrild, B. and Lykke-Andersen, J. (2005) Multiple processing body factors and the ARE-binding protein TTP activate mRNA decapping. *Mol Cell*, **20**, 905-915.
- Fong, N. and Bentley, D.L. (2001) Capping, splicing, and 3' processing are independently stimulated by RNA polymerase II: different functions for different segments of the CTD. *Genes Dev*, **15**, 1783-1795.
- Frischmeyer, P.A., van Hoof, A., O'Donnell, K., Guerrierio, A.L., Parker, R. and Dietz, H.C. (2002) An mRNA surveillance mechanism that eliminates transcripts lacking termination codons. *Science*, **295**, 2258-2261.
- Furuichi, Y., Morgan, M., Shatkin, A.J., Jelinek, W., Salditt-Georgieff, M. and E., D.J. (1975) Methylated, Blocked 5' Termini in HeLa Cell mRNA. *Proc. Nat. Acad. Sci. USA*, **72** 1904-1908.
- Gabelli, S.B., Bianchet, M.A., Bessman, M.J. and Amzel, L.M. (2001) The structure of ADP-ribose pyrophosphatase reveals the structural basis for the versatility of the Nudix family. *Nat Struct Biol*, **8**, 467-472.
- Gang, G. and Lavers, G.C. (1980) Detection of an enzyme activity which cleaves m⁷GUANINE from m⁷GMP in an extract of embryonic chick lens cells. *Mol Bio Rep*, **6**, 35-38.
- Gao, M., Fritz, D.T., Ford, L.P. and Wilusz, J. (2000) Interaction between a Poly(A)-Specific Ribonuclease and the 5' Cap Influences mRNA Deadenylation Rates In Vitro. *Molecular Cell*, **5**, 479-488.
- Garneau, N.L., Wilusz, J. and Wilusz, C.J. (2007) The highways and byways of mRNA decay. *Nat Rev Mol Cell Biol*, **8**, 113-126.
- Gasteiger, E., Hoogland, C., Gattiker, A., Duvaud, S., Wilkins, M.R., Appel, R.D. and Bairoch, A. (2005) Protein Identification and Analysis Tools on the ExPASy Server. (In) John M. Walker (ed): The Proteomics Protocols Handbook. Humana Press. pp. 571-607

- Geerlings, T.H., Vos, J.C. and Raue, H.A. (2000) The final step in the formation of 25S rRNA in *Saccharomyces cerevisiae* is performed by 5' 3' exonucleases. *RNA*, **6**, 1698–1703.
- Gerber, H.P., Hagmann, M., Seipel, K., Georgiev, O., West, M.A.L., Litington, Y., Schaffner, W. and Corden, J.L. (1995) RNA polymerase II C-terminal domain required for enhancer-driven transcription. *Nature*, **374** 660 - 662
- Ghosh, T., Peterson, B., Tomasevic, N. and Peculis, B.A. (2004) *Xenopus* U8 snoRNA Binding Protein Is a Conserved Nuclear Decapping Enzyme. *Mol Cell*, **13**, 817-828.
- Gill, S.C. and von Hippel, P.H. (1989) Calculation of protein extinction coefficients from amino acid sequence data. *Anal Biochem*, **182**, 319-326.
- Gingerich, T.J., Feige, J.J. and LaMarre, J. (2004) AU-rich elements and the control of gene expression through regulated mRNA stability. *Anim Health Res Rev*, **5**, 49-63.
- Gingras, A.C., Raught, B. and Sonenberg, N. (1999) eIF4 INITIATION FACTORS: Effectors of mRNA Recruitment to Ribosomes and Regulators of Translation. *Annu Rev Biochem*, **68**, 913-963.
- Gordon, P.M., Sontheimer, E.J. and Piccirilli, J.A. (2000) Metal ion catalysis during the exon-ligation step of nuclear pre-mRNA splicing: extending the parallels between the spliceosome and group II introns. *RNA*, **6**, 199-205.
- Gu, M., Fabrega, C., Liu, S.W., Liu, H., Kiledjian, M. and Lima, C.D. (2004) Insights into the structure, mechanism, and regulation of scavenger mRNA decapping activity. *Mol Cell*, **14**, 67-80.
- Gu, M. and Lima, C.D. (2005) Processing the message: structural insights into capping and decapping mRNA. *Curr Opin Struct Biol*, **15**, 99-106.
- Guhaniyogi, J. and Brewer, G. (2001) Regulation of mRNA stability in mammalian cells. *Gene*, **265**, 11-23.
- Guranowski, A. (2000) Specific and nonspecific enzymes involved in the catabolism of mononucleoside and dinucleoside polyphosphates. *Pharmacol Ther*, **87**, 117-139.
- Hamm, J. and Mattaj, I.W. (1990) Monomethylated cap structures facilitate RNA export from the nucleus. *Cell*, **63**, 109-118.
- Han, G.W., Schwarzenbacher, R., McMullan, D., Abdubek, P., Ambing, E., Axelrod, H., Biorac, T., Canaves, J.M., Chiu, H.J., Dai, X., Deacon, A.M., DiDonato, M., Elsliger, M., Godzik, A., Grittini, C., Grzechnik, S.K., Hale, J., Hampton, E.,

- Haugen, J., Hornsby, M., Jaroszewski, L., Klock, H.E., Koesema, E., Kreusch, A., Kuhn, P., Lesley, S.A., McPhillips, T.M., Miller, M.D., Moy, K., Nigoghossian, E., Paulsen, J., Quijano, K., Reyes, R., Spraggon, G., Stevens, R.C., Bedem, H.v.d., Velasquez, J., Vincent, J., White, A., Wolf, G., Xu, Q., Hodgson, K.O., Wooley, J. and Wilson, I.A. (2005) Crystal Structure of an Apo mRNA Decapping Enzyme (DcpS) from Mouse at 1.83 Å Resolution. *PROTEINS: Structure, Function, and Bioinformatics*, **60**, 797–802.
- Henry, Y., Wood, H., Morrissey, J.P., Petfalski, E., Kearsey, S. and Tollervey, D. (1994) The 5' end of yeast 5.8S rRNA is generated by exonucleases from an upstream cleavage site. *Embo J*, **13**, 2452-2463.
- Houseley, J., LaCava, J. and Tollervey, D. (2006) RNA-quality control by the exosome. *Nat Rev Mol Cell Biol*, **7**, 529-539.
- Howe, K.J. (2002) RNA polymerase II conducts a symphony of pre-mRNA processing activities. *Biochim Biophys Acta*, **1577**, 308-324.
- Hsu, C.L. and Stevens, A. (1993) Yeast cells lacking 5'→3' exoribonuclease 1 contain mRNA species that are poly(A) deficient and partially lack the 5' cap structure. *Mol Cell Biol*, **13**, 4826-4835.
- Inoue, K., Ohno, M., Sakamoto, H. and Shimura, Y. (1989) Effect of the cap structure on pre-mRNA splicing in *Xenopus* oocyte nuclei. *Genes & Dev.*, **3**, 1472-1479.
- Izaurrealde, E. and Mattaj, I.W. (1995) RNA export. *Cell*, **81**, 153-159.
- Izaurrealde, E., Stepinski, J., Darzynkiewicz, E. and Mattaj, I.W. (1992) A cap binding protein that may mediate nuclear export of RNA polymerase II-transcribed RNAs. *J. Cell Biol.*, **118**, 1287-1295.
- Jacobs, J.S., Anderson, A.R. and Parker, R.P. (1998) The 3' to 5' degradation of yeast mRNAs is a general mechanism for mRNA turnover that requires the SKI2 DEVH box protein and 3' to 5' exonucleases of the exosome complex. *Embo J*, **17**, 1497-1506.
- Jarmolowski, A., Boelens, W.C., Izaurrealde, E. and Mattaj, I.W. (1994) Nuclear export of different classes of RNA is mediated by specific factors. *J Cell Biol*, **124**, 627-635.
- Jiao, X., Trifillis, P. and Kiledjian, M. (2002) Identification of Target Messenger RNA Substrates for the Murine Deleted in Azoospermia-Like RNA-Binding Protein. *Biol Reprod*, **66**, 475-485.
- Jiao, X., Wang, Z. and Kiledjian, M. (2006) Identification of an mRNA-Decapping Regulator Implicated in X-Linked Mental Retardation. *Mol Cell*, **24**, 713-722.

- Johnson, A.W. (1997) Rat1p and Xrn1p are functionally interchangeable exoribonucleases that are restricted to and required in the nucleus and cytoplasm, respectively. *Mol Cell Biol*, **17**, 6122-6130.
- Khanna, R. and Kiledjian, M. (2004) Poly(A)-binding-protein-mediated regulation of hDcp2 decapping in vitro. *Embo J*, **23**, 1968-1976.
- Kijas, A.W., Harris, J.L., Harris, J.M. and Lavin, M.F. (2006) Aprataxin forms a discrete branch in the HIT (histidine triad) superfamily of proteins with both DNA/RNA binding and nucleotide hydrolase activities. *J Biol Chem*, **281**, 13939-13948.
- Kim, E., Du, L., Bregman, D.B. and Warren, S.L. (1997) Splicing factors associate with hyperphosphorylated RNA polymerase II in the absence of pre-mRNA. *J Cell Biol*, **13**, 19-28.
- Kim, M., Krogan, N.J., Vasiljeva, L., Rando, O.J., Nedeia, E., Greenblatt, J.F. and Buratowski, S. (2004) The yeast Rat1 exonuclease promotes transcription termination by RNA polymerase II. *Nature*, **432**, 517-522.
- Konarska, M.M., Padgett, R.A. and Sharp, P.A. (1984) Recognition of cap structure in splicing in vitro of mRNA precursors. *Cell*, **38**, 731-736.
- Koonin, E.V. (1993) A highly conserved sequence motif defining the family of MutT-related proteins from eubacteria, eukaryotes and viruses. *Nucleic Acids Res*, **21**, 4847.
- Korner, C.G. and Wahle, E. (1997) Poly(A) tail shortening by a mammalian poly(A)-specific 3'-exoribonuclease. *J Biol Chem*, **272**, 10448-10456.
- Korner, C.G., Wormington, M., Muckenthaler, M., Schneider, S., Dehlin, E. and Wahle, E. (1998) The deadenylating nuclease (DAN) is involved in poly(A) tail removal during the meiotic maturation of *Xenopus* oocytes. *Embo J*, **17**, 5427-5437.
- Koshland, D.E. (1996) The structural basis of negative cooperativity: receptors and enzymes. *Curr Opin Struct Biol*, **6**, 757-761.
- Koshland, D.E. and Hamadani, K. (2002) Proteomics and models for enzyme cooperativity. *J Biol Chem*, **277**, 46841-46844.
- Kuai, L., Das, B. and Sherman, F. (2005) A nuclear degradation pathway controls the abundance of normal mRNAs in *Saccharomyces cerevisiae*. *Proc Natl Acad Sci USA*, **102**, 13962-13967.
- Kufel, J., Bousquet-Antonelli, C., Beggs, J.D. and Tollervey, D. (2004) Nuclear pre-mRNA decapping and 5' degradation in yeast require the Lsm2-8p complex. *Mol Cell Biol*, **24**, 9646-9657.

- Kumagai, H., Kon, R., Hoshino, T., Aramaki, T., Nishikawa, M., Hirose, S. and Igarashi, K. (1992) Purification and properties of a decapping enzyme from rat liver cytosol. *Biochim Biophys Acta*, **1119**, 45-51.
- LaCava, J., Houseley, J., Saveanu, C., Petfalski, E., Thompson, E., Jacquier, A. and Tollervey, D. (2005) RNA degradation by the exosome is promoted by a nuclear polyadenylation complex. *Cell*, **121**, 713-724.
- LaGrandeur, T.E. and Parker, R. (1998) Isolation and characterization of Dcp1p, the yeast mRNA decapping enzyme. *Embo J*, **17**, 1487-1496.
- Le Hir, H., Gatfield, D., Izaurralde, E. and Moore, M.J. (2001) The exon-exon junction complex provides a binding platform for factors involved in mRNA export and nonsense-mediated mRNA decay. *Embo J*, **20**, 4987-4997.
- Le Hir, H., Izaurralde, E., Maquat, L.E. and Moore, M.J. (2000) The spliceosome deposits multiple proteins 20-24 nucleotides upstream of mRNA exon-exon junctions. *Embo J*, **19**, 6860-6869.
- Lee, J.M. and Greenleaf, A.L. (1997) Modulation of RNA polymerase II elongation efficiency by C-terminal heptapeptide repeat domain kinase I. *J Biol Chem*, **272**, 10990-10993.
- Lejeune, F., Li, X. and Maquat, L.E. (2003) Nonsense-mediated mRNA decay in mammalian cells involves decapping, deadenylating, and exonucleolytic activities. *Mol Cell*, **12**, 675-687.
- Lima, C.D., Klein, M.G. and Hendrickson, W.A. (1997) Structure-based analysis of catalysis and substrate definition in the HIT protein family. *Science*, **278**, 286-290.
- Liu, H. and Kiledjian, M. (2005) Scavenger decapping activity facilitates 5' to 3' mRNA decay. *Mol Cell Biol*, **25**, 9764-9772.
- Liu, H. and Kiledjian, M. (2006) Decapping the message: a beginning or an end. *Biochem Soc Trans*, **34**, 35-38.
- Liu, H., Rodgers, N.D., Jiao, X. and Kiledjian, M. (2002) The scavenger mRNA decapping enzyme DcpS is a member of the HIT family of pyrophosphatases. *Embo J*, **21**, 4699-4708.
- Liu, S.W., Jiao, X., Liu, H., Gu, M., Lima, C.D. and Kiledjian, M. (2004) Functional analysis of mRNA scavenger decapping enzymes. *Rna*, **10**, 1412-1422.
- Lopez, P.J. and Seraphin, B. (2000) Uncoupling yeast intron recognition from transcription with recursive splicing. *EMBO Rep*, **1**, 334-339.

- Lowell, J.E., Rudner, D.Z. and Sachs, A.B. (1992) 3'-UTR-dependent deadenylation by the yeast poly(A) nuclease. *Genes Dev*, **6**, 2088-2099.
- Lund, M.K. and Guthrie, C. (2005) The DEAD-box protein Dbp5p is required to dissociate Mex67p from exported mRNPs at the nuclear rim. *Mol Cell*, **20**, 645-651.
- Luo, M.J. and Reed, R. (1999) Splicing is required for rapid and efficient mRNA export in metazoans. *Proc Natl Acad Sci USA*, **96**, 14937-14942.
- Lykke-Andersen, J. (2002) Identification of a human decapping complex associated with hUpf proteins in nonsense-mediated decay. *Mol Cell Biol*, **22**, 8114-8121.
- Mühlemann, O. (2005) Applying the brakes on gene expression. *Nat Struct Mol Biol*, **12**, 1024-1025.
- Malys, N., Carroll, K., Miyan, J., Tollervey, D. and McCarthy, J.E. (2004) The 'scavenger' m7GpppX pyrophosphatase activity of Dcs1 modulates nutrient-induced responses in yeast. *Nucleic Acids Res*, **32**, 3590-3600.
- Malys, N. and McCarthy, J.E.G. (2006) Dcs2, a Novel Stress-induced Modulator of m7GpppX Pyrophosphatase Activity that Locates to P Bodies. *J Mol Biol*, **363**, 370-382.
- Mandel, C.R., Kaneko, S., Zhang, H., Gebauer, D., Vethantham, V., Manley, J.L. and Tong, L. (2006) Polyadenylation factor CPSF-73 is the pre-mRNA 3'-end-processing endonuclease. *Nature*, **444**, 953-956.
- Martinez, J., Ren, Y.G., Nilsson, P., Ehrenberg, M. and Virtanen, A. (2001) The mRNA cap structure stimulates rate of poly(A) removal and amplifies processivity of degradation. *J Biol Chem*, **276**, 27923-27929.
- Martinez, J., Ren, Y.G., Thuresson, A.C., Hellman, U., Astrom, J. and Virtanen, A. (2000) A 54-kDa fragment of the Poly(A)-specific ribonuclease is an oligomeric, processive, and cap-interacting Poly(A)-specific 3' exonuclease. *J Biol Chem*, **275**, 24222-24230.
- McCracken, S., Fong, N., Rosonina, E., Yankulov, K., Brothers, G., Siderovski, D., Hessel, A., Foster, S., Shuman, S. and Bentley, D.L. (1997a) 5'-Capping enzymes are targeted to pre-mRNA by binding to the phosphorylated carboxy-terminal domain of RNA polymerase II. *Genes Dev*, **11**, 3306-3318.
- McCracken, S., Fong, N., Yankulov, K., Ballantyne, S., Pan, G., Greenblatt, J., Patterson, S.D., Wickens, M. and Bentley, D.L. (1997b) The C-terminal domain of RNA polymerase II couples mRNA processing to transcription. *Nature*, **385**, 357-361.

- Meininghaus, M., Chapman, R.D., Horndasch, M. and Eick, D. (2000) Conditional expression of RNA polymerase II in mammalian cells. Deletion of the carboxyl-terminal domain of the large subunit affects early steps in transcription. *J Biol Chem* **275**, 24375-24382.
- Mejean, V., Salles, C., Bullions, L.C., Bessman, M.J. and Claverys, J.P. (1994) Characterization of the mutX gene of *Streptococcus pneumoniae* as a homologue of *Escherichia coli* mutT, and tentative definition of a catalytic domain of the dGTP pyrophosphohydrolases. *Mol Microbiol*, **11**, 323-330.
- Meyer, S., Temme, C. and Wahle, E. (2004) Messenger RNA turnover in eukaryotes: pathways and enzymes. *Crit Rev Biochem Mol Biol*, **39**, 197-216.
- Milone, J., Wilusz, J. and Bellofatto, V. (2004) Characterization of deadenylation in trypanosome extracts and its inhibition by poly(A)-binding protein Pab1p. *RNA*, **10**, 448-457.
- Mitchell, P., Petfalski, E., Shevchenko, A., Mann, M. and Tollervey, D. (1997) The exosome: a conserved eukaryotic RNA processing complex containing multiple 3'→5' exoribonucleases. *Cell*, **91**, 457-466.
- Mitchell, P. and Tollervey, D. (2000b) Musing on the structural organization of the exosome complex. *Nat Struct Biol*, **7**, 843-846.
- Mitchell, P. and Tollervey, D. (2003) An NMD pathway in yeast involving accelerated deadenylation and exosome-mediated 3'→5' degradation. *Mol Cell*, **11**, 1405-1413.
- Moore, M.J. (2002) Nuclear RNA turnover. *Cell*, **108**, 431-434.
- Morillon, A., O'Sullivan, J., Azad, A., Proudfoot, N. and Mellor, J. (2003) Regulation of elongating RNA polymerase II by forkhead transcription factors in yeast. *Science*, **300**, 492-495.
- Mortillaro, M.J., Blencowe, B.J., Wei, X., Nakayasu, H., Du, L., Warren, S.L., Sharp, P.A. and Berezney, R. (1996) A hyperphosphorylated form of the large subunit of RNA polymerase II is associated with splicing complexes and the nuclear matrix. *Proc Natl Acad Sci U S A*, **93**, 8253-8257.
- Mossessova, E. and Lima, C.D. (2000) Ulp1-SUMO crystal structure and genetic analysis reveal conserved interactions and a regulatory element essential for cell growth in yeast. *Mol Cell*, **5**, 865-876.

- Muhlrad, D., Decker, C.J. and Parker, R. (1994) Deadenylation of the unstable mRNA encoded by the yeast MFA2 gene leads to decapping followed by 5'→3' digestion of the transcript. *Genes Dev*, **8**, 855-866.
- Muhlrad, D., Decker, C.J. and Parker, R. (1995) Turnover mechanisms of the stable yeast PGK1 mRNA. *Mol Cell Biol*, **15**, 2145-2156.
- Murray, E.L. and Schoenberg, D.R. (2007) A+U-rich instability elements differentially activate 5'-3' and 3'-5' mRNA decay. *Mol Cell Biol*, **27**, 2791-2799.
- Muthukrishnan, S., Both, G.W., Furuichi, Y. and Shatkin, A.J. (1975) 5'-Terminal 7-methylguanosine in eukaryotic mRNA is required for translation. *Nature*, **255**, 33-37.
- Neugebauer, K.M. (2002) On the importance of being co-transcriptional. *J Cell Sci*, **115**, 3865-3871.
- Newbury, S. and Woollard, A. (2004) The 5'-3' exoribonuclease xrn-1 is essential for ventral epithelial enclosure during *C. elegans* embryogenesis. *Rna*, **10**, 59-65.
- Newbury, S.F. (2006) Control of mRNA stability in eukaryotes. *Biochem Soc Trans*, **34**, 30-34.
- Niedzwiecka, A., Marcotrigiano, J., Stepinski, J., Jankowska-Anyszka, M., Wyslouch-Cieszyńska, A., Dadlez, M., Gingras, A.C., Mak, P., Darzynkiewicz, E., Sonenberg, N., Burley, S.K. and Stolarski, R. (2002) Biophysical studies of eIF4E cap-binding protein: recognition of mRNA 5' cap structure and synthetic fragments of eIF4G and 4E-BP1 proteins. *J Mol Biol*, **319**, 615-635.
- Nuss, D.L. and Furuichi, Y. (1977) Characterization of the m7G(5')pppN-pyrophosphatase activity from HeLa cells. *J Biol Chem*, **252**, 2815-2821.
- Nuss, D.L., Furuichi, Y., Koch, G. and Shatkin, A.J. (1975) Detection in HeLa cell extracts of a 7-methyl guanosine specific enzyme activity that cleaves m7GpppNm. *Cell*, **6**, 21-27.
- Ougland, R., Zhang, C.M., Liiv, A., Johansen, R.F., Seeberg, E., Hou, Y.M., Remme, J. and Falnes, P.Ø. (2004) AlkB restores the biological function of mRNA and tRNA inactivated by chemical methylation. *Mol Cell*, **16**, 107-116.
- Pace, H.C., Garrison, P.N., Robinson, A.K., Barnes, L.D., Draganescu, A., Rosler, A., Blackburn, G.M., Siprashvili, Z., Croce, C.M., Huebner, K. and Brenner, C. (1998) Genetic, biochemical, and crystallographic characterization of Fhit- substrate complexes as the active signaling form of Fhit. *Proc Natl Acad Sci U S A*, **95**, 5484-5489.

- Paddison, P.J., Caudy, A.A., Bernstein, E., Hannon, G.J. and Conklin, D.S. (2002) Short hairpin RNAs (shRNAs) induce sequence-specific silencing in mammalian cells. *Genes Dev*, **16**, 948-958.
- Parker, R. and Song, H. (2004) The enzymes and control of eukaryotic mRNA turnover. *Nat Struct Mol Biol*, **11**, 121-127.
- Peculis, B.A. and Steitz, J.A. (1993) Disruption of U8 nucleolar snRNA inhibits 5.8S and 28S rRNA processing in the *Xenopus* oocyte. *Cell*, **73**, 1233-1245.
- Petfalski, E., Dandekar, T., Henry, Y. and Tollervey, D. (1998) Processing of the precursors to small nucleolar RNAs and rRNAs requires common components. *Mol Cell Biol*, **18**, 1181-1189.
- Phatnani, H.P. and Greenleaf, A.L. (2006) Phosphorylation and functions of the RNA polymerase II CTD. *Genes & Dev* **20**, 2922-2936.
- Piccirillo, C., Khanna, R. and Kiledjian, M. (2003) Functional characterization of the mammalian mRNA decapping enzyme hDcp2. *Rna*, **9**, 1138-1147.
- Piccoli, R., Di Donato, A. and D'Alessio, G. (1988) Co-operativity in seminal ribonuclease function. Kinetic studies. *Biochem J*, **253**, 329-336.
- Piccoli, R., Di Donato, A., Dudkin, S. and D'Alessio, G. (1982) Bovine seminal ribonuclease: non-hyperbolic kinetics in the second reaction step. *FEBS Lett*, **140**, 307-310.
- Piccoli, R., Tamburrini, M., Piccialli, G., Di Donato, A., Parente, A. and D'Alessio, G. (1992) The dual-mode quaternary structure of seminal RNase. *Proc Natl Acad Sci U S A*, **89**, 1870-1874.
- Ramirez, C.V., Vilela, C., Berthelot, K. and McCarthy, J.E. (2002) Modulation of eukaryotic mRNA stability via the cap-binding translation complex eIF4F. *J Mol Biol*, **318**, 951-962.
- Reed, R. and Hurt, E. (2002) A conserved mRNA export machinery coupled to pre-mRNA splicing. *Cell*, **108**, 523-531.
- Rodgers, N.D., Wang, Z. and Kiledjian, M. (2002) Regulated alpha-globin mRNA decay is a cytoplasmic event proceeding through 3'-to-5' exonuclease-dependent decapping. *Rna*, **8**, 1526-1537.
- Rodriguez, M.S., Dargemont, C. and Stutz, F. (2004) Nuclear export of RNA. *Biol Cell*, **96**, 639-655.

- Salehi, Z., Geffers, L., Vilela, C., Birkenhager, R., Ptushkina, M., Berthelot, K., Ferro, M., Gaskell, S., Hagan, I., Stapley, B. and McCarthy, J.E. (2002) A nuclear protein in *Schizosaccharomyces pombe* with homology to the human tumour suppressor Fhit has decapping activity. *Mol Microbiol*, **46**, 49-62.
- Sanford, J.R. and Caceres, J.F. (2004) Pre-mRNA splicing: life at the centre of the central dogma. *J Cell Sci*, **117**, 6261-6263.
- Schirmer, T. and Evans, P.R. (1990) Structural basis of the allosteric behaviour of phosphofructokinase. *Nature*, **343**, 140 - 145
- Schmitt, C., von Kobbe, C., Bachi, A., Panté, N., Rodrigues, J.P., Boscheron, C., Rigaut, G., Wilm, M., Séraphin, B., Carmo-Fonseca, M. and Izaurralde, E. (1999) Dbp5, a DEAD-box protein required for mRNA export, is recruited to the cytoplasmic fibrils of nuclear pore complex via a conserved interaction with CAN/Nup159p. *EMBO J*, **18**, 4332-4347.
- Schwartz, D.C. and Parker, R. (1999) Mutations in translation initiation factors lead to increased rates of deadenylation and decapping of mRNAs in *Saccharomyces cerevisiae*. *Mol Cell Biol*, **19**, 5247-5256.
- Schwartz, D.C. and Parker, R. (2000) mRNA decapping in yeast requires dissociation of the cap binding protein, eukaryotic translation initiation factor 4E. *Mol Cell Biol*, **20**, 7933-7942.
- Segref, A., Sharma, K., Doye, V., Hellwig, A., Huber, J., Lührmann, R. and Hurt, E. (1997) Mex67p, a novel factor for nuclear mRNA export, binds to both poly(A)+ RNA and nuclear pores. *EMBO J* **16**, 3256–3271.
- Seraphin, B. (1992) The HIT protein family: a new family of proteins present in prokaryotes, yeast and mammals. *DNA Seq*, **3**, 177-179.
- Shatkin, A.J. and Manley, J.L. (2000) The ends of the affair: capping and polyadenylation [In Process Citation]. *Nat Struct Biol*, **7**, 838-842.
- She, M., Decker, C.J., Chen, N., Tumati, S., Parker, R. and Song, H. (2006) Crystal structure and functional analysis of Dcp2p from *Schizosaccharomyces pombe*. *Nat Struct Mol Biol*, **13**, 63-70.
- Shuman, S. (1997) Origins of mRNA identity: Capping enzymes bind to the phosphorylated C-terminal domain of RNA polymerase II. *Proc Natl Acad Sci U S A* **94**, 2758–12760.
- Sigler, P.B., Xu, Z., Rye, H.S., Burston, S.G., Fenton, W.A. and Horwich, A.L. (1998) Structure and function in GroEL-mediated protein folding. *Annu Rev Biochem*, **67**, 581-608.

- Simon, E., Camier, S. and Seraphin, B. (2006) New insights into the control of mRNA decapping. *Trends Biochem Sci*, **31**, 241-243.
- Sonenberg, N. (1988) Cap-binding proteins of eukaryotic messenger RNA: functions in initiation and control of translation. *Prog Nucleic Acid Res Mol Biol*, **35**, 173-207.
- Steiger, M., Carr-Schmid, A., Schwartz, D.C., Kiledjian, M. and Parker, R. (2003) Analysis of recombinant yeast decapping enzyme. *Rna*, **9**, 231-238.
- Stevens, A. (1980) Purification and characterization of a *Saccharomyces cerevisiae* exoribonuclease which yields 5'-mononucleotides by a 5' leads to 3' mode of hydrolysis. *J Biol Chem*, **255**, 3080-3085.
- Stewart, M. (2007) Ratcheting mRNA out of the nucleus. *Mol Cell*, **25**, 327-330.
- Tange, T.Ø., Nott, A. and Moore, M.J. (2004) The ever-increasing complexities of the exon junction complex. *Curr Opin Cell Biol*, **16**, 279-284.
- Tharun, S., He, W., Mayes, A.E., Lennertz, P., Beggs, J.D. and Parker, R. (2000) Yeast Sm-like proteins function in mRNA decapping and decay. *Nature*, **404**, 515-518.
- Till, D.D., Linz, B., Seago, J.E., Elgar, S.J., Marujo, P.E., Elias, M.L., Arraiano, C.M., McClellan, J.A., McCarthy, J.E. and Newbury, S.F. (1998) Identification and developmental expression of a 5'-3' exoribonuclease from *Drosophila melanogaster*. *Mech Dev*, **79**, 51-55.
- Tucker M, S.R., Valencia-Sanchez MA, Muhlrads D, Parker R. (2002) Ccr4p is the catalytic subunit of a Ccr4p/Pop2p/Notp mRNA deadenylase complex in *Saccharomyces cerevisiae*. *Embo J*, **21**, 1427-1436.
- Tucker M, V.-S.M., Staples RR, Chen J, Denis CL, Parker R. . (2001) The transcription factor associated Ccr4 and Caf1 proteins are components of the major cytoplasmic mRNA deadenylase in *Saccharomyces cerevisiae*. *Cell*, **104**, 377-386.
- Uchida, N., Hoshino, S. and Katada, T. (2004) Identification of a human cytoplasmic poly(A) nuclease complex stimulated by poly(A)-binding protein. *J Biol Chem*, **279**, 1383-1391.
- Valadkhan, S. and Manley, J.L. (2001) Splicing-related catalysis by protein-free snRNAs. *Nature*, **413**, 701-707.
- van Dijk, E., Cougot, N., Meyer, S., Babajko, S., Wahle, E. and Seraphin, B. (2002) Human Dcp2: a catalytically active mRNA decapping enzyme located in specific cytoplasmic structures. *Embo J*, **21**, 6915-6924.

- van Dijk, E., Le Hir, H. and Seraphin, B. (2003) DcpS can act in the 5'-3' mRNA decay pathway in addition to the 3'-5' pathway. *Proc Natl Acad Sci U S A*, **100**, 12081-12086.
- van Hoof, A., Frischmeyer, P.A., Dietz, H.C. and Parker, R. (2002) Exosome-mediated recognition and degradation of mRNAs lacking a termination codon. *Science*, **295**, 2262-2264.
- van Hoof, A. and Parker, R. (1999) The exosome: a proteasome for RNA? *Cell*, **99**, 347-350.
- van Hoof, A., Staples, R.R., Baker, R.E. and Parker, R. (2000) Function of the ski4p(Csl4p) and Ski7 proteins in 3' to 5' degradation of mRNA. *Mol Cell Biol*, **20**, 8230-8243.
- Vasiljeva, L. and Buratowski, S. (2006) Nrd1 interacts with the nuclear exosome for 3' processing of RNA polymerase II transcripts. *Mol Cell*, **21**, 239-248.
- Villa, T., Pleiss, J.A. and Guthrie, C. (2002) Spliceosomal snRNAs: Mg²⁺-Dependent Chemistry at the Catalytic Core? *Cell*, **149-152**, 149-152.
- Vincent, M., Lauriault, P., Dubois, M.F., Lavoie, S., Bensaude, O. and Chabot, B. (1996) The nuclear matrix protein p255 is a highly phosphorylated form of RNA polymerase II largest subunit which associates with spliceosomes. *Nucleic Acids Res*, **24**, 4649-4652.
- Wagner, E., Clement, S.L. and Lykke-Andersen, J. (2007) An unconventional human Ccr4-Caf1 deadenylase complex in nuclear cajal bodies. *Mol Cell Biol* **27**, 1686-1695.
- Wahle, E. and Keller, W. (1992) The biochemistry of 3'-end cleavage and polyadenylation of messenger RNA precursors. *Annu Rev Biochem*, **61**, 419-440.
- Wang, Z., Day, N., Trifillis, P. and Kiledjian, M. (1999) An mRNA stability complex functions with poly(A)-binding protein to stabilize mRNA in vitro. *Mol Cell Biol*, **19**, 4552-4560.
- Wang, Z., Jiao, X., Carr-Schmid, A. and Kiledjian, M. (2002) The hDcp2 protein is a mammalian mRNA decapping enzyme. *Proc Natl Acad Sci U S A*, **99**, 12663-12668.
- Wang, Z. and Kiledjian, M. (2001) Functional Link between the Mammalian Exosome and mRNA Decapping. *Cell*, **107**, 751-762.
- Watts, R.W. (1983) Some regulatory and integrative aspects of purine nucleotide biosynthesis and its control: an overview. *Adv Enzyme Regul*, **21**, 33-51.

- Wetterberg, I., Bauren, G. and Wieslander, L. (1996) The intranuclear site of excision of each intron in Balbiani ring 3 pre-mRNA is influenced by the time remaining to transcription termination and different excision efficiencies for the various introns. *RNA*, **2**, 641-651.
- Wetterberg, I., Zhao, J., Masich, S., Wieslander, L. and Skoglund, U. (2001) In situ transcription and splicing in the Balbiani ring 3 gene. *EMBO J*, **20**, 2564-2574.
- Wilson, G.M. and Brewer, G. (1999) Identification and characterization of proteins binding A + U-rich elements. *Methods*, **17**, 74-83.
- Wilusz, C.J., Gao, M., Jones, C.L., Wilusz, J. and Peltz, S.W. (2001) Poly(A)-binding proteins regulate both mRNA deadenylation and decapping in yeast cytoplasmic extracts. *Rna*, **7**, 1416-1424.
- Wilusz, C.J. and Wilusz, J. (2004) Bringing the role of mRNA decay in the control of gene expression into focus. *Trends Genet*, **20**, 491-497.
- Wyers, F., Rougemaille, M., Badis, G., Rousselle, J.C., Dufour, M.E., Boulay, J., Regnault, B., Devaux, F., Namane, A., Seraphin, B., Libri, D. and Jacquier, A. (2005) Cryptic pol II transcripts are degraded by a nuclear quality control pathway involving a new poly(A) polymerase. *Cell*, **121** 725-737.
- Wyngaarden, J.B. (1976) Regulation of purine biosynthesis and turnover. *Adv Enzyme Regul*, **14**, 25-42.
- Yamashita, A., Chang, T.C., Yamashita, Y., Zhu, W., Zhong, Z., Chen, C.Y. and Shyu, A.B. (2005) Concerted action of poly(A) nucleases and decapping enzyme in mammalian mRNA turnover. *Nat Struct Mol Biol*, **12**, 1054-1063.
- Yean, S.L., Wuenschell, G., Termini, J. and Lin, R.J. (2000) Metal-ion coordination by U6 small nuclear RNA contributes to catalysis in the spliceosome. *Nature*, **408**, 881-884.
- Yu, B., Edstrom, W.C., Benach, J., Hamuro, Y., Weber, P.C., Gibney, B.R. and Hunt, J.F. (2006) Crystal structures of catalytic complexes of the oxidative DNA/RNA repair enzyme AlkB. *Nature*, **439**, 879-884.
- Yu, J.H., Yang, W.H., Gulick, T., Bloch, K.D. and Bloch, D.B. (2005) Ge-1 is a central component of the mammalian cytoplasmic mRNA processing body. *RNA*, **11**, 1795-1802.
- Yue, Z., Maldonado, E., Pillutla, R., Cho, H., Reinberg, D. and Shatkin, A.J. (1997) Mammalian capping enzyme complements mutant *Saccharomyces cerevisiae*

lacking mRNA guanylyltransferase and selectively binds the elongating form of RNA polymerase II. *Proc Natl Acad Sci U S A*, **94**, 12898-12903.

Zhao, J., Hyman, L. and Moore, C. (1999) Formation of mRNA 3' ends in eukaryotes: mechanism, regulation, and interrelationships with other steps in mRNA synthesis. *Microbiol Mol Biol Rev*, **63**, 405-445.

Zuberek, J., Jemielity, J., Niedzwiecka, A., Stepinski, J., Wyslouch-Cieszyńska, A., Stolarski, R. and Darzynkiewicz, E. (2003) Influence of the length of the phosphate chain in mRNA 5' cap analogues on their interaction with eukaryotic initiation factor 4E. *Nucleosides Nucleotides Nucleic Acids*, **22**, 1707-1710.

Zuk, D. and Jacobson, A. (1998) A single amino acid substitution in yeast eIF-5A results in mRNA stabilization. *Embo J*, **17**, 2914-2925.

Curriculum Vitae

- 1997 B.V.M. Veterinary Medicine, National Chung-Hsing University, Taiwan.
- 1999 M.S. Veterinary Microbiology, National Chung-Hsing University, Taiwan.
- 2007 Ph.D. Cell and Developmental Biology, Rutgers University.

Publications:

1. **Liu, S.W.**, Jiao, X., Welch, S., and Kiledjian, M. (2007) Analysis of mRNA decapping. In preparation.
2. **Liu, S.W.**, Rajagopal, V., Patel, S.S. and Kiledjian, M. (2007) Mechanistic and kinetic analysis of the DcpS scavenger decapping enzyme. In preparation.
3. Shen, V., **Liu, S.W.**, Liu, H., Jiao, X., and Kiledjian, M. (2007) The DcpS scavenger decapping enzyme functions in pre-mRNA Splicing and mRNA translation. Submitted.
4. **Liu, S.W.**, Jiao X., Liu H., Gu M., Lima C.D. and Kiledjian, M. (2004) Functional analysis of mRNA scavenger decapping enzymes. *RNA* 10:1412-22
5. Gu, M., Fabrega C., **Liu, S.W.**, Liu, H., Kiledjian M. and Lima, C.D. (2004) Insights into the structure, mechanism, and regulation of scavenger mRNA decapping activity. *Mol Cell* 9:14:67-80.
6. Chung, Y.T., **Liu, S.W.** and Lin, C.F. (1998) Cloning and sequence analysis of the infectious bovine rhinotracheitis virus (IBRV) gene encoding the envelope glycoprotein gC. *Taiwan J. Vet. Med. & Anim. Husb.* 68: 113-124. (in Chinese).
7. Chung, Y.T., Hsu, W. and **Liu, S.W.** (1996) Production and purification of recombinant infectious bovine rhinotracheitis virus uracil-DNA glycosylase. *Taiwan J. Vet. Med. Anim. Husb.* 66:265-275. (in Chinese).